AN EXAMINATION OF BLUE WHALE FORAGING AND ITS KRILL PREY FIELD IN THE MONTEREY BAY SUBMARINE CANYON

A Dissertation

Presented to the Faculty of the Graduate School

of Cornell University

In Partial Fulfillment of the Requirements for the Degree of

Doctor of Philosophy

by

Louise Patricia McGarry

May 2014

AN EXAMINATION OF BLUE WHALE FORAGING AND ITS KRILL PREY FIELD IN THE MONTEREY BAY SUBMARINE CANYON

Louise Patricia McGarry, Ph. D.

Cornell University, 2014

The purpose of this study is to advance the application of hydroacoustic techniques in the study of marine ecosystems. In the Monterey Bay Submarine Canyon on the coast of California, USA, 120 kHz and 200 kHz hydroacoustic data was collected with scientific echosounders. Zooplankton specimens were collected using MOCNESS stratified net tows from the strongly scattering krill sound-scattering layer (SSL). A suite of zooplankton scattering models were used to predict the backscatter expected from the specimens collected in the nets. The results of this work demonstrate that the backscatter from rare and inconspicuous but strongly scattering gas-bearing siphonophores can dominate the backscatter observed from the sound-scattering layers dominated by krill biomass. Failure to account for the contribution to observed backscatter by the gas-bearing siphonophores will results in overestimates of acoustic-derived euphausiid abundance and the nutritional quality of these krill sound-scattering layers.

Blue whales, the largest animal on the planet, feed on the krill aggregations found to coincide with the SSLs adjacent to the walls of the Monterey Bay Submarine Canyon. In this study the foraging-dives of a blue whale were tracked and its krill prey-field was remotely sensed using hydroacoustic techniques. The foraging behavior

of the whale as it searched and exploited the krill SSL was examined in the context of its krill prey-field, and the foraging efficiency achieved by the whale was estimated. The results of this study suggest that the search behavior of the whale is consistent with behavior that theory predicts would optimize their encounter rate with krill patches of sufficiently high prey density. The results also provide compelling evidence that within the foraging habitat, the whale focused its foraging effort in a discrete high-density patch where the achievable foraging efficiency was an order of magnitude greater than in other regions tested and rejected by the whale.

BIOGRAPHICAL SKETCH

Louise Patricia McGarry earned a Bachelor of Science, with Distinction, in Business Administration from the University of Maine in 1983. In 1997, she earned a Bachelor of Science, *magna cum laude*, in Geological Sciences from the University of Maine. In 2003, she joined the doctoral program in Ocean Science and Technology within the graduate field of Geological Sciences at Cornell University.

Honors offered by the Department of Earth and Atmospheric Sciences and awarded to Dr. McGarry included Most Outstanding Graduate Student (Estwing Award), Outstanding Graduate Student Dedicated to Academia and the Human Aspects of Life (Meyer Bender Memorial Scholarship), and Outstanding Teaching Assistant.

While pursuing her degree, Dr. McGarry was a teaching assistant for many courses within the Department of Earth and Atmospheric Sciences including Introduction to Oceanography, Marine Ecosystem Dynamics, and Climate Dynamics, among others. In addition she created and taught a first-year writing course entitled Sustainable Earth, Energy, and Environmental Systems for which she created an associated speaker series that was open to the public and recognized by the Tompkins County Signs Of Sustainability award for public education on sustainability issues. Her contribution to the University extended outside of her department by invitation to assume teaching assistant responsibilities for Teaching Writing, and mentoring in the Sustainable Energy Fellowship program hosted by Cornell University.

Through her advisor, Dr. Charles H. Greene, Dr. McGarry has had a strong association with the Bioacoustical Oceanography Workshop funded by the Office of Naval Research. Her affiliation with the workshop has progressed from participant to teaching assistant to instructor.

DEDICATION

To those that came before me who, by their dedication and sacrifices, made it possible for me to choose what for them was not possible.

ACKNOWLEDGMENTS

No graduate program would be successful without the good and kind care and engagement of colleagues, mentors, friends, family, and sometimes even strangers.

First and foremost, with deepest gratitude, I would like to acknowledge the gifted, kind, brilliant men on my academic steering committee: Charles H. Greene, Patrick J. Sullivan, Lars G. Rudstam, and Andrew J. Pershing. For their good guidance, encouragement, affirmation, support, patience, engagement, and generosity of spirit and intellect, I thank them all. I couldn't have accomplished the work that is represented by this dissertation without the support of each of them.

In addition, it is with deep gratitude that I thank my colleagues at Woods Hole Oceanographic Institution who, in their enthusiasm for their own work and science, generously shared their knowledge, collegiality, and the Matlab coding used in this work for the zooplankton digitization, zooplankton backscattering modeling, and kriging: Peter Wiebe, Nancy Copley, Andone Lavery, Tim Stanton, Dezhang Chu, and Gareth Lawson. I particularly want to recognize and thank Peter Wiebe for his generosity in inviting me to work in his lab for the extended periods required for the identification and measurement of the zooplankton that illuminated the importance of siphonophores of Chapter 2, and for his generosity to allow Nancy Copley the time to teach me. And Nancy Copley who not only taught me specimen handling, zooplankton identification, and silhouette and digitizing techniques, but also befriended me, gave me rest at her house, and the joy of bicycling on a beautiful gift-of-a-day on Martha's Vineyard. Included in the Woods Hole crowd is Ken Foote who I originally met through the bioacoustical oceanography workshop but who spent time with me to talk

about my work and encourage my investigations of geospatial statistical techniques. Included in that number is Joe Warren of StonyBrook University, who will probably be surprised to find his name on my list, but he too was generous with his time and knowledge to give me a primer on backscattering from physical sources. And Mark Benfield of Louisiana State University and Duncan McGehee of Cuyamaca College who, too, will likely be surprised to find their names among this list, but who, while conversing among themselves as we trekked to the dining commons one day during my first bioacoustical workshop at the Friday Harbor Marine Labs, made a remark to me that consisted of a question and a comment, and in that moment left an indelible mark on my scroll that carried me through some of the rough spots of graduate school. Indeed, small moments can get emblazoned on the scroll, and we never know when we deliver those large messages in the small moments.

And then there is “office west”. John K. Horne and the Fisheries Acoustics Research (FAR) lab at the University of Washington, Seattle. It was my good fortune to meet John at that first bioacoustical oceanography course on my way into graduate school. And my great good fortune that he was another who is generous with his time and knowledge and experience. And in the midst of the busy-ness of the bioacoustics courses, taking the time for conversation, crab (Dungeness), and cribbage. In addition, opening the FAR lab and the expertise of its members to me, particularly the ever-funny, ever-brilliant, David Barbee.

Included in the FAR Lab is Sandra Parker-Stetter, a colleague who I met as she was finishing up at Cornell, and then re-met during my passages through Seattle on the way to Friday Harbor, and from there became first colleague and mentor, and then

friend and chief cheer-leader. Sandy, I am so honored to know you and count you as Friend.

And when not traveling to other labs, there was a whole passel of people in Ithaca and surroundings helping me keep body and soul together by offering housing, a meal, friendship, and a place to rest my weary spirit: Pete Nester and Elizabeth Humbert, Stephanie Devlin, Carrie Brindisi, Katie Tamulonis, Tiffany Tchakarides, Brian Ruskin, Herdis Schopka, and Kathy Mills who continue to be part of my life and heart although they are long gone from Cornell. And Julie Pett-Ridge, although our contact has loosened since she left Cornell, during our time together here, her friendship was deeply valued. Professors within the department who opened their hearts and homes to me in my time of need, and coincidently were also the ones who opened their office doors to me: Lou Derry and Alex Moore, Terry Jordan and Rick Allmendinger, and Larry and Mary Helen Cathles. Their generosity of heart and home touches me deeply and stays with me. And two couples whose friendship carried over from my earlier excursion to Ithaca: Keith and Paula Davis, and Bob and Anne Terrell. And my Cortland crowd: Renee McLain, Shelia Murray, Kevin Murray, and dearest Carol Horton including her David and her son Tom. Carol, your generosity of heart nourishes my body, soul, and spirit. You are truly an angel in our midst. And Janet Shortall with whom I share so much in terms of heart and spirit. Our breakfasts at the State, treks at Burns Road or Cass Park, time together kept me grounded in the wide reality of my world which incorporated both heart and head. And Dee Bailey: without our standing Sunday night “phone dates” my world would be so much less rich.

And then there is Bruce Monger: funny, brilliant, kind, and ever “awesome”. I met Bruce when he generously agreed to drive me, a stranger, the 7 hours from Ithaca to

Woods Hole where we were to board a ship for a GLOBEC cruise. In the intervening 17 years since, he has generously offered counsel, advice, knowledge, many small kindnesses, and his book shelves. My life, my teaching, and my dissertation is richer because of your presence in my life.

Erin Gutbrod-Meyer and Ian Brosnan, I am glad my turn at Cornell lasted long enough to have met both of you. You are the kind of labmates one wishes for. And although you arrived at a time of particular challenge for me, you took me into your worlds with grace and care. Your bright minds, and bright, strong hearts willing to take me in brought me strength, focus, and clarity while I moved through a really challenging time and back into the land of the living. Your joyful presences helped me to remember joy, and that it too, would come back into my world.

And then there are the members of the front office staff in Snee, particularly Judy Starr and Savannah Williams. You helped me navigate the logistical needs as both a student and as an instructor, but in the midst of all that, also offered me your friendship. I cherish you both.

And no graduate program can be accomplished without financial support. I am deeply grateful to the Office of Naval Research. The financial support they provided has supported this research throughout the dissertation process including my work, the bioacoustical oceanography workshops through which the data for this dissertation was collected, and through which I received excellent training. This research was also partially funded by the NASA/New York Space Grant Consortium (NASA Grant Number NNG05GH17H), and Shell Oil Summer Support. And to Chuck Greene who

continued to believe in me and in my work even after my world became complicated in a way that hindered my professional progress.

To make this work complete, countless hours were invested by Tracey Steig of Hydroacoustic Technologies, Inc. Seattle, to resurrect data and metadata and answer my questions associated with the 1997 bioacoustical oceanography workshop in Santa Cruz, CA in which he participated in the collection of the acoustic data. Truly, without his help, I would not have been able to reconstruct the metadata required to appropriately interpret the acoustic data underlying the work of Chapter 2. In addition, Peter Wiebe, also present in that workshop, dug through his own records to find his personal logs and photographs of those days at sea, and reconstructed the MOCNESS setup used in that survey more than a decade earlier in order to help me understand the net-collected specimen data underlying the work of Chapter 2. Without the generosity of both Tracey and Peter, my interpretation of the data forming the foundation of the work of Chapter 2 would be far less complete. I am deeply grateful to both of them.

I thank Don Croll, my “blue whale guy” at UC Santa Cruz, who along with his colleagues during the bioacoustics workshop of 1996, tagged the blue whale which provided the opportunity to develop the amazing story of Chapter 3. And I thank him for the enthusiasm he showed when I arrived in his lab to show him an early rendition of what was coming out of the work. And I thank him for his generosity in granting Kelly Newton the time to assist me by locating data and metadata that were instrumental in interpretation of the whale data.

Indeed, I need to thank all the instructors, advisors, crew, and participants of those 1996 and 1997 bioacoustics workshops in Santa Cruz who collected all the data underlying the work of this dissertation.

A special thank you needs to go out to Ian Higginbottom, founder of Myriax Software Pty. Ltd. in Hobart Australia. After seeing my presentation of the early work of Chapter 3 at the joint meeting of the Japanese and American acoustical societies, he and I met for hours to discuss the analytical needs of the data and the analytical capabilities of Echoview, a Myriax software designed for processing echosounder data. At the end of that conversation, he handed me a copy of the software and told me to "go do what you need to do to finish up that Ph.D." The original generosity and support of Ian Higginbottom was continued by Bernd Wechner, Sales Manager for Myriax. I deeply, deeply thank them both. They saved me from spending my time thinking about constructing "if-then" statements in Matlab, and instead allowed me to spend my time thinking about the ecological questions I was trying to answer while their Echoview software did the heavy-lifting of the calculations involving the acoustic data.

A deeply grateful thank you goes out to Chris Pelkie of Cornell University, an amazing teacher with seemingly infinite patience who launched me up the learning curve of Data Explorer. Without his help, I would not have been able to produce the quality data visualizations that help me communicate the findings of this amazing data set. His enthusiasm for scientific visualization, creativity in thinking about communicating through visual methods, and his commitment to my data and my learning are deeply appreciated.

In addition to the support of my scientific growth, Chuck Greene has nurtured other aspects important to me, including teaching. Through his support I have participated in six bioacoustical oceanography workshops held at the Friday Harbor Marine Labs affiliated with the University of Washington on San Juan Island off the coast of Washington. My participation in the workshops moved from student to teaching assistant to instructor. The opportunity to be among a bioacoustical oceanography community for a few weeks each of those summers was a joy. In that space I could "fire on all 4 cylinders". It was a very social setting of intellectual growth, teaching and learning, in an aesthetically beautiful place. To be among a group of instructors, participants, guests all driven by the same goal of advancing our understanding of this work is a deep privilege. And I want to acknowledge the contribution to those experiences made by the staff of the Friday Harbor Marine Labs whether the staff was in the front office, the stockroom, dining, housing, grounds, library, computing technology, or marine operations. Their constant enthusiasm and support of us and of our endeavors for this course with its heavy classroom, computer, and marine operations requirements allowed us to focus on our work at hand.

The other teaching opportunity that Chuck Greene made possible for me was the development of a first-year writing seminar and associated speaker series through the Knight Writing Institute at Cornell. I am deeply grateful for his vision of an integrated learning environment that would provide the students not only with the classroom content, but also the associated seminar series that would bring researchers from across campus "into our classroom", and by opening the series to the campus and surrounding community, bring that knowledge to a much wider audience. His question: "Would you like to create and teach a first-year writing seminar entitled Sustainable Earth, Energy and Environmental Systems? And, oh, by the way, create a

speaker series to go with it?" opened a door of possibility for me, and allowed my brain to lift up out of my dissertation and create in a new way. I am deeply grateful to Chuck and the Knight Writing Institute for that opportunity. And for the fact that that experience brought Kim Todt into my life, first as my TA in the Writing 7100 course, and then as friend. And her son Ewan who made a charming and beautiful hand-drawn cartoon story of krill and whales and dragons as a gift for me at the time of the defense of the work included in this dissertation.


Dragons and Krill
By Ewan
A long, long, long, long, I mean long time ago, when dragons roamed, they loved to eat Krill.
Dude, Krill is awesome!
But guess who else liked Krill, Whales
Indeed
They are yummy in my tummy
As dragons and wales ate more and more krill the krill population was
dying
yesterday
today
Thats a lot less
The wars lasted for many many years
Whales and dragons had battles to get the krill
All this war over me. Thanks a lot!
The war stopped after a new food came for the dragons. HUMANS!
Now only Whales worry the Krill.
Krill!
We want Humans
oh no

And then there is family. Without them I would not be who I am. First I want to thank Denise M. Simoneau. You and your family, both your family of origin and the family you made, have been a refuge of sanity, peace, and love. I carry you deep in my heart. And to that end I thank my brothers Paul and Kenneth, my sisters Patricia and Nancy for their love and patience while my time and attention was diverted elsewhere. And to my sister Tricia and her husband Robert Clark, I am deeply grateful for stepping in with temporary support when factors outside of school overwhelmed my resources. And to my parents Francis P. and Anita B. McGarry: the resonance, form, and structure of my life came from you. I am so deeply grateful. Go with God.

TABLE OF CONTENTS

LIST OF FIGURES

LIST OF TABLES

CHAPTER 1

Background, motivation, and work of others

The Motivation for Studying Zooplankton

Zooplankton are found throughout the world's oceans and are the essential food-web link between primary producers and upper trophic levels in marine ecosystems. For populations that feed directly on zooplankton, such as many species of fish, seabirds, and marine mammals, the abundance and distribution of the zooplankton directly influences the abundance and distribution of these upper trophic-level organisms. However, aggregations of zooplankton are patchy and ephemeral in multiple scales of space (centimeters to kilometers) and time (daily, seasonally, and interannually) (Marine Zooplankton Colloquium I, 1989; Skjoldal *et al.*, 2000; Marine Zooplankton Colloquium II, 2001). Consequently, in order to understand and predict the distributions of the upper trophic-level populations, biological oceanographers seek to understand the highly heterogeneous distributions of zooplankton populations and the mechanisms giving rise to the observed patterns (Marine Zooplankton Colloquium I, 1989; Marine Zooplankton Colloquium II, 2001; Fogarty and Powell, 2002).

From Net Tows to Hydroacoustic Techniques

Our understanding of the species and general distribution of zooplankton arose from examination of the contents of net tow surveys (Wiebe and Benfield, 2003).

However, net tow sampling by its nature provides data on zooplankton distribution and abundance that is too sparse, discrete, and integrative to determine the biological and physical mechanisms that influence the zooplankton patchy distribution and abundance at a scale relevant to predators. To address the need for higher resolution data, remote-sensing hydroacoustic techniques, in which scientific echosounders interrogate synoptic regions with fine-scale sampling, have been developed (Holliday and Pieper, 1995; Medwin and Clay, 1998; Foote and Stanton, 2000; Chu and Wiebe, 2005). A pulse of a sound pressure wave is released into the water, and the proportion of the pressure wave backscattered, or returned to the echosounder, is recorded (Medwin and Clay, 1998). The use of calibrated scientific echosounders (Foote *et al.*, 1987) provide results such that the measurements can be compared among surveys. However, it is the conversion of the measured backscatter into biologically-grounded metrics that provides meaningful information from hydroacoustic surveys.

Predicting Backscatter

The efficiency with which organisms backscatter sound pressure waves, and therefore contribute to the total measured backscatter, is a complex function of the shape and material properties of each individual, the orientation of the individual relative to the incident sound wave, and the size of the animal relative to the wavelength of the acoustic source (Stanton and Chu, 2000, and references therein). The acoustical responsiveness, or target strength, of an organism is strongly influenced by the individual's acoustically dominant material property. The material properties found in zooplankton have been generalized into three broad categories: elastic-shelled (capable of supporting a shear wave), fluid-like (may be thin shelled but does not support a shear

wave, and with a body composition for which the sound speed and density is very similar to that of the surrounding seawater), or gas-filled (capable of resonance) (Stanton *et al.*, 1998b; Foote and Stanton, 2000; Stanton and Chu, 2000). Among the material property categories, the difference in the backscattering strength is succinctly demonstrated by the 19,000-fold difference in target strength measured for a 2-mm-long elastic-shelled strongly scattering gastropod relative to the target strength measured for a 26-mm-long fluid-like weakly scattering salp, on an echo-energy per unit biomass basis at 200 kHz (Stanton *et al.*, 1994; Stanton *et al.*, 1996). Therefore, to appropriately infer the ecologically meaningful metrics of taxon abundance, biomass, or distribution from observed backscatter, an understanding and quantification of the frequency-dependent backscatter characteristics of each taxon is required.

To understand the echo level patterns and variability associated with the backscattering physics of zooplankton, a series of experiments was undertaken (Stanton *et al.*, 1994; Stanton *et al.*, 1996; Stanton *et al.*, 1998c) from which a suite of taxon-specific zooplankton backscattering models was developed (Lavery *et al.*, 2007, and references therein). The models provide a representative quantification of the frequency-dependent backscatter efficiency of individual organisms and consequently, establish the relationship between the remotely-sensed acoustic data and the *in situ* specimens that are collected via net, pump, or video systems.

Employing the Acoustic Models in the Field

The model ensemble by Stanton and colleagues (Stanton *et al.*, 1994; Stanton *et al.*, 1998a; reviewed by Stanton and Chu, 2000; as modified by Lavery *et al.*, 2007) has been field-tested for robustness in prediction of the field-measured acoustic volume

backscatter (Wiebe *et al.*, 1996; Wiebe *et al.*, 1997), and investigated for the applicability of the model ensemble for ground-truthing the remotely-sensed hydroacoustic data (Greene *et al.*, 1998). Individual predictive models for crustacean and gas-bearing taxa were field-tested by targeting layers of enhanced backscatter from relatively homogeneous and mono-specific assemblages (Trevorrow *et al.*, 2005). The results of these studies highlighted opportunities for refinement of the models (Greene *et al.*, 1998; Mair *et al.*, 2005; Trevorrow *et al.*, 2005) and opportunities that identify methodological problems occurring during the *in situ* net sampling (Greene *et al.*, 1998; Mair *et al.*, 2005). In addition, the need to account for physical sources of the field-measured backscatter such as that arising from sound-speed fluctuations associated with physical microstructure was identified (Bucklin *et al.*, 2002). Based on the findings from the application of the models in field and experimental studies, new solutions have been incorporated into the models for estimating the contribution to measured backscatter by physical boundaries (Warren *et al.*, 2003; Warren and Wiebe, 2008; Lavery *et al.*, 2010; Ross and Lavery, 2010; Ross and Lavery, 2012) and by the gas-bearing taxa (Lavery *et al.*, 2007). Extension of the model suite to include backscatter by physical sources expanded the physical settings in which the taxon-specific models can be used. Lavery and colleagues (2007) provide a comprehensive summary of the techniques for interpreting backscatter from a mixed zooplankton assemblage.

Concurrent with the development, testing, and refinement of the ensemble of backscatter models, the models have been used in the service of important ecological questions, such as characterizing the ecosystem context for single-species measurements (Bucklin *et al.*, 2002), identifying the ecological sources of the vertical

pattern of observed backscatter (Benfield *et al.*, 2003) and, after predicting the likely sources of acoustic backscatter, using the results to make inferences concerning the spatial variability in zooplankton biomass (Lawson *et al.*, 2004; Lawson *et al.*, 2008). One consequence of using the suite of models to identify the source of the field-measured total backscatter is the confirmation that the relative intensity of measured backscatter is not necessarily proportional to biomass (Stanton *et al.*, 1994; Wiebe *et al.*, 1996; Benfield *et al.*, 2003; Lawson *et al.*, 2004; Lavery *et al.*, 2007). Therefore when conducting zooplankton surveys, quantifying the relationship between the observed zooplankton assemblage and the field-measured backscatter is required in order to infer biologically meaningful metrics from the observed backscatter.

The Motivation for Investigating Euphausiids in Monterey Bay

In the work presented here, the suite of zooplankton backscattering models is applied in the service of addressing ecological questions in the Monterey Bay Submarine Canyon (MBSC), an ecological setting with unique characteristics. Monterey Bay, California, USA, is an open embayment, ~ 1,200 km^2, located on the eastern boundary of the North Pacific Ocean in the transition zone between the subarctic and equatorial waters of the California Current System (CCS) (Brinton, 1962; Bolin and Abbot, 1963; Hickey, 1979; Lynn and Simpson, 1987; Collins *et al.*, 2003; Breaker, 2005). The continental shelf underlying the Bay is bisected by the MBSC, a large, deep canyon which starts ~ 100 m offshore of Moss Landing, traverses 20 km to the mouth of the bay, where, having reached a depth of ~ 2 km, joins the deep ocean (Skogsberg and Phelps, 1946; Baduini, 1997; Petruncio *et al.*, 1998). The canyon

establishes a broad diversity of habitats within the bay, from shallow near-shore to deep ocean. The richness of habitats, the Bay's location downstream from a nutrient-rich seasonal, eastern-boundary-current upwelling center at Pt. Año Nuevo (Tracy, 1990; Rosenfeld *et al.*, 1994; Ramp *et al.*, 2005), and the presence of the transition zone hydrography and biology, support a highly productive and biologically diverse ecosystem in Monterey Bay (Ryther, 1969; Barber and Smith, 1981; Croll *et al.*, 2005; Ryan *et al.*, 2005). The unique ecological significance of the region was formally recognized by the US Congress in 1992 with the establishment of the Monterey Bay National Marine Sanctuary (MBNMS), which included a congressional mandate to protect the resources within its jurisdiction using a broad, ecosystem-based perspective.

Euphausiids, a pelagic shrimp-like crustacean (Mauchline and Fisher, 1969; Everson, 2000) and a prominent zooplankter in the CCS, Monterey Bay, and the MBSC, is one of the key prey taxa consumed by fish, seabirds, and marine mammals (Ainley *et al.*, 1996; Simard and Lavoie, 1999; Abraham and Sydeman, 2004; Ish *et al.*, 2004; Ballon *et al.*, 2011), thereby contributing to the high productivity of the region. In recognition of the fundamental role of euphausiids in the Monterey Bay ecosystem trophic structure, a ban was placed on the harvest of euphausiids within MBNMS waters. In 2006, the ban was expanded by the Pacific Fishery Management Council to include all species of euphausiids in the west coast waters of the U.S. Exclusive Economic Zone (EEZ). These protection efforts were federally recognized by the issuance of a final rule and Federal regulation in July 2009 which placed all species of euphausiids in the west coast EEZ in the category of "prohibited harvest species" (NOAA, 2009). By this sequence of events, the protection of euphausiids in the west

coast U.S. waters started with the recognition of the critical role of euphausiids as prey in Monterey Bay and its surrounding marine ecosystem.

The Challenge for Hydroacoustic Surveys of Euphausiids in Monterey Bay

In the MBSC, euphausiids are found seasonally in dense, patchy, ephemeral aggregations adjacent to the canyon wall (Barham, 1956; Schoenherr, 1991; Croll *et al.*, 2005). On hydroacoustic echograms, the locations of these aggregations appear as conspicuous regions of intense backscatter. Net samples confirm that the zooplankton assemblage within these layers is dominated by euphausiids, or 'krill', and hence the strongly scattering layers are known as krill sound-scattering layers (SSLs). Biomass of euphausiids within the SSLs is orders of magnitude greater than in regions outside the layers of intense backscatter (Schoenherr, 1991; Marinovic *et al.*, 2002; Croll *et al.*, 2005). Surface concentrations and feeding-dive behavior of stenographic euphausiid-consuming whales are commonly observed to target the regions of intense backscatter (Schoenherr, 1991; Croll *et al.*, 2005), further supporting the co-occurrence of SSLs with dense aggregations of euphausiids in Monterey Bay and its associated canyon.

The association of high krill biomass and intense backscatter has long been noted in the literature in Monterey Bay (Barham, 1956), in Saanich Inlet, British Columbia, Canada (Bary and Pieper, 1970), Oregon, USA (Greenlaw and Pearcy, 1985), Gulf of St. Lawrence, Quebec, Canada (Sameoto, 1976, 1983). Relying on the association of densely aggregated krill with regions of intense backscattering, investigators target the SSLs to estimate krill biomass in Monterey Bay (Schoenherr, 1991; Benson *et al.*, 2002; Marinovic *et al.*, 2002; Croll *et al.*, 2005). In a mixed assemblage of zooplankton such as that found in the SSLs where euphausiids dominate

the biomass, among the fluid-like organisms, euphausiids are the dominant backscatterer at hydroacoustic frequencies commonly used in zooplankton surveys (e.g. 120 kHz and 200 kHz). However, physonect siphonophores, a relatively rare but gas-bearing zooplankter, are a predator of, and co-occur with, euphausiids (Mackie *et al.*, 1987; Robison *et al.*, 1998). The gas-bearing properties of the physonect siphonophores make them extremely efficient backscatterers, disproportionately strong relative to their biomass, at the frequencies used in hydroacoustic surveys targeting the fluid-like euphausiids (Barham, 1963; Stanton *et al.*, 1994; Warren *et al.*, 2001; Benfield *et al.*, 2003; Lavery *et al.*, 2007), thereby requiring that investigators account for the backscattering from siphonophores when executing euphausiid surveys.

Siphonophores

Siphonophores are a cnidarian Order consisting of 170 described species of pelagic, free-swimming, polymorphic, colonial hydrozoans that are widely distributed in the open ocean (Dunn *et al.*, 2005). The colonies are referred to as 'super organisms' (Mackie, 1963) because of their distinctive feature of polyps and medusa, or zooids, which are each homologous to free-living animals but physiologically integrated and genetically identical (Dunn and Wagner, 2006). The specialized functions of the zooids include locomotion, feeding, defense, excretion, or reproduction (Dunn *et al.*, 2005). Based on the presence or absence of the swimming bells that provide locomotion, and the presence or absence of a gas-filled apical organ, the Order is divided into three Sub-orders (Kirkpatrick and Pugh, 1984). Acoustically the two sub-orders of interest are the physonectae and cystonectae for which the gas-filled organ, the pneumatophore, is present. The fluid-like material properties of the zooids and the central stem to which

they are attached do not substantially contribute to backscattering relative to the pneumatophores (Stanton *et al.*, 1998c). However, although small, rare, and inconspicuous, the scattering strength of the gas-filled pneumatophore is one to three orders of magnitude greater than an individual euphausiid (Stanton *et al.*, 1994; Stanton *et al.*, 1996). In Monterey Bay, gas-bearing siphonophores are important predators of euphausiids (Robison *et al.*, 1998) and consequently co-occur with euphausiid aggregations. Allocating backscatter among the taxa, to include the strongly scattering gas-bearing siphonophores, is crucial for acoustically-derived distribution and abundance estimates of the trophically important euphausiid in the MBSC. The goal of apportioning the total measured backscatter among euphausiids and all other taxa is to make the results of acoustic surveys a better proxy for euphausiid distribution and abundance.

The First Goal of This Study

To advance our understanding of the potential to use hydroacoustic methods to survey euphausiids in the MBSC, in the first section of the work reported here we undertook to 1) investigate the skill of the suite of zooplankton backscatter models to reproduce the backscatter measured in the MBSC, 2) apportion the total measured backscatter among taxa in the mixed assemblage, 3) evaluate the relative contribution of euphausiid backscatter and the resulting acoustically-derived estimates of euphausiid abundance, and 4) provide recommendations for using these techniques to survey euphausiids.

Although establishing the distribution and abundance of euphausiids is important, the results take on particular meaning when put into an ecological context.

Therefore, in the second section of this study, we examine the diving behavior of a blue whale foraging on an acoustically surveyed krill aggregation.

The Blue Whales

Blue whales (*Balaenoptera musculus*) are the largest animal on the planet, reaching sizes that exceed 30 m in length, and mass that can well exceed 100 ton (Rice, 1978; Yochem and Leatherwood, 1985). The paradox presented by blue whale ecology is that they support the enormous energetic demands (Rice, 1978) of their great size, mammalian metabolism, and energetic investment of mammalian reproduction by employing an energetically costly lunge-feeding behavior (Brodie, 1993; Acevedo-Gutierrez *et al.*, 2002; Goldbogen *et al.*, 2006) to feed on patchy, ephemeral aggregations of tiny krill (Gaskin, 1982; Croll *et al.*, 2005). The blue whales achieve this success while undertaking an annual basin-scale migration from low-latitude winter mating and breeding grounds to high-latitude productive summer feeding grounds (Mate *et al.*, 1999; Gilpatrick and Perryman, 2008; Block *et al.*, 2011). The high inter-annual variability of the ocean environment (Bograd *et al.*, 2009), and the subsequent high inter-annual variability of the krill abundance and distribution (Chelton *et al.*, 1982; Brinton and Reid, 1986) makes the success of this gigantic sea-going animal particularly intriguing.

Blue whale basin-scale movement and feeding grounds

During the last few decades advances in data-logging tag technologies and satellite telemetry have augmented traditional sight and photo-capture surveys to increase our understanding of the details of the blue whale basin-scale migratory

patterns (Rivers, 1997; Stafford *et al.*, 1999; Block *et al.*, 2003; Burtenshaw *et al.*, 2004; Calambokidis and Barlow, 2004; Moore *et al.*, 2006; Bailey and Thompson, 2009; Calambokidis *et al.*, 2009; Bograd *et al.*, 2010; Block *et al.*, 2011). Members of the eastern North Pacific stock of blue whales range from the Costa Rica Dome, 9° N, to British Columbia and the Gulf of Alaska, 59° N (Reilly and Thayer, 1990; Stafford *et al.*, 1999; Burtenshaw *et al.*, 2004; Bailey and Thompson, 2009; Calambokidis *et al.*, 2009; Matteson, 2009; Block *et al.*, 2011). Although the year-round presence of individuals in some regions has unexpectedly been revealed (Reilly and Thayer, 1990), the presumptive pattern of an annual meridional migration to take advantage of the seasonal prey increases in temperate and polar waters has been confirmed by the new technologies recording the whale's seasonal movements (Bailey *et al.*, 2010; Block *et al.*, 2011).

The timing of the migration of the eastern North Pacific blue whales tracks northward, lagging the northward bloom of primary production, such that the animals arrive at the feeding grounds at peak euphausiid biomass (Burtenshaw *et al.*, 2004; Croll *et al.*, 2005). Two modes of movement during the northward migration are evident in the satellite tracking data; transiting and area-restricted search (ARS) (Kareiva and Odell, 1987; Bailey *et al.*, 2010). Bailey and colleagues (2010) describe the transiting mode as characterized by generally high speed and minimal turning allowing the whales to cover long distances, while the ARS mode is characterized by decreased travel speed and increased turning angles keeping the whales on the feeding grounds for an average of 21 days . The locations where the ARS mode is exhibited suggests preferential targeting of high productivity locations (Reilly and Thayer, 1990; Munger *et al.*, 2009;

Block *et al.*, 2011) which, in turn, are locations that support high prey density (Dolphin, 1987; Piatt and Methven, 1992; Macaulay *et al.*, 1995; Fiedler *et al.*, 1998; Fiedler, 2002). Because these animals return with high inter-annual fidelity to feeding sites, a regularity of threshold density of prey at these sites is suggested (Acevedo-Gutierrez *et al.*, 2002; Bailey *et al.*, 2010). In further support of the notion that the whales target regions reaching a sufficient threshold density of prey, during the strong 1997-1998 El Niño event, which altered krill distribution and abundance in the California Current System, the blue whales of the eastern North Pacific were found in increased numbers in Monterey Bay, and increased numbers farther north than usual (Benson *et al.*, 2002; Burtenshaw *et al.*, 2004). And, again 2005, another year of low prey abundance, found the blue whales responding by traveling farther north (Calambokidis *et al.*, 2009; Bailey *et al.*, 2010). However, the strategies, tactics, and cues by which these animals return to feeding grounds or select feeding grounds farther north when prey aggregations are low, and then locate and exploit krill aggregations of sufficient density are unknown.

Migratory and foraging strategies: a conceptual model

Kenney and colleagues (2001) proposed a multi-scaled, hierarchical, conceptual model of basin-scale whale migratory and foraging strategies. Their work focuses on the western North Atlantic right whale population, a baleen whale that feeds primarily on surface aggregations of copepods in the region of the Gulf of Maine, from Cape Cod to Nova Scotia. However, the concepts in their model can be of use in considering migratory and foraging strategies of the eastern North Pacific blue whale. In both cases, the western North Atlantic right whale and the eastern North Pacific blue whale, winter

in low latitude regions and undertake a northward migration to feeding grounds in the spring and summer (Winn *et al.*, 1986; Mate *et al.*, 1999; Block *et al.*, 2011). The feeding habitats of both populations are specialized and restricted, and located generally in or near continental shelf waters (Baumgartner *et al.*, 2003; Croll *et al.*, 2005; Santora *et al.*, 2012). High-use feeding areas, or locations of extended stops, have been identified within the migration route of each of these populations (Murison and Gaskin, 1989; Mayo and Goldman, 1992; Bailey *et al.*, 2010). However, aggregations of their respective zooplankton prey are patchy and ephemeral in time and space (Mauchline and Fisher, 1969; Beardsley *et al.*, 1996). Once on the feeding grounds, the whales must locate patches of sufficiently high prey density (Wishner *et al.*, 1988; Goldbogen *et al.*, 2011), suggesting, as Kenney and colleagues (2001) propose, that the movements of these whales reflect adaptive responses to the distribution of prey at many scales.

Challenges of characterizing movement of the whales at the scale of its prey field

While the satellite tracking has given us more detail into the timing and movements of the whales through their basin-scale habitat, details of how this predator interacts with its prey field still eludes us. The ocean environment presents special challenges to observing the behavior of blue whales in the context of their krill prey-fields. To collect *in situ* measurements from an undisturbed prey-field, remote-sensing hydroacoustic techniques have been developed. These techniques provide measures of backscatter, a proxy however, for which the conversion to biologically meaningful metrics of biomass and krill density is not trivial (see Chapter 2). In addition, the foraging behavior of the blue whale takes place at depths of 150 to 200 m, the depths of

the dense daytime aggregations of krill (Schoenherr, 1991; Croll *et al.*, 2005). Therefore, to observe the behavior of a feeding blue whale requires a data logger attached to the whale which allows the whale to move freely, undisturbed, while the details of its movements are being recorded. The original loggers used in the 1960s were simple time-depth recorders (TDR) for which time was limited to an hour (Kooyman, 1966). Advances in subsequent decades, particularly with the emergence of microprocessors, efficient power and data storage, and the inclusion of hydrophones and underwater cameras has increased the sophistication, duration, and data collection capabilities (Calambokidis *et al.*, 2002; Kooyman, 2004; Naito, 2004; Goldbogen *et al.*, 2006; Calambokidis *et al.*, 2007; Ropert-Coudert *et al.*, 2010). With the advent of the modern, sophisticated data loggers, research into the metabolic costs of lunge-feeding behavior could begin in earnest.

Energetic costs of feeding dives

Feeding-dive durations for blue whales are substantially shorter than that predicted for their great size (Croll *et al.*, 2001; Acevedo-Gutierrez *et al.*, 2002). For example, from the records of 231 dives executed by 7 blue whales, the longest recorded dive was 14.7 min, whereas the calculated theoretical aerobic dive limit estimated for an animal of that size is 31.2 min, suggestive of a high energetic cost to the lunge-feeding maneuver (Croll *et al.*, 2001). The modern data loggers have made possible a focused effort by Goldbogen and colleagues to investigate the lunge-feeding biomechanics, hydrodynamics, and energetics (Goldbogen *et al.*, 2013; and references therein). From their results, they have developed a model of the metabolic costs of the lunge-feeding

behavior (Goldbogen *et al.*, 2011). They conclude that the lunge-feeding behavior is indeed energetically costly, and therefore limits the time between oxygen-replenishing, breathing events, shortening the dive durations, and thereby limiting the amount of feeding events possible during each dive (Goldbogen *et al.*, 2011). With feeding events limited for each dive, the feeding whale is dependent on the density of its krill prey in order to obtain sufficient energetic gains to cover the costs of the dive and to replenish its stores.

The second goal of this study

The success of the foraging ultimately depends on the success of the whale in locating and exploiting prey patches of sufficient density. In the second part of this study, we have the rare opportunity to investigate the foraging behavior and energetics of an individual blue whale as it exploits the krill SSL along the wall of the MBSC. With this study, we undertook to (1) develop a three-dimensional characterization of the krill sound-scattering layer and place the whale movement within the context of the foraging habitat, (2) using the results of the model developed by Goldbogen and colleagues (2011) and our characterization of the prey field, estimate the foraging efficiency experienced by the whale, and (3) develop hypotheses regarding blue whale foraging decision making in the presence of its foraging habitat.

REFERENCES

Abraham, C. L., and Sydeman, W. J. (**2004**). "Ocean climate, euphausiids and auklet nesting: inter-annual trends and variation in phenology, diet and growth of a planktivorous seabird, Ptychoramphus aleuticus," Marine Ecology-Progress Series **274**, 235-250.

Acevedo-Gutierrez, A., Croll, D. A., and Tershy, B. R. (**2002**). "High feeding costs limit dive time in the largest whales," Journal of Experimental Biology **205**, 1747-1753.

Ainley, D. G., Spear, L. B., and Allen, S. G. (**1996**). "Variation in the diet of Cassin's auklet reveals spatial, seasonal, and decadal occurrence patterns of euphausiids off California, USA," Marine Ecology-Progress Series **137**, 1-10.

Baduini, C. L. (**1997**). "Spatial and temporal patterns of zooplankton biomass in Monterey Bay, California, during the 1991-1993 El Niño, and an assessment of the sampling design," California Cooperative Oceanic Fisheries Investigations Reports **38**, 193-198.

Bailey, H., and Thompson, P. M. (**2009**). "Using marine mammal habitat modelling to identify priority conservation zones within a marine protected area," Marine Ecology-Progress Series **378**, 279-287.

Bailey, H., Mate, B. R., Palacios, D. M. *et al.* (**2010**). "Behavioural estimation of blue whale movements in the Northeast Pacific from state-space model analysis of satellite tracks," Endangered Species Research **10**, 93-106.

Ballon, M., Betrand, A., Lebourges-Dhaussy, A. *et al.* (**2011**). "Is there enough zooplankton to feed forage fish populations off Peru? An acoustic (positive) answer.," Progress in Oceanography **91**, 360-381.

Barber, R. T., and Smith, R. L. (**1981**). "Coastal Upwelling Ecosystems," in *Analysis of Marine Ecosystems*, edited by A. R. Longhurst (Academic Press, New York), pp. 31-68.

Barham, E. G. (**1956**). "The Ecology of Sonic Scattering Layers in the Monterey Bay area, California," in *Biological Sciences* (Stanford University, Palo Alto, CA).

Barham, E. G. (**1963**). "Siphonophores and Deep Scattering Layer," Science **140**, 826-828.

Bary, B. M., and Pieper, R. E. (**1970**). "Sonic-Scattering Studies in Saanich Inlet, British Columbia: A Preliminary Report," in *International Symposium on Biological Sound Scattering in the Ocean*, edited by G. B. Farquhar (Maury Center for Ocean Science, Department of the Navy, Washington, DC, Airlie House Conference Center, Warrenton, VA).

Baumgartner, M. F., Cole, T. V. N., Clapham, P. J. *et al.* (**2003**). "North Atlantic right whale habitat in the lower Bay of Fundy and on the SW Scotian Shelf during 1999-2001," Marine Ecology-Progress Series **264**, 137-154.

Beardsley, R. C., Epstein, A. W., Chen, C. S. *et al.* (**1996**). "Spatial variability in zooplankton abundance near feeding right whales in the Great South Channel," Deep-Sea Research Part II-Topical Studies in Oceanography **43**, 1601-1625.

Benfield, M. C., Lavery, A. C., Wiebe, P. H. *et al.* (**2003**). "Distributions of physonect siphonulae in the Gulf of Maine and their potential as important sources of acoustic scattering," Canadian Journal of Fisheries and Aquatic Sciences **60**, 759-772.

Benson, S. R., Croll, D. A., Marinovic, B. B. *et al.* (**2002**). "Changes in the cetacean assemblage of a coastal upwelling ecosystem during El Niño 1997-98 and La Niña 1999," Progress in Oceanography **54**, 279-291.

Block, B. A., Costa, D. P., Boehlert, G. W. *et al.* (**2003**). "Revealing pelagic habitat use: the tagging of Pacific pelagics program," Oceanologica Acta **25**, 255-266.

Block, B. A., Jonsen, I. D., Jorgensen, S. J. *et al.* (**2011**). "Tracking apex marine predator movements in a dynamic ocean," Nature **475**, 86-90.

Bograd, S. J., Schroeder, I., Sarkar, N. *et al.* (**2009**). "Phenology of coastal upwelling in the California Current," Geophysical Research Letters **36**, 5.

Bograd, S. J., Block, B. A., Costa, D. P. *et al.* (**2010**). "Biologging technologies: new tools for conservation. Introduction," Endangered Species Research **10**, 1-7.

Bolin, R. L., and Abbot, D. P. (**1963**). "Studies on the marine climate and phytoplankton of the central coastal area of California 1954-1960," California Cooperative Oceanic Fisheries Investigations Reports **9**, 23-45.

Breaker, L. C. (**2005**). "What's happening in Monterey Bay on seasonal to interdecadal time scales," Continental Shelf Research **25**, 1159-1193.

Brinton, E. (**1962**). "The Distribution of Pacific Euphausiids," Bulletin of the Scripps Institution of Oceanography of the University of California, La Jolla, California **8**, 51-270.

Brinton, E., and Reid, J. L. (**1986**). "On the effects of interannual variations in circulation and temperature upon euphausiids of the California Current," in *UNESCO Technical Paper Marine Science*, pp. 25-34.

Brodie, P. F. (**1993**). "Noise Generated by the Jaw Actions of Feeding Fin Whales," Canadian Journal of Zoology-Revue Canadienne De Zoologie **71**, 2546-2550.

Bucklin, A., Wiebe, P. H., Smolenack, S. B. *et al.* (**2002**). "Integrated biochemical, molecular genetic, and bioacoustical analysis of mesoscale variability of the euphausiid *Nematoscelis difficilis* in the California Current," Deep-Sea Research Part I-Oceanographic Research Papers **49**, 437-462.

Burtenshaw, J. C., Oleson, E. M., Hildebrand, J. A. *et al.* (**2004**). "Acoustic and satellite remote sensing of blue whale seasonality and habitat in the Northeast Pacific," Deep-Sea Research Part II-Topical Studies in Oceanography **51**, 967-986.

Calambokidis, J., Francis, J., Marshall, G. *et al.* (**2002**). "Underwater Behavior of Blue Whales Using a Suction-cup Attached CRITTERCAM. Final Technical Report. Grant Number: N00014-00-1-0942."

Calambokidis, J., and Barlow, J. (**2004**). "Abundance of blue and humpback whales in the eastern North Pacific estimated by capture-recapture and line-transect methods," Marine Mammal Science **20**, 63-85.

Calambokidis, J., Schorr, G. S., Steiger, G. H. *et al.* (**2007**). "Insights into the underwater diving, feeding, and calling behavior of blue whales from a suction-cup-attached video-imaging tag (CRITTERCAM)," Marine Technology Society Journal **41**, 19-29.

Calambokidis, J., Barlow, J., Ford, J. K. B. *et al.* (**2009**). "Insights into the population structure of blue whales in the Eastern North Pacific from recent sightings and photographic identification," Marine Mammal Science **25**, 816-832.

Chelton, D. B., Bernal, P. A., and McGowan, J. A. (**1982**). "Large-Scale Interannual Physical and Biological Interaction in the California Current," Journal of Marine Research **40**, 1095-1125.

Chu, D. Z., and Wiebe, P. H. (**2005**). "Measurements of sound-speed and density contrasts of zooplankton in Antarctic waters," ICES Journal of Marine Science **62**, 818-831.

Collins, C. A., Pennington, J. T., Castro, C. G. *et al.* (**2003**). "The California Current system off Monterey, California: physical and biological coupling," Deep-Sea Research Part II-Topical Studies in Oceanography **50**, 2389-2404.

Croll, D. A., Acevedo-Gutierrez, A., Tershy, B. R. *et al.* (**2001**). "The diving behavior of blue and fin whales: is dive duration shorter than expected based on oxygen stores?," Comparative Biochemistry and Physiology a-Molecular & Integrative Physiology **129**, 797-809.

Croll, D. A., Marinovic, B., Benson, S. *et al.* (**2005**). "From wind to whales: trophic links in a coastal upwelling system," Marine Ecology-Progress Series **289**, 117-130.

Dolphin, W. F. (**1987**). "Prey Densities and Foraging of Humpback Whales, Megaptera-Novaeangliae," Experientia **43**, 468-471.

Dunn, C. W., Pugh, P. R., and Haddock, S. H. D. (**2005**). "Molecular phylogenetics of the Siphonophora (Cnidaria), with implications for the evolution of functional specialization," Systematic Biology **54**, 916-935.

Dunn, C. W., and Wagner, G. P. (**2006**). "The evolution of colony-level development in the Siphonophora (Cnidaria : Hydrozoa)," Development Genes and Evolution **216**, 743-754.

Everson, I. (ed). (**2000**). *Krill Biology Ecology and Fisheries* (Blackwell Science, Malden MA).

Fiedler, P. C., Reilly, S. B., Hewitt, R. P. *et al.* (**1998**). "Blue whale habitat and prey in the California Channel Islands," Deep-Sea Research Part II-Topical Studies in Oceanography **45**, 1781-1801.

Fiedler, P. C. (**2002**). "The annual cycle and biological effects of the Costa Rica Dome," Deep-Sea Research Part I-Oceanographic Research Papers **49**, 321-338.

Fogarty, M. J., and Powell, T. M. (**2002**). "An overview of the U.S. GLOBEC program," Oceanography **15**, 4-12.

Foote, K. G., Knudsen, H. P., Vestnes, G. *et al.* (**1987**). "Calibration of Acoustic Instruments for Fish Density Estimation: A Practical Guide," in *Cooperative*

Research Report (International Council for the Exploration of the Sea, Copenhagen, Denmark).

Foote, K. G., and Stanton, T. K. (**2000**). "Acoustical Methods," in *ICES Zooplankton Methodology Manual* (Academic Press), pp. 223-258.

Gaskin, D. E. (**1982**). *Ecology of Whales and Dolphins* (Heinemann, London).

Gilpatrick, J. W., and Perryman, W. L. (**2008**). "Geographic variation in external morphology of North Pacific and Southern Hemisphere blue whales (Balaenoptera musculus)," Journal of Cetacean Research and Management **10**, 9-21.

Goldbogen, J. A., Calambokidis, J., Shadwick, R. E. *et al.* (**2006**). "Kinematics of foraging dives and lunge-feeding in fin whales," Journal of Experimental Biology **209**, 1231-1244.

Goldbogen, J. A., Calambokidis, J., Oleson, E. *et al.* (**2011**). "Mechanics, hydrodynamics and energetics of blue whale lunge feeding: efficiency dependence on krill density," Journal of Experimental Biology **214**, 131-146.

Goldbogen, J. A., Friedlaender, A. S., Calambokidis, J. *et al.* (**2013**). "Integrative Approaches to the Study of Baleen Whale Diving Behavior, Feeding Performance, and Foraging Ecology," Bioscience **63**, 90-100.

Greene, C. H., Wiebe, P. H., Pershing, A. J. *et al.* (**1998**). "Assessing the distribution and abundance of zooplankton: a comparison of acoustic and net-sampling methods with D-BAD MOCNESS," Deep-Sea Research Part II-Topical Studies in Oceanography **45**, 1219-1237.

Greenlaw, C. F., and Pearcy, W. G. (**1985**). "Acoustical patchiness of mesopelagic micronekton," Journal of Marine Research **43**, 163-178.

Hickey, B. M. (**1979**). "The California Current system - hypotheses and facts," Progress in Oceanography **8**, 191-279.

Holliday, D. V., and Pieper, R. E. (**1995**). "Bioacoustical Oceanography at High-Frequencies," ICES Journal of Marine Science **52**, 279-296.

Ish, T., Dick, E. J., Switzer, P. V. *et al.* (**2004**). "Environment, krill and squid in the Monterey Bay: from fisheries to life histories and back again," Deep-Sea Research Part II-Topical Studies in Oceanography **51**, 849-862.

Kareiva, P., and Odell, G. (**1987**). "Swarms of predators exhibit "preytaxis: if individual predators use area-restricted search," American Naturalist **130**, 233-270.

Kenney, R. D., Mayo, C. A., and Winn, H. E. (**2001**). "Migration and foraging strategies at varying spatial scales in western North Atlantic right whales: a review of hypotheses," Journal of Cetacean Research and Management **2**, 251-260.

Kirkpatrick, P. A., and Pugh, P. R. (**1984**). *Siphonophores and Velellids* (E.J. Brill Publishing Company, London).

Kooyman, G. L. (**1966**). "Maximum diving capacities of Weddell Seal, *Leptonychotes weddelli*," Science **151**, 1553-1554.

Kooyman, G. L. (**2004**). "Genesis an evolution of bio-logging devices: 1963-2002," Memoirs of the National Institute of Polar Research **58**, 15-22.

Lavery, A. C., Wiebe, P. H., Stanton, T. K. *et al.* (**2007**). "Determining dominant scatterers of sound in mixed zooplankton populations," Journal of the Acoustical Society of America **122**, 3304-3326.

Lavery, A. C., Chu, D. Z., and Moum, J. N. (**2010**). "Measurements of acoustic scattering from zooplankton and oceanic microstructure using a broadband echosounder," ICES Journal of Marine Science **67**, 379-394.

Lawson, G. L., Wiebe, P. H., Ashjian, C. J. *et al.* (**2004**). "Acoustically-inferred zooplankton distribution in relation to hydrography west of the Antarctic Peninsula," Deep-Sea Research Part II-Topical Studies in Oceanography **51**, 2041-2072.

Lawson, G. L., Wiebe, P. H., Ashjian, C. J. *et al.* (**2008**). "Euphausiid distribution along the Western Antarctic Peninsula - Part B: Distribution of euphausiid aggregations and biomass, and associations with environmental features," Deep-Sea Research Part II-Topical Studies in Oceanography **55**, 432-454.

Lynn, R. J., and Simpson, J. J. (**1987**). "The California Current System - the Seasonal Variability of Its Physical Characteristics," Journal of Geophysical Research-Oceans **92**, 12947-12966.

Macaulay, M. C., Wishner, K. F., and Daly, K. L. (**1995**). "Acoustic Scattering from Zooplankton and Micronekton in Relation to a Whale Feeding Site near Georges Bank and Cape-Cod," Continental Shelf Research **15**, 509-537.

Mackie, G. O. (**1963**). "Siphonophores, bud colonies and superorganisms," in *The Lower Metazoa*, edited by E. C. Dougherty (University of California Press, Berkeley), pp. 329-337.

Mackie, G. O., Pugh, P. R., and Purcell, J. E. (**1987**). "Siphonophore Biology," Advances in Marine Biology **24**, 97-262.

Mair, A. M., Fernandes, P. G., Lebourges-Dhaussy, A. *et al.* (**2005**). "An investigation into the zooplankton composition of a prominent 38-kHz scattering layer in the North Sea," Journal of Plankton Research **27**, 623-633.

Marine Zooplankton Colloquium I (**1989**). "Future marine zooplankton research - a perspective," Marine Ecology-Progress Series **55**, 197-206.

Marine Zooplankton Colloquium II (**2001**). "Future marine zooplankton research - a perspective," Marine Ecology-Progress Series **222**, 297-308.

Marinovic, B. B., Croll, D. A., Gong, N. *et al.* (**2002**). "Effects of the 1997-1999 El Niño and La Niña events on zooplankton abundance and euphausiid community composition within the Monterey Bay coastal upwelling system," Progress in Oceanography **54**, 265-277.

Mate, B. R., Lagerquist, B. A., and Calambokidis, J. (**1999**). "Movements of North Pacific blue whales during the feeding season off southern California and their southern fall migration," Marine Mammal Science **15**, 1246-1257.

Matteson, R. S. (**2009**). "The Costa Rica Dome: A study of physics, zooplankton, and blue whales," in *Department of Oceanography*.

Mauchline, J., and Fisher, L. R. (eds). (**1969**). *The Biology of Euphausiids* (Academic Press Inc., New York, NY).

Mayo, C. A., and Goldman, L. (**1992**). "Right whale foraging and the plankton resources in Cape Cod and Massachusetts Bays," in *The Right Whale in the Western North Atlantic: A Science and Management Workshop*, edited by J. Hain (National Marine Fisheries Service, Northeast Fisheries Science Center, Conservation and Utilization Division, Woods Hole, MA).

Medwin, H., and Clay, C. S. (**1998**). *Fundamentals of Acoustical Oceanography* (Academic Press, San Diego).

Moore, S. E., Stafford, K. M., Mellinger, D. K. *et al.* (**2006**). "Listening for large whales in the offshore waters of Alaska," Bioscience **56**, 49-55.

Munger, L. M., Camacho, D., Havron, A. *et al.* (**2009**). "Baleen whale distribution relative to surface temperature and zooplankton abundance off southern California, 2004-2008," California Cooperative Oceanic Fisheries Investigations Reports **50**, 155-168.

Murison, L. D., and Gaskin, D. E. (**1989**). "The Distribution of Right Whales and Zooplankton in the Bay-of-Fundy, Canada," Canadian Journal of Zoology-Revue Canadienne De Zoologie **67**, 1411-1420.

Naito, Y. (**2004**). "New steps in bio-logging science," Memoirs of the National Institute of Polar Research **58**, 50-57.

NOAA (**2009**). "Fisheries Off West Coast States; Coastal Pelagic Species Fishery; Amendment 12 to the Coastal Pelagic Species Fishery Management Plan; Final Rule," in *50 CFR Part 660, Docket No. 071106669-81372-03, RIN 0648-AU26* (National Marine Fisheries Service (NMFS), National Oceanic and Atmospheric Administration (NOAA), Department of Commerce), pp. 33372-33373.

Petruncio, E. T., Rosenfeld, L. K., and Paduan, J. D. (**1998**). "Observations of the internal tide in Monterey Canyon," Journal of Physical Oceanography **28**, 1873-1903.

Piatt, J. F., and Methven, D. A. (**1992**). "Threshold Foraging Behavior of Baleen Whales," Marine Ecology-Progress Series **84**, 205-210.

Ramp, S. R., Paduan, J. D., Shulman, I. *et al.* (**2005**). "Observations of upwelling and relaxation events in the northern Monterey Bay during August 2000," Journal of Geophysical Research-Oceans **110**.

Reilly, S. B., and Thayer, V. G. (**1990**). "Blue whale (Balaenoptera musculus) distribution in the eastern tropical Pacific," Marine Mammal Science **6**, 265-277.

Rice, D. W. (**1978**). "Blue Whale," in *Marine Mammals of Eastern North Pacific and Arctic Waters*, edited by D. Haley (Pacific Search Press, Seattle), pp. 31-35.

Rivers, J. A. (**1997**). "Blue Whale, *Balaenoptera musculus*, vocalizations from the waters off central California," Marine Mammal Science **13**, 186-195.

Robison, B. H., Reisenbichler, K. R., Sherlock, R. E. *et al.* (**1998**). "Seasonal abundance of the siphonophore, *Nanomia bijuga*, in Monterey Bay," Deep-Sea Research Part II-Topical Studies in Oceanography **45**, 1741-1751.

Ropert-Coudert, Y., Beaulieu, M., Hanuise, N. *et al.* (**2010**). "Diving into the world of biologging," Endangered Species Research **10**, 21-27.

Rosenfeld, L. K., Schwing, F. B., Garfield, N. *et al.* (**1994**). "Bifurcated Flow from an Upwelling Center - a Cold-Water Source for Monterey Bay," Continental Shelf Research **14**, 931-964.

Ross, T., and Lavery, A. (**2010**). "Acoustic Detection of Oceanic Double-Diffusive Convection: A Feasibility Study," Journal of Atmospheric and Oceanic Technology **27**, 580-593.

Ross, T., and Lavery, A. C. (**2012**). "Acoustic scattering from density and sound speed gradients: Modeling of oceanic pycnoclines," Journal of the Acoustical Society of America **131**, EL54-EL60.

Ryan, J. P., Chavez, F. P., and Bellingham, J. G. (**2005**). "Physical-biological coupling in Monterey Bay, California: topographic influences on phytoplankton ecology," Marine Ecology-Progress Series **287**, 23-32.

Ryther, J. H. (**1969**). "Photosynthesis and Fish Production in Sea," Science **166**, 72-76.

Sameoto, D. D. (**1976**). "Distribution of Sound Scattering Layers Caused by Euphausiids and Their Relationship to Chlorophyll-a Concentrations in Gulf of St-Lawrence Estuary," Journal of the Fisheries Research Board of Canada **33**, 681-687.

Sameoto, D. D. (**1983**). "Euphausiid Distribution in Acoustic Scattering Layers and Its Significance to Surface Swarms," Journal of Plankton Research **5**, 129-143.

Santora, J. A., Field, J. C., Schroeder, I. D. *et al.* (**2012**). "Spatial ecology of krill, micronekton and top predators in the central California Current: Implications for defining ecologically important areas," Progress in Oceanography **106**, 154-174.

Schoenherr, J. R. (**1991**). "Blue Whales Feeding on High-Concentrations of Euphausiids around Monterey Submarine-Canyon," Canadian Journal of Zoology-Revue Canadienne De Zoologie **69**, 583-594.

Simard, Y., and Lavoie, D. (**1999**). "The rich krill aggregation of the Saguenay - St. Lawrence Marine Park: hydroacoustic and geostatistical biomass estimates, structure, variability and signficance for whales," Canadian Journal of Fisheries and Aquatic Sciences **56**, 1182-1197.

Skjoldal, H. R., Wiebe, P. H., and Foote, K. G. (**2000**). "Sampling and experimental design," in *Zooplankton Methodology Manual*, edited by R. Harris, P. H. Wiebe, J. Lenz, H. R. Skjoldal, and M. Huntley (Elsevier Academic Press, New York), pp. 33-53.

Skogsberg, T., and Phelps, A. (**1946**). "Hydrography of Monterey Bay, California, Thermal Conditions, Part II (1934-1937)," Proceedings of the American Philosophical Society **90**, 350-386.

Stafford, K. M., Nieukirk, S. L., and Fox, C. G. (**1999**). "An acoustic link between blue whales in the eastern tropical Pacific and the northeast Pacific," Marine Mammal Science **15**, 1258-1268.

Stanton, T. K., Wiebe, P. H., Chu, D. Z. *et al.* (**1994**). "On Acoustic Estimates of Zooplankton Biomass," ICES Journal of Marine Science **51**, 505-512.

Stanton, T. K., Chu, D. Z., and Wiebe, P. H. (**1996**). "Acoustic scattering characteristics of several zooplankton groups," ICES Journal of Marine Science **53**, 289-295.

Stanton, T. K., Chu, D. Z., and Wiebe, P. H. (**1998a**). "Sound scattering by several zooplankton groups. II. Scattering models," Journal of the Acoustical Society of America **103**, 236-253.

Stanton, T. K., Chu, D. Z., and Wiebe, P. H. (**1998b**). "Ray Solutions to Sound Scattering by Complex Bodies: Application to Zooplankton," in *New Perspectives on Problems in Classical and Quantum Physics: Acoustic propagation and scattering, electronic scattering*, edited by H. Uberall, P. P. Delsanto, and A. W. Saenz (Gordon and Breach Science Publishers).

Stanton, T. K., Chu, D. Z., Wiebe, P. H. *et al.* (**1998c**). "Sound scattering by several zooplankton groups. I. Experimental determination of dominant scattering mechanisms," Journal of the Acoustical Society of America **103**, 225-235.

Stanton, T. K., and Chu, D. Z. (**2000**). "Review and recommendations for the modelling of acoustic scattering by fluid-like elongated zooplankton: euphausiids and copepods," ICES Journal of Marine Science **57**, 793-807.

Tracy, D. E. (**1990**). "Source of cold water in Monterey Bay observed by AVHRR satellite imagery," (Naval Postgraduate School, Monterey, California).

Trevorrow, M. V., Mackas, D. L., and Benfield, M. C. (**2005**). "Comparison of multifrequency acoustic and *in situ* measurements of zooplankton abundances in

Knight Inlet, British Columbia," Journal of the Acoustical Society of America **117**, 3574-3588.

Warren, J. D., Stanton, T. K., Benfield, M. C. *et al.* (**2001**). "*In situ* measurements of acoustic target strengths of gas-bearing siphonophores," ICES Journal of Marine Science **58**, 740-749.

Warren, J. D., Stanton, T. K., Wiebe, P. H. *et al.* (**2003**). "Inference of biological and physical parameters in an internal wave using multiple-frequency, acoustic-scattering data," ICES Journal of Marine Science **60**, 1033-1046.

Warren, J. D., and Wiebe, P. H. (**2008**). "Accounting for biological and physical sources of acoustic backscatter improves estimates of zooplankton biomass," Canadian Journal of Fisheries and Aquatic Sciences **65**, 1321-1333.

Wiebe, P. H., Mountain, D. G., Stanton, T. K. *et al.* (**1996**). "Acoustical study of the spatial distribution of plankton on Georges Bank and the relationship between volume backscattering strength and the taxonomic composition of the plankton," Deep-Sea Research Part II-Topical Studies in Oceanography **43**, 1971-2000.

Wiebe, P. H., Stanton, T. K., Benfield, M. C. *et al.* (**1997**). "High-frequency acoustic volume backscattering in the Georges Bank coastal region and its interpretation using scattering models," IEEE Journal of Oceanic Engineering **22**, 445-464.

Wiebe, P. H., and Benfield, M. C. (**2003**). "From the Hensen net toward four-dimensional biological oceanography," Progress in Oceanography **56**, 7-136.

Winn, H. E., Price, C. J., and Sorensen, P. W. (**1986**). "The Distributional Biology of the Right Whale (*Eubalaena glacialis*) in the Western North Atlantic," Reports of the International Whaling Commission **Special Issue 10**, 129-138.

Wishner, K., Durbin, E., Durbin, A. *et al.* (**1988**). "Copepod Patches and Right Whales in the Great South Channel Off New-England," Bulletin of Marine Science **43**, 825-844.

Yochem, P. K., and Leatherwood, S. (**1985**). "Blue whale (*Baleaenoptera musculus*) (Linnaeus, 1758)," in *Handbook of marine mammals*, edited by S. H. Ridgway, and R. J. Harrison (Academic Press, London), pp. 193-240.

CHAPTER 2

Relative contributions of euphausiids and siphonophores to the measured acoustic backscatter from krill sound-scattering layers in the Monterey Bay Submarine Canyon

ABSTRACT

The krill sound-scattering layers (SSLs) commonly observed adjacent to the walls of the Monterey Bay Submarine Canyon provide an important source of nutrition for blue whales during their late summer migration on the California coast. The SSL, although dominated by krill biomass, includes a diverse assemblage of zooplankton taxa. This study was undertaken to investigate the relative contribution to acoustic backscatter by the taxa present in the assemblage. Zooplankton scattering models, parameterized with size and abundance data from net samples collected in the krill SSLs, were used to predict the expected backscatter at 120 and 200 kHz. Our results demonstrate that although euphausiids dominate the biomass in the krill SSLs, gas-bearing siphonophores substantially contribute to the acoustic backscatter measured at these two frequencies. We conclude that failure to account for the contribution of siphonophores to the backscatter measured during acoustic surveys of krill SSLs will

result in overestimates of euphausiid abundance and the nutritional quality of these SSLs to foraging blue whales.

INTRODUCTION

The Monterey Bay Submarine Canyon (MBSC) is recognized as an important feeding ground for blue whales and other predators that rely on euphausiids as their principal source of nutrition (Schoenherr, 1991; Yen *et al.*, 2004; Croll *et al.*, 2005). The euphausiids, a very small shrimp-like order of crustaceans (Mauchline and Fisher, 1969), are commonly found in dense daytime aggregations adjacent to the walls of the submarine canyon (Schoenherr, 1991; Croll *et al.*, 2005). When studied with high-frequency echosounders, these daytime aggregations appear on echograms as conspicuous layers of intense acoustic backscatter (Barham, 1956; Schoenherr, 1991; Marinovic *et al.*, 2002; Croll *et al.*, 2005). Because the biomass in these layers is dominated by euphausiids, these acoustically conspicuous regions are commonly referred to as krill sound-scattering layers (SSLs).

Relying on the association of the high biomass of krill and the strong backscattering layers, investigations in the Bay have used high-frequency echosounders to detect krill SSLs and estimate the numerical abundance of euphausiids within them (Schoenherr, 1991; Marinovic *et al.*, 2002; Croll *et al.*, 2005). Although it is widely recognized that a mixed zooplankton assemblage comprises these krill SSLs (Barham, 1956; Schoenherr, 1991; Marinovic *et al.*, 2002), methods to attribute the observed backscatter among the taxa present have not been made explicit. Without a method to apportion the observed backscatter, an assumption that all backscatter is attributable to euphausiids would not result in large biases in the acoustic-derived estimates of euphausiid abundance if all organisms contributing to the acoustic backscatter in these

layers are characterized as fluid-like, weak sound scatterers as are the euphausiids. However, there is ample evidence that physonect siphonophores, which are strong sound scatterers due to the presence of gas-filled pneumatophores, commonly co-occur with euphausiids (Pickwell *et al.*, 1970; Mackie, 1985), including *Nanomia bijuga* the most commonly observed gelatinous animal and year-round resident in Monterey Bay (Robison *et al.*, 1998).

The backscattering efficiency, or target strength, of an organism is a complex, frequency-dependent response to the animal's size, shape and orientation, and the contrast of the density and sound speed characteristics of each animal relative to that of its seawater medium (Stanton and Chu, 2000). Consequently, the physonect siphonophore, a polymorphic coelenterate with a gas-bearing float, is an organism with strongly scattering material properties (Stanton *et al.*, 1996, 1998a; Stanton *et al.*, 1998b). The structure of the float, the pneumatophore, includes an inner compartment, the pneumatocyst, separated from the outer wall by a void (Totton, 1965). It is the gas-bearing inner pneumatocyst, filled mainly with carbon monoxide (Pickwell *et al.*, 1964), that is acoustically important, whereas the remainder of the organism with "jelly"-like material properties not so different from its seawater medium contributes little to overall scattering (Stanton *et al.*, 1998a; Stanton *et al.*, 1998b). Relative to the gas-filled pneumatophores, the euphausiids with fluid-like material properties are weak scatterers (Stanton *et al.*, 1994). Therefore, although euphausiids dominate the biomass in these krill SSLs, one must be cautious in assuming a direct relationship between the intensity of acoustic backscatter and the abundance of euphausiids (Stanton *et al.*, 1994; Wiebe *et al.*, 1996; Benfield *et al.*, 2003; Lawson *et al.*, 2004; Lavery *et al.*, 2007).

Failure to account for the presence of only a few strongly scattering organisms within the krill SSLs can bias the results and lead to significant overestimates of euphausiid abundance. Hence, the question addressed in this study is how to best employ acoustic techniques to survey krill in the mixed assemblages that constitute the krill SSLs in the Monterey Bay Submarine Canyon.

In order to employ acoustic methods to quantify the abundance and distribution of euphausiids, a technique is needed to apportion the backscatter between the abundant, but weakly sound-scattering euphausiids and the rare, but strongly sound-scattering gas-bearing siphonophores. In this study, we investigate the feasibility of using a suite of sound-scattering models to quantitatively establish the relationship between acoustic backscatter and the biological properties of the individuals sampled from the SSL, solving the forward problem (Wiebe *et al.*, 1997; Greene *et al.*, 1998), and using the results to apportion backscatter measured from the SSL among the taxa.

METHODS

Survey and Sampling Locations

Monterey Bay (36.76° N, 122.0° W) is an open embayment on the central California continental shelf; its mouth measures 40 km in width between Point Santa Cruz and Point Piños. The Monterey Bay Submarine Canyon bisecting the shelf underlying the bay starts ~ 100 m offshore of Moss Landing, CA and traverses 20 km west across the Bay where the canyon joins the deep ocean at a depth of ~ 2 km (Skogsberg, 1936; Baduini, 1997). A hydroacoustic survey of the canyon was

conducted August 6-9, 1997 aboard the RV Roger Revelle. At eight locations, a Multiple Opening Closing Net and Environmental Sensing System (MOCNESS) (Wiebe *et al.*, 1985) was deployed from the stern of the ship to sample zooplankton concurrent with the acoustic backscatter measurements. We analyzed data from three of the eight sampling sites; Tows 5, 9, and 10 (Figure 2.1). At all three sites, the net sampling targeted an intense daytime krill SSL that forms adjacent to the canyon wall between 100 m and 250 m depth. Environmental data, including conductivity, temperature, and depth (CTD), were concurrently collected at net sampling sites by environmental sensors attached to the MOCNESS frame.

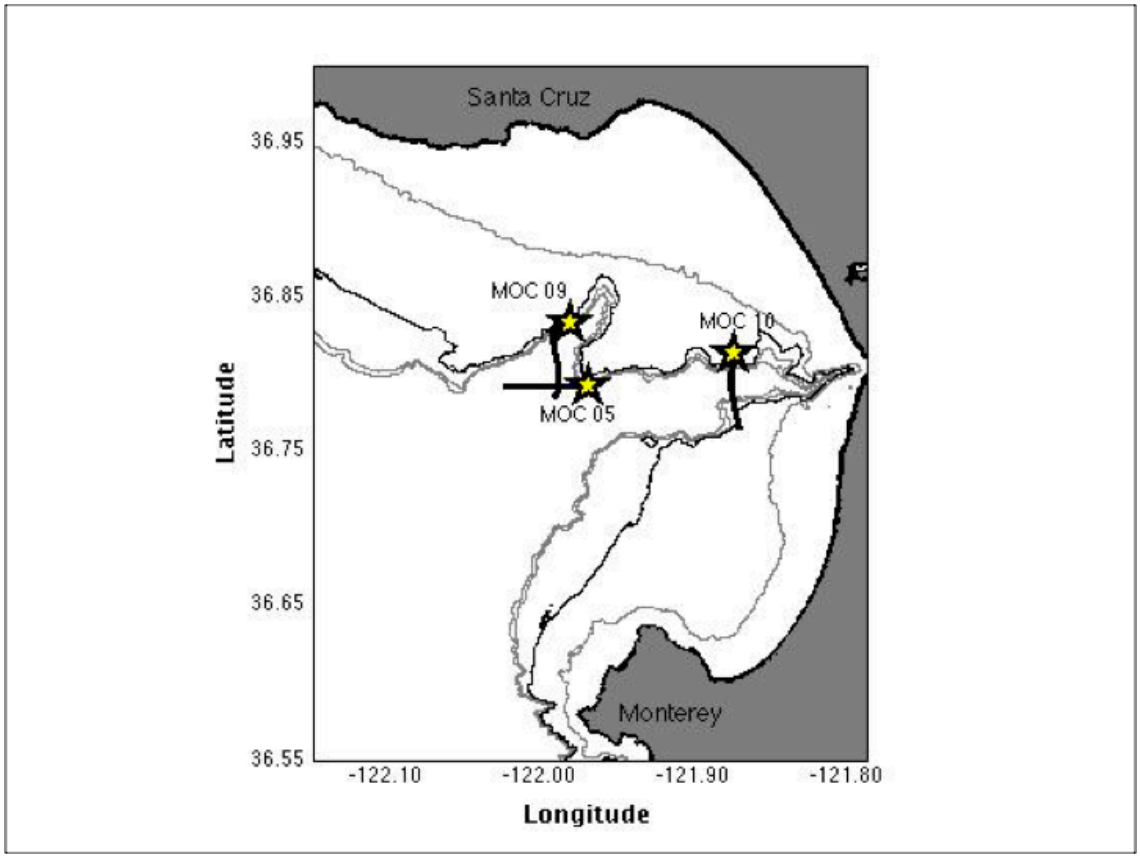

FIGURE 2.1: MOCNESS Zooplankton Sampling Locations
Monterey Bay Submarine Canyon, California. Stars indicate start location of daytime tows used in this study. Contours: 0 to 200 m in 50 m intervals. 0 and 100 m emphasized in black.

Acoustic Survey Methods

Acoustic survey data were collected using Hydroacoustic Technology Inc. (HTI Seattle, WA) Model 244 split-beam echosounders operating at 120 and 200 kHz. The 120- and 200-kHz transducers with nominal beam widths of 3° and 6°, respectively, were mounted on a tow body deployed ~ 4 m below the surface. Acoustic data were recorded starting 1 m from the face of the transducer to eliminate near-field effects. A 5 msec, 10 kHz-window, frequency-modulated (FM)-slide chirp signal (Ehrenberg and Torkelson, 2000) was produced by each transducer sequentially at a rate of one ping per second. A matched filter was applied to the signal to enhance the signal-to-noise ratio and extend the depth range of usable data (Stanton *et al.*, 1998b; Ehrenberg and Torkelson, 2000). The matched filtering resulted in an effective pulse length of 0.18 msec (J. Ehrenberg, personal communication), with a signal-to-noise enhancement of 28 times over a conventional, continuous-wave signal for the equivalent vertical resolution of 0.135 m (Ehrenberg and Torkelson, 2000). All volume backscattering strengths are reported in units of dB re 1 m^{-1}.

During the net tows, the acoustic survey data were echo integrated over 15 s intervals, yielding a horizontal resolution of ~ 15 m at the 2-knot average speed of the ship. The echo-integrated data were resolved vertically in 1-m depth bins starting 5 m from the surface and extending to 230 m in depth. Spurious position data recorded in the acoustic data acquisition file was corrected using the Global Positioning System (GPS) data recorded in the ship's underway position file.

Because the transducers were deployed from a towed platform rather than hull-mounted, and the ship speed was slowed from 8 knots to 2 knots during the net tows,

the operational depth of the acoustic tow-body platform was variable. To confirm the depths inferred from the acoustic record, the bathymetry along the shiptrack was extracted from a 25-m resolution bathymetric database (Monterey Bay Aquarium Research Institute, Moss Landing, CA) and compared to the bathymetric depth recorded by the hydroacoustic system. Depth adjustments of 1 to 2 meters were made accordingly.

Due to a failure in the cable connector for the 120-kHz transducer near the end of day three of this four-day cruise, only one frequency, 200 kHz, was available for some parts of this analysis. Where available, both the 120 kHz and 200 kHz data were used.

MOCNESS Sampling Methods

Zooplankton sampling was conducted with a 1-m^2 MOCNESS (Wiebe *et al.*, 1985), equipped with nine 335-μm mesh nets. The first net (Net 0), an integrated sample collected on descent from the surface to ~ 250 m for each tow, was not used in this study. Nets 1 through 8 were used to collect stratified samples from ~ 250 m on ascent to the surface, with the two deepest nets (Nets 1 and 2) sampling ~ 50 m intervals and all subsequent nets sampling ~ 25 m intervals. The Environmental-Sensing System (ESS) instruments attached to the net frame recorded time, conductivity, temperature, pressure, salinity, volume filtered, and net opening and closing depths at 4-s intervals. Ship position in latitude and longitude was concurrently recorded from the shipboard GPS.

Net samples were split into halves using a Folsom plankton splitter (McEwen *et al.*, 1954) while at sea. One half was preserved in 95% ethyl alcohol for a separate molecular study (Jarman *et al.*, 2000; Bucklin *et al.*, 2007), and one half was preserved in 10% buffered formalin in seawater for the biovolume (Wiebe *et al.*, 1975; Wiebe, 1988) and silhouette analyses in this study. Net samples from Tows 5, 9, and 10 were subsampled and analyzed for length frequency distribution for twenty-eight taxa using the standard silhouette photographic methods (Davis and Wiebe, 1985; Foote, 2000; Little and Copley, 2003). Net samples from Tow 5 were subjected to a more detailed analysis specific to characterizing the sound-scattering properties of gas-bearing siphonophores.

The size of the gas-filled inclusions of the siphonophores was characterized using the size of the pneumatocyst, rather than the larger pneumatophore size measurable with the silhouette method. The length and width dimensions of both the pneumatocysts and pneumatophores from the Tow 5 net samples were measured using a microscope. The microscopically determined conversion from pneumatophore length to pneumatocyst length ($r=0.78$), and pneumatocyst length-to-width ratio ($r=0.76$) were assumed to be representative for gas-bearing siphonophores collected in Tows 9 and 10. The average volume of the estimated pneumatocyst sizes (Tow 5: 1.47 mm^3, Tow 9: 1.31 mm^3, Tow 10: 1.35 mm^3) fell within the range of fresh specimens of *Nanomia bijuga* found at the San Diego Trough, 0.25 mm^3 to 2.5 mm^3 (Pickwell *et al.*, 1964). Recognizing that the measurements were made on preserved, deflated pneumatophores, the contribution to total backscatter by the rare, but strongly scattering gas-bearing siphonophores may be greater than that calculated in this study.

Euphausiid length measurements as determined from the silhouette procedures required conversion to the 'acoustic length' requisite for the backscatter models. The length measurement in the silhouette procedure corresponds to the euphausiid standard length 3 (SL3), defined by Mauchline (1980) as "the lateral distance between the base of the eye-stalk and the posterior margin of the sixth abdominal segment". The acoustic length is defined as "(the lateral distance) from the anterior of the eye to the end of the sixth abdominal segment" (Lawson *et al.*, 2008). Measurements of the SL3 and acoustic lengths were made on 60 individuals from the Tow 5 aliquot sample for Nets 1 and 2, and a conversion factor of 1.09 was determined. This conversion factor was applied to all euphausiid SL3 lengths for subsequent backscatter modeling.

For all taxa except euphausiids and the gas-bearing portion of the siphonophores, length-to-width ratios were based on values from the literature (Table 2.1). For euphausiids, the average body length-to-width ratio was determined as the mean ratio of acoustic length to width measured for 60 specimens from the Tow 5 net samples. The pneumatocyst length-to-width ratio for gas-bearing siphonophores was determined as the mean ratio measured for all specimens from the Tow 5 net samples as described above. Unmeasured parameters, including orientation distributions as well as sound-speed contrast (g) and density contrast (h) of the organisms relative to the surrounding seawater, were based on values from the literature (Table 2.1).

Table 2.1: Scattering models and parameters for backscattering prediction.
Legend appears at the end of the table.

Table 2.1 (Continued) Target zooplankton taxa and potentially acoustically important taxa.

TAXA	scattering model	Length-to-Width ratio β_D**	Orientation (Mean, STD)	Density Contrast (g)	Sound Speed Contrast (h)
TARGET TAXA and related					
euphausiids*	DWBA uniformly bent cylinder	8.2[b]	(0, 30)[e]	1.038[f]	1.041[f]
decapod shrimp and mysids	DWBA uniformly bent cylinder	5.3576[c]	(20, 20)[a]	if (L)>25; g = 5.485e-4 *nanmean(L)+1.002; else h = 1.0157; end;[a]	if (L)>25; h = 5.942e-4 *nanmean(L)+1.004; else h = 1.0189; end;[a]
TAXA: POTENTIALLY ACOUSTICALLY IMPORTANT (gas-bearing, elastic shelled)					
siphonophore – pneumatophores*	hybrid fluid-filled sphere	[d]	[d]	0.0011[h]	0.225[h]
pteropod – limacina*	spherical elastic shell	[d]	[d]	[d] r is hard coded so no g r = 0.5[i]	[d] r is hard coded so no h r = 0.5[i]
fish larvae	DWBA uniformly bent cylinder	4.0	(0, 30)[g]	1.03[g]	1.03[g]
medusae*	DWBA two prolate spheroidal surfaces	2	(0, 20)	1.02[a]	1.02[a]

Table 2.1 (Continued) Numerically abundant taxa.

TAXA	scattering model	Length-to-Width ratio β_D**	Orientation (Mean, STD)	Density Contrast (g)	Sound Speed Contrast (h)
TAXA: NUMERICALLY ABUNDANT					
siphonophore – bracts and nectophores	fluid sphere	[d]	[d]	1.02[a]	1.02[a]
amphipods	DWBA uniformly bent cylinder	3.0021[a]	(0, 30)[a]	1.058[a]	1.058[a]
copepods*	DWBA prolate spheroid	2.5497[a]	(0, 30)[g]	1.02[a]	1.058[a]
chaetognaths	DWBA uniformly bent cylinder	17.151[a]	(0, 30)[a]	1.03[a]	1.03[a]
crustacean larvae	DWBA uniformly bent cylinder	2.5497[a]	(0, 30)[a]	1.058[a]	1.058[a]
eggs	elastic shell	[d]	[d]	0.979[a] used to calculate r	1.017[a] used to calculate r
larvacean	DWBA uniformly bent cylinder	1.83	(0, 30)	1.03	1.03
ostracod	DWBA uniformly bent cylinder	2.5497[a]	(0, 30)[a]	1.03[a]	1.03[a]
polychaets	DWBA uniformly bent cylinder	17.151[a]	(0, 30)[a]	1.03[a]	1.03[a]
pteropod - gymnosome	DWBA uniformly bent cylinder	1.83[a]	(0, 30)[a]	1.03[a]	1.03[a]
radiolarian	high-pass fluid sphere	[d]	[d]	2.147[g]	3.979[g]
salp*	DWBA uniformly bent cylinder	4.0[a]	(0, 30)[a]	1.0041[a]	1.0041[a]

Table 2.1 (Continued) Legend

*	model validation: Asterisks (*) indicate those models that have been validated through comparisons of model predictions to laboratory measurements of scattering from the animal of interest; elsewhere, models were deemed appropriate on the basis of what is known about the animal's structure, but not on experimental verifications. (from: Lawson *et al.,* 2004)
**	length-to-width: reported at length-to-diameter (β_D) not to be confused with length-to-radius (β from Stanton *et al.,* 1998a) that used in modeling ($2*(\beta_D)$)
a	Lavery e*t al.,* (2007): Table 1 and text.
b	Measured this study. Note: The 8.2 is the β_D for euphausiids after conversion from silhouette measured length (SL3) to acoustic length.
c	NOTE: these were values encoded in the models. As there was an order of magnitude less of shrimp and mysids relative to euphausiids, these parameters were accepted.
d	Parameter not applicable for modeling this taxa.
e	Lawson *et al.,* (2006) in situ measurements for *Euphausia superba*. (Laboratory measurements for *E pacifica* by Miyashita *et al*., (1996) demonstrates swimming angle is dependent on swimming speed.)
f	Mikami *et al.,* (2000) E pacifica density (g) and sound speed (h) contrasts measured on live animals. Density contrast (g) used here (1.038) is the average of their findings for July 1999 (1.039) and September 1999 (1.037). Sound speed contrast (h) used here (1.041) is the average of their findings for July 1999 for temperature ranges 8°C through 10°C.
g	Lawson *et al.,* (2004): Table 1
h	A. Lavery personal communication. Values for g and h reported elsewhere in the literature (0.0022 and 0.22 respectively) are for air (e.g. Stanton *et al.,* 1998a). Values used here are for carbon monoxide (content of pneumatocyst per Pickwell *et al.,* 1964).
i	Stanton *et al.,* (1994)

Specimens from twenty-eight taxa were digitized and counted in the samples. Seventeen taxa found at the depths of interest, 100 m to 250 m, were identified as acoustically important and therefore included in the forward problem calculations. Taxa qualified as acoustically important by meeting any of the following criteria, (1) a numerical abundance greater than 1 m^{-3}, (2) the body includes strongly backscattering material properties, such as gas-bearing or hard-shelled taxa, or (3) euphausiids, the taxa of interest, and related, such as shrimp and mysids.

Predicting Acoustic Backscatter from Zooplankton

We used idealized models developed by Stanton and colleagues (Stanton *et al.*, 1994; Stanton *et al.*, 1998a; reviewed by Stanton and Chu, 2000; as modified by Lavery *et al.*, 2007): to predict the acoustic characteristics associated with three general types of sound-scattering zooplankton: (1) strongly scattering, hard elastic-shelled organisms, (2) strongly scattering, gas-filled organisms, and (3) weakly scattering, fluid-like organisms. Simplified shapes corresponding to bent-cylinders, spheroids, and ellipsoids were used in the idealized models (Table 2.1). All calculations were made using the linear forms of the equations for both the backscattering from individual organisms, the backscattering cross-section with units of m^2, and backscattering from the specimens in a volume, the backscattering coefficient with units of m^2/m^3, hereafter referred to as σ_{bs} and s_v, respectively. The results were converted to the logarithmic forms of target strength (TS) with units of decibel (dB) relative to 1 m^2 and mean volume backscattering strength (S_v) with units of dB relative to 1 m^{-1}, respectively, using the following relationships (MacLennan *et al.*, 2002):

$$TS = 10 * log_{10}(\sigma_{bs})$$ EQUATION 2.1

$$S_v = 10 * log_{10}(s_v)$$ EQUATION 2.2

Using the sound-scattering model appropriate for each taxonomic group (Table 2.1), the taxon-specific backscattering cross-section (σ_{bs}) at 120 and 200 kHz was calculated for each of the specimens measured. The backscattering cross-sections were summed within each taxon for each frequency and scaled by the appropriate aliquot fraction and the volume of water filtered by the net as recorded by the MOCNESS data acquisition system. Thus, the summed total σ_{bs} predicted for each taxon at each frequency estimated the total biologically associated volume backscattering coefficient (s_v) at each frequency for each net. This procedure to estimate the total volume backscattering coefficient (s_v), in units of m^2/m^3, from all targets within the sampled volume is summarized in its general form by the following equation (Lavery *et al.*, 2007):

$$s_v(f_q, d_k) = \frac{1}{V_k} \sum_{i=1}^{N_k} \sum_{j=1}^{M_k} \left\langle \sigma_{bs}^{ij}\left(f_q, d_k, \psi_{ij}\right) \right\rangle$$ EQUATION 2.3

where f_q is the frequency, V_k is the volume of water sampled in the depth range d_k, N_k is the number of zooplanktonic organisms of a particular taxon in the depth range d_k, M_k is the number of zooplanktonic taxa in the depth range d_k, and $\langle \sigma_{bs}^{ij}(f_q, d_k, \psi_{ij}) \rangle$ is the backscattering cross section of each individual of size i, taxon j, at frequency f_q, in the depth of range d_k. The term $\langle ... \rangle$ represents an average over angles of orientation. The ψ_{ij} includes the dependence of σ_{bs} on a number of taxon-specific parameters not

explicitly written into the equation, such as shape and material properties. All parameters are assumed to be constant for all individuals of a given taxon, other than size. Multiple sources of scattering in the same sampling volume are accounted for by assuming their contributions add incoherently.

The backscattering model for the gas-bearing portion of the siphonophores incorporates two assumptions biologically consistent with *Nanomia bijuga*, the most abundant siphonophore in Monterey Bay (Robison *et al.*, 1998). The model prediction incorporates a resonance damping effect imparted by the tissue surrounding the gas bearing pneumatocyst (Lavery *et al.*, 2007). In addition, the size of the gas-bearing pneumatocyst was assumed equal to the size measured at the surface regardless of the depth at which the specimen was captured, and consequently the density and sound speed contrast to the surrounding seawater was adjusted to account for gas density within the pneumatocyst that was accordingly secreted by the animal to equalize the pressure within the pneumatocyst with the linearly increasing water pressure with depth (Benfield *et al.*, 2003). This parameterization is consistent with *N. bijuga* physiology that demonstrates that the pneumatophore is a hydrostatic organ required for depth-control of the animal (Mackie *et al.*, 1987), and is consistent with supporting observations of no apparent depth dependence of the radii of the measured pneumatophores (Pickwell, 1970; Benfield *et al.*, 2003).

In the absence of high-resolution vertical microstructure data from which to predict a contribution to the total observed volume backscatter from physical sources (Lavery *et al.*, 2003; Lavery *et al.*, 2007), seawater density profiles and the hydroacoustic echograms were visually inspected for evidence of potentially significant

contributions to the observed backscatter by hydrographic microstructure. The density profiles were calculated from the temperature, salinity, and pressure data recorded in the MOCNESS data acquisition files. Unstable or nearly vertical sections in the density profiles were absent in the depth range of interest, 100 m to 250 m, as was any visible evidence of internal waves in the echograms. In the absence of any visible evidence of physical microstructure, all volume backscatter was assumed to be biological in origin. Any bias introduced in the prediction of total volume backscattering strength is assumed negligible or generally constant.

Comparing Model-Predicted with Observed Backscatter

The model-predicted volume backscattering strengths for each net were examined for reasonableness relative to the observed. The observed backscatter was defined as the backscatter recorded from the echogram region delimited by a parallelogram for which the track of the net system through the water column served as the centerline. The track of the net system was co-located to the acoustic data by calculating the 'setback' of the towed net system relative to the physical location of the transducers. Given the uncertainties inherent in the sampled geometry and placement of the nets relative to the hydroacoustic data, we tested the sensitivity of the observed total volume backscattering strength for each net by systematically shifting the net sampling placement relative to the hydroacoustic echogram and recalculated the observed total volume backscattering strengths. Additionally, any nets for which the model-predicted and the observed volume backscattering strength differed by more than 10 dB were investigated for sources of data quality issues.

The model results were tested for the sensitivity of total predicted volume backscattering strength (S_v) to the presence of the pneumatocysts and to potential net avoidance by euphausiids or siphonophores. The models were run excluding the pneumatocysts entirely and then run with sequentially increasing multiples of the frequency distributions measured from the net samples. The abundance factors tested, using the size distribution from the measured samples, were 0x, 1x, 2x, 3x, 4x, and 5x. To test the sensitivity to additions of single pneumatocysts, up to 7 total, at the mean size found in the aliquot, were also tested. The models were also run sequentially using the original frequency distribution and parameters for all taxa while increasing the multiples of euphausiid abundances from the net. The euphausiid abundance factors tested were 1x, 2x, 4x, 6x, 8x, and 10x.

Estimating Euphausiid Abundance

Euphausiid abundance estimates from the net samples were compared with those estimated from the observed acoustic backscatter using the relationship between the volume backscatter coefficient (s_v) and the individual backscattering cross-section (σ_{bs}) (MacLennan *et al.*, 2002):

$$s_v^j(f_q, d_k) = \frac{n_j}{V_k} * \bar{\sigma}_{bs}^j \qquad \text{EQUATION 2.4}$$

where s_v^j is the volume backscattering coefficient contribution for taxon j at frequency f_q in the depth range d_k , n_j is the number of individuals in taxon j per V_k, the volume of water sampled in the depth range d_k, and $\bar{\sigma}_{bs}^j$ is the backscattering cross-section

predicted for one individual in taxon j. We used the weighted mean euphausiid backscattering cross-section estimated at each frequency for $\bar{\sigma}_{bs}^{j}$.

Further euphausiid abundance analysis was performed for the nets inferred to have sampled within the krill SSL which was defined as the region where the observed mean volume backscattering strength exceeded -75 dB at 200 kHz within the 100 m to 250 m depth range. The additional analysis was performed to test the sensitivity of euphausiid abundance estimates to assumptions about net avoidance and assumptions about the presence of pneumatocysts. Three scenarios were investigated using equation (4). The first scenario assumed 100% of the observed backscatter in the region of the net sample was from euphausiids. The second scenario assumed that for nets in which backscatter was under-predicted, the low values were entirely attributable to net avoidance by the euphausiids. The third assumed that for nets in which backscatter was under-predicted, the low values were attributable to net avoidance by all taxa present in the sample in proportion to their contribution to the predicted mean volume backscattering strength. These three acoustic estimates of euphausiid abundance, at two frequencies when available, were compared to one another and to abundance estimates determined directly from the net samples.

RESULTS

Acoustic Survey Results

Echograms of the acoustic data collected during the net sampling revealed a layer of intense sound scattering at depths of 100 m or greater (Figure 2.2). The observed 200-kHz mean volume backscattering strength (S_v) for the depth range of the

sound-scattering layer ranged from -68.5 dB (Tow 10) to -65.2 dB (Tow 9), about 5 dB, or approximately three times higher, than background mean S_v outside of the intense layers.

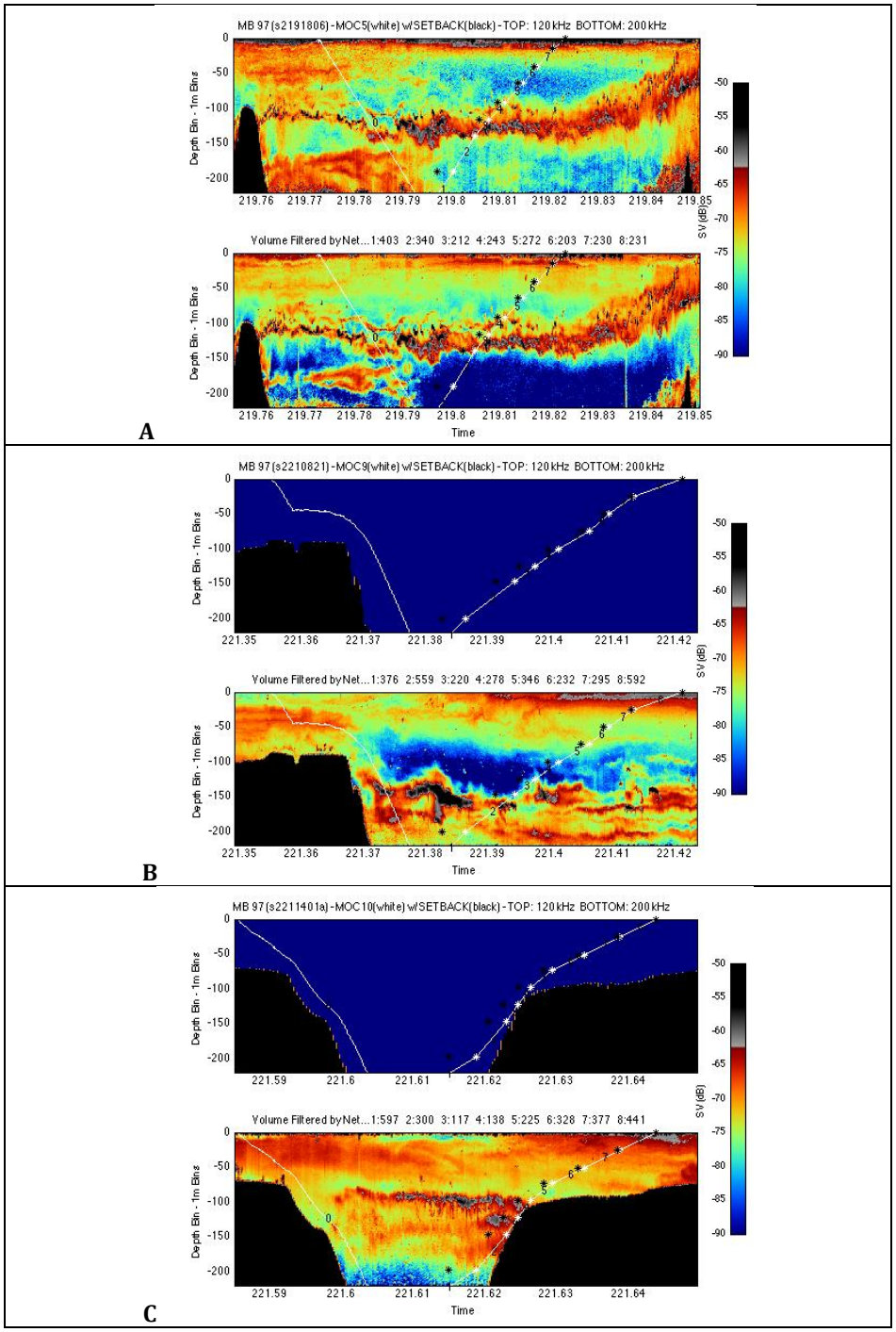

FIGURE 2.2: Echograms of Measured Backscatter
A) Tow 5. B) Tow 9. C) Tow 10. For each tow, top panel is 120 kHz data and bottom panel is 200 kHz data. Black is canyon bathymetry. White line marked with stars is the trace of the MOCNESS recovery. White stars are locations at which one net was closed and the succeeding net was opened. Black stars show setback location. For net tows completed after the failure of the 120 kHz echosounder (Tow 9 and Tow 10), flat blue has been substituted in the top panel in place of the missing 120 kHz data.

MOCNESS Sampling Results

Zooplankton samples collected by the depth-stratified net tows confirmed that the highest biomass concentrations of euphausiids coincided with the location of the SSL, the region sampled by nets 1 through 4 in each of the tows. Data combined from the three tows showed that euphausiid biomass concentrations within the SSL, nets 1 through 4, were on average 40 times greater than that found above the SSL, nets 5 through 8. Localized variability in biomass as captured within individual nets showed that the biomass could be as high as 2000 times that seen outside the SSL. Nets 5 through 8 for each tow sampled above the intense backscattering layer that encompasses the high krill biomass, and are excluded from this study. All references to nets include only nets 1 through 4 for each of the tows.

The animals within the SSL were comprised of a mixed assemblage of zooplankton for which the biomass was dominated by euphausiids and copepods, but included decapod shrimp, chaetognaths, medusa, siphonophores, and fish larvae among others. Euphausiids dominated the biomass in samples from nets 1, 2, and 3 in Tow 5, accounting for 57%, 88%, and 96%, respectively, and accounted for 74% of the biomass in samples from Net 2 of Tow 9. The net with the highest percentage of euphausiid biomass coincided with the region of the most intense backscatter recorded within each tow. This was true also for Tow 10, in which samples from Net 3 had the highest percentage of euphausiid biomass and the most intense observed backscatter. Copepods were present in all net samples but dominated the biomass in only Net 4 of Tows 5 and 10 at 53% and 83%, respectively. Pneumatophores were found in all net samples except for Net 4 of Tows 9 and 10. These strongly backscattering gas-bearing

floats of the siphonophores were present at abundances several orders of magnitude less than the euphausiids and contributed negligible amounts to the biomass. Other animals present in the assemblage did not dominate the biomass in any of the samples except for medusa at 64% in Net 1 of Tow 9, and decapod shrimp at 54% in Net 1 of Tow 10.

Collecting samples in near proximity to the canyon wall presented special challenges that resulted in both contact with the canyon wall for Tows 5 and 10, and, in order to avoid contact with the canyon wall, increased vertical velocity during the collection of nets 3 and 4 of Tow 10. During the descent phase of Tow 5, the net system struck and dragged down the canyon wall before the system was righted. Considerable vibration was likely sustained by the MOCNESS frame and consequently compromised the net closures. Benthic animals and sand were excluded from the analysis of the contents of Tow 5. Tow 10 experienced brief contact with the wall during the descent of the net system. No evidence of compromised net closures was noted for this tow. In order to avoid additional collisions with the canyon wall during the collection of the nets 3 and 4 samples for Tow 10, the vertical velocity at which the net system was towed was increased from a nominal 6 m/min (10 cm/s) to greater than 10 m/min (16.7 cm/s). The increased vertical velocity resulted in ~ 50% reduced volumes filtered by nets 3 and 4 during this tow relative to nets 3 and 4 of the other tows also sampling a nominal depth range of 25 m each.

Acoustic Backscatter Prediction Results

Model predictions of acoustic backscatter for the zooplankton assemblage at 120 kHz and 200 kHz revealed that although euphausiids dominated the biomass, they did not contribute to the backscatter in the same proportion as their biomass. This was

particularly true at 120 kHz in the presence of the rare, but strongly scattering pneumatophores. For example, in Net 3 of Tow 5 euphausiids dominated the biomass, comprising 96% of the sample and pneumatophores contributed negligible amounts to the biomass but were present at an abundance of 1% of that of the euphausiids. However, in the presence of the pneumatophores, despite comprising 96% of the biomass, euphausiids accounted for only 27% and 64% of the predicted backscatter at 120 kHz and 200 kHz, respectively. Pneumatophores, present in the net at an abundance nearly two orders of magnitude less than the euphausiids, accounted for 68% and 28% of the predicted backscatter at 120 kHz and 200 kHz, respectively. On average, for nets in which pneumatophores were present, they accounted for 68% and 61% of the total predicted backscatter at 120 kHz and 200 kHz, respectively, contributing a disproportionate amount to total volume backscattering relative to their negligible contribution to biomass and total animal abundance. Likewise, this presence of only a few pneumatophores reduced the relative euphausiid contribution to the total mean volume backscattering to 25% (n=4, STD: 27) and 29% (n=10, STD: 28) at 120 kHz and 200 kHz, respectively.

Copepods, a fluid-like scatterer but much smaller than the euphausiids, made substantial contributions to the biomass of the samples in Net 4 in each of the tows, ~ 50%; however, only in Tow 10 with no pneumatophores present did they contribute substantially to the predicted volume backscattering, 66% and 71% at 120 kHz and 200 kHz, respectively. The substantial contribution to the predicted backscatter by the copepods may have been an artifact of the increased towing speed disproportionately

reducing the capture efficiency of euphausiids and thereby biasing the backscatter predicted from the net samples.

Thus, the euphausiids and the gas-bearing floats of the siphonophores were the two dominant contributors to the predicted backscatter, combined accounting for 90% or more of the total predicted backscatter within the SSL. Copepods contributed little to the total predicted backscatter, generally less than 5% at both 120 kHz and 200 kHz, except for Net 4 of Tow 9 where the contribution was ~ 15% at 120 kHz and 200 kHz and, Net 4 of Tow 10 as described above. For all nets, the small amount of predicted acoustic backscatter not accounted for by the euphausiids, pneumatophores, and copepods, was contributed primarily by decapod shrimp, chaetognaths, and the "jelly" portions of the siphonophores.

Model Predictions Compared with Observed Backscatter

Sixteen predictions of total mean volume backscattering strength were calculated and compared to the observed: four nets for Tow 5 at 120 kHz, and four nets each for Tows 5, 9, and 10 at 200 kHz. The difference between the predicted and observed ranged from a minimum of 0.1 dB to a maximum difference of 18.4 dB. The net-shifting exercise ruled out error in the setback locations as the source of the mismatch between the predicted and observed total mean volume backscattering strength. The span of observed values for each net in the net-shifting exercise ranged from a minimum of 0.3 dB to a maximum of 6.6 dB. In only one case, Net 2 of Tow 5 at 200 kHz for which the difference between the original predicted and observed was 0.1 dB, did the span of net-shifted observed values encompass the predicted value. For the remainder of the predictions, all of which had an original difference greater than

0.1 dB between the predicted and observed, the mismatch was not resolved by the net-shifting exercise.

Three predictions were subsequently excluded from analyses due to data-quality issues. Tow 5 Net 1 was excluded because nearly 70% of the observed values were not recorded in the 200-kHz file and consequently may account for a predicted backscattering exceeding the observed value for that net by an anomalous ~ 12 dB. Tow 10 nets 3 and 4 were excluded when predicted backscattering anomalously under-predicted the observed values by ~ 15 dB and ~ 19 dB, respectively. The higher than usual tow speeds, and the consequent lower than usual volume of seawater filtered, associated with these two nets likely contributed to a reduced net catch efficiency and consequently led to large mismatches between the predicted and observed backscatter.

The thirteen remaining predictions of mean volume backscattering strength (S_v) produced results that were within 7 dB, or a factor of 5, of the observed values. The mean difference between predicted and observed values was an under-prediction of 1.6 dB (SD: 4.2). A Model II regression analysis of observed versus predicted mean volume backscattering strength (S_v) produced a slope of 1.4 (r2 = 0.67), indicating a tendency for under-prediction in the nets with higher observed backscatter, although not statistically different from a one-to-one line. The difference between the observed and predicted values, when pneumatophores were excluded, resulted in a mean under-prediction of 7.1 dB (SD: 6.2), with a regression slope of 1.4 (r2 = 0.28), again, not statistically different from a one-to-one line (Figure 2.3).

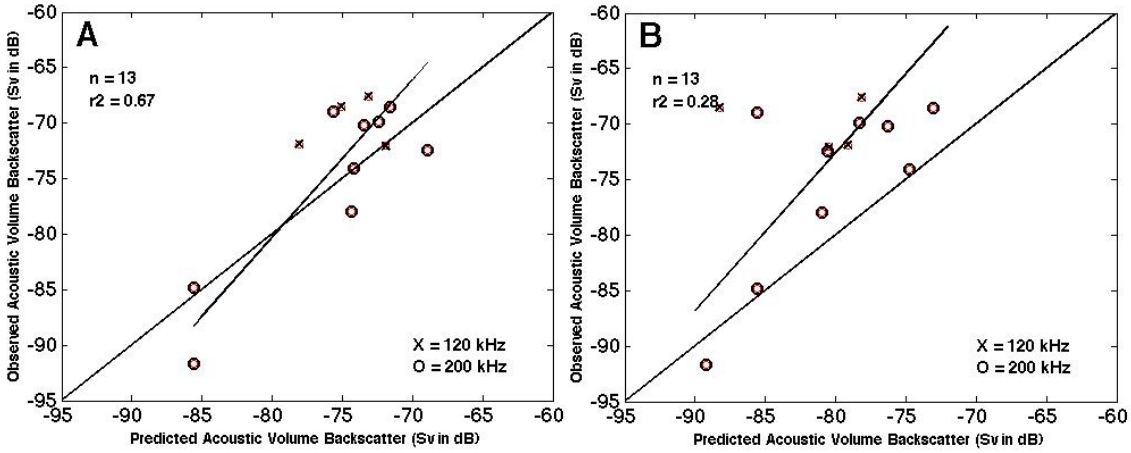

FIGURE 2.3: Measured and Predicted Backscatter by Net for 13 Nets
X: predictions at 120 kHz. Circles: predictions at 200 kHz. Nets for which predicted backscatter equals observed backscatter would fall on the diagonal one-to-one line. Nets for which the predicted backscatter is less than the observed backscatter fall above the one-to-one line. Regression line through the data is also plotted.

Euphausiid Abundance Estimates

Of the thirteen net samples analyzed, Tow 9 Nets 3 and 4, and Tow 10 Net 1, were excluded from the euphausiid abundance estimates because their observed mean volume backscattering strengths at 200 kHz were less than the −75 dB minimum threshold for inclusion as part of the SSL, leaving ten net samples for which we analyzed the acoustic-derived euphausiid abundance estimates versus the abundance estimated from the animals captured by the nets.

The euphausiid abundances estimated from the observed backscatter were markedly affected by the assumption regarding the source of the backscatter. When the backscatter within the krill SSL was assumed to be produced exclusively by euphausiids, the acoustic-derived estimate of euphausiid abundance exceeded the net-derived estimate by a range that varied from a minimum factor of 1.3 up to a factor of 360, or two orders of magnitude greater than that derived from the animals found within

the nets. However, when the observed backscatter was apportioned among the taxa according to the relative backscatter contribution predicted from the animals found within the nets, including the pneumatophores, the amount by which the acoustic-derived estimated euphausiid abundance exceeded the net-derived estimates were reduced from a maximum factor of 360 to a maximum factor of 4.6.

Although the maximum factor by which the acoustic-derived estimate exceeded the net-derived was reduced to a reasonable 4.6, the acoustic derived euphausiid abundance estimates differed between frequencies. For the nets in Tow 5 for which measured backscatter was available at both frequencies, in each case, the acoustic-derived abundance estimated from the 120-kHz data exceeded the abundance estimated from the 200-kHz data. The frequency-mismatch in the euphausiid abundance predictions at 120 kHz relative to the 200-kHz predictions was a factor of 4.0 for Net 2, a factor of 1.8 for Net 3, and good agreement with a factor of 1.0 for Net 4, a net, it should be noted, in which the pneumatophores accounted for greater than 90% of the predicted backscatter at both frequencies (Table 2). Efforts to reconcile the acoustic-derived estimates at the two frequencies were unsuccessful at finding a combination of euphausiid net avoidance and siphonophore under-representation factors to resolve the discrepancy between the estimates and bring the estimates at the two frequencies into agreement.

DISCUSSION

The krill sound-scattering layers of the Monterey Bay Submarine Canyon are characterized by conspicuously strong sound-scattering and a diverse assemblage of

zooplankton dominated by krill biomass which ranged up to greater than 90% of the biomass captured in the net samples. The results of this study demonstrate that despite the dominance of the krill presence within the SSL, that even when present in quantities orders of magnitude less than the euphausiids, the rare and inconspicuous gas-filled floats of siphonophores can contribute substantially to the observed backscatter at the frequencies used here: 120 kHz and 200 kHz. Accordingly, careful attention must be given to the small, rare, but strongly scattering gas-bearing pneumatophores when using acoustic techniques to survey krill.

The importance of accounting for the backscatter contribution by the pneumatophores is evident in all four analyses in this study: (1) comparison of euphausiid biomass relative to observed S_v for nets within each tow, (2) total mean volume backscattering strength (S_v) predicted for each net relative to the observed, (3) euphausiid contribution to the total predicted mean S_v relative to their contribution to captured biomass, and (4) acoustic-derived euphausiid abundance estimates relative to the abundance calculated from the net samples.

Although the strongest observed mean S_v within each tow was associated with the net with both the highest biomass and the highest percentage contribution by euphausiids to that biomass, these associations appear tenuous in the presence of the strongly scattering gas-bearing pneumatophores. In Tow 5, there is only a small difference of 23% and 12% (0.9 dB and 0.5 dB) in the total observed mean S_v for the nets with the two highest recorded mean S_v values in the tow, at 120 kHz and 200 kHz, respectively. Despite this small difference in mean S_v there is a full order of magnitude less total biomass in the net with the lower backscatter, 15 mg m^{-3} versus 210 mg m^{-3},

and euphausiids contribute substantially less to total biomass, 38% versus 96%. The weakly scattering copepods, a crustacean with fluid-like material properties and on the order of 1 to 2 mm in length, account for 53% of the biomass in the net with the substantially reduced biomass contribution by euphausiids. Under a scenario of more copepod contribution and less euphausiid contribution, at the frequencies used in this study, one would expect a decrease in the observed mean S_v by 85% and 70%, rather than 23% and 12%, at 120 kHz and 200 kHz, respectively. In this case, we don't see the substantial drop in observed backscatter that we might expect with a drop of an order of magnitude of biomass. The presence of the pneumatophores, with their negligible contribution to biomass but strong scattering, account for 95% and 90% of the backscatter in the net with the substantially reduced biomass, at 120 kHz and 200 kHz, respectively. Therefore, although in this case the net sampled region with the highest observed mean S_v was co-located with the net with the highest euphausiid biomass, this relationship may not be reliable when the strongly scattering gas-bearing siphonophores are present in sufficient numbers. The caution that this presents is that within the krill SSL, variability of biomass and backscatter contributions require investigation through the methods presented here to appropriately attribute sound scattering among the taxa present, and that strong backscatter within the SSL does not necessarily equate to either high euphausiid biomass nor backscattering dominated by euphausiid contributions.

In the second analysis, model results show good agreement with observed mean S_v when the predicted pneumatophore contribution to total backscatter is included. The good agreement is evident in both the mean of the difference between the predicted and observed mean S_v values, and in the coefficient of determination associated with the

Model II regression line describing the relationship of the observed backscatter to the model-predicted backscatter. When the pneumatophore contribution is included, the mean difference between the model-predicted and the observed S_v is an under-prediction of 1.6 dB (〖SE〗_$\bar{x}$: 1.2), not significantly different from zero, whereas when the pneumatophore contribution is excluded, the mean difference increases to an under-prediction of 7.1 dB (〖SE〗_$\bar{x}$: 1.7), significantly different from zero. And although the slope of the Model II regression line remains at 1.4 and not significantly different from a one-to-one line whether the pneumatophore contribution was included or excluded, the coefficient of determination, r2, that provides a measure of the proportion of the total variation of outcomes explained by the models is reduced from 0.67 when the pneumatophore contribution is included to 0.28 when the pneumatophore contribution to backscatter is excluded. Both of those measures, the mean difference and the coefficient of determination, indicate that inclusion of the pneumatophore contribution is important in the attribution of the observed backscatter to its sources in the krill SSL in the Monterey Bay canyon.

In the third analysis, accounting for the backscatter contribution from the pneumatophores reduces the euphausiid contribution to backscatter relative to the euphausiid contribution to biomass. If the pneumatophores had contributed to the backscatter in a measure proportionate to their insignificant size and abundance, we would have expected the krill dominance of the biomass to be indicative of the krill relative contribution to backscatter. However, only in the nets in which no pneumatophores were present did the krill contribution to total predicted mean S_v meet or exceed the krill contribution to biomass. Because of the strong predicted target

strength of the pneumatophores, the krill contribution to the predicted backscattering is less than its contribution to total biomass for nets in which pneumatophores are present. This mismatch between the krill contribution to biomass and the contribution to predicted backscatter in the presence of the pneumatophores emphasizes the usefulness in employing the forward problem to infer the sources generating the observed volume backscattering.

And finally, in the analysis of the acoustic-derived euphausiid abundance, when the pneumatophore contribution to total backscatter is excluded, the euphausiid abundance estimated from the observed mean S_v is up to a factor of 360 greater than that derived from the net contents. Accounting for the pneumatophore contribution brings the amount by which the acoustically-derived euphausiid abundance estimate exceeds the net-derived estimate down to a reasonable 4.6 as discussed below. Thus, accounting for the backscatter contribution by these small, rare, and inconspicuous gas-bearing pneumatophores is important to the outcome of generating a biologically meaningful metric for krill when using acoustic surveys.

Pneumatophore contribution to backscatter is disproportionate to their physical presence in the nets because of the strongly scattering gas-bearing nature of their material properties relative to the aggregation of fluid-like krill and copepods that dominate the biomass and abundance of individuals found in the nets (Stanton *et al.*, 1998b; Warren *et al.*, 2001). The suite of zooplankton scattering models (Stanton *et al.*, 1994; 1998a; reviewed by Stanton and Chu, 2000; as modified by Lavery *et al.*, 2007) provides an important tool by which to estimate the frequency-specific contribution to

total volume backscattering strength from each taxon found in the nets, and thereby a method by which to apportion the total observed backscatter among the taxa.

The accordance of the outcome of the model suite relative to the observed backscatter is influenced by: (1) model and parameter selection, (2) representativeness of the net sample contents, (3) the quality of the acoustic record and calibration, and (4) the ability to match the net-sample volume with the acoustic record. Discussion of each of these follows.

The scattering efficiency, or target strength (TS), of an animal is a complex, frequency-dependent function of an animal's size, shape and orientation, and the contrast of the density and sound speed characteristics of each animal relative to that of its seawater medium (Stanton and Chu, 2000). When possible we chose models tested on, and parameters measured from, appropriate taxa. Model results, therefore, while generally representative of a taxon's contribution to total backscatter, do include uncertainty. Sensitivity analyses of some of the parameters are discussed elsewhere in the literature (Mikami *et al.*, 2000; Stanton and Chu, 2000; Lavery *et al.*, 2002; Lawson *et al.*, 2006).

Because of the substantial backscattering contribution predicted for the gas-bearing portion of the siphonophores, it was important that we modify the procedures for enumerating and measuring the pneumatophores. First, in the silhouette method, the small and inconspicuous, but strongly scattering pneumatophores can be obscured from view by entanglement with parts of the siphonophore colony. Use of the microscope to extract the pneumatophores from the aliquot assures that all pneumatophores within the aliquot are included in scattering predictions. Second, use of the microscope allowed us

to measure the size of the inner gas-bearing pneumatocyst (Totton, 1965) rather than the outer, larger, pneumatophore dimensions visible in the silhouettes, and thereby calculate the conservative estimate of the backscatter contribution from each pneumatophore.

Quantitative zooplankton sampling is an area of ongoing development (Wiebe and Benfield, 2003). The representativeness of net sample contents is challenged by; animal behavior (e.g. net avoidance), sampling procedures (e.g. net washdown or sample handling), and collection methodologies (e.g. deployment of the net system). Net avoidance by euphausiids is a known issue (Brinton, 1967; Wiebe *et al.*, 1982; Everson and Bone, 1986), but one for which quantification is an continuing effort (Sameoto *et al.*, 1993; Wiebe *et al.*, 2004; Wiebe *et al.*, 2013). Quantification of a net avoidance factor for euphausiids in the absence of empirical data, especially in an environment with strong backscatterers such as the gas-bearing siphonophores in this study, is difficult. Under-representation of specimens captured within the nets is a function of the unquantified net avoidance factors for each of the taxa, and potentially a size bias for krill in that underrepresentation (Wiebe *et al.*, 2004; Wiebe *et al.*, 2013). So although the most reasonable acoustic-derived euphausiid abundance relative to the net-derived abundance, with a maximum factor of 4.6, was attained in the procedure in which any under-predicted backscatter was allocated among the taxa based on their net-derived predicted backscattering contribution, it is implicitly assuming under-sampling factors for taxa where net-capture efficiency has not been quantified.

An undersampling or net avoidance factor of 4.6 for euphausiids is well within the daytime net avoidance factor of 11 quantified for euphausiids in the Gulf of Maine in a study which used equivalent net sampling gear, a 1-m^2 MOCNESS, outfitted with a

strobe light (Wiebe *et al.*, 2013). Strobe light studies suggest a preferential catch-enhancement of larger euphausiid specimens (Wiebe *et al.*, 2004; Wiebe *et al.*, 2013). Although a catchment size-bias has not been tested in Monterey Bay, the length distribution of euphausiids found in whale fecal samples relative to the length distributions captured by a bongo net system (Croll *et al.*, 2005) suggest that a preferential catch-enhancement of larger euphausiids may be found for the species of the submarine canyon if a strobe light is included with net instrumentation. Similar studies are needed to delimit the range of net avoidance and any potential size bias for the euphausiid species of Monterey Bay. Likewise, undersampling of gas-bearing siphonophores while using net collection techniques has been noted (Warren *et al.*, 2001), but not quantified.

One advantage of integrating the forward problem modeling into acoustic survey techniques is that methodological problems can come to light (Greene *et al.*, 1998; Trevorrow *et al.*, 2005). Three nets with data quality issues were identified from the anomalously high difference of one to two orders of magnitude between the predicted and observed mean S_v values. For the anomalously over-predicted net, the associated observed 200-kHz record was revealed to be a partial record, raising doubt as to its representativeness of the backscatter associated with the net-sampled volume. An anomalously fast vertical towing speed, to avoid collision with the canyon wall, was associated with the two nets for which an anomalously large under-prediction was identified. The catch-efficiency of the net system may have been compromised by the unusually fast vertical towing speed and thereby compromised the representativeness of the net sample contents. Identification of nets with anomalously large differences

between the predicted and observed S_v values allowed us to identify nets for which methodological issues compromised the reliability of the data quality of acoustic or net sample data.

In acoustically variable environments such as that found here, with both patchy, intense backscattering regions within the SSL and SSL edges, co-location of the net sampled volume and the acoustically interrogated volume can have a substantial impact on the apparent success of the model predictions. The reliability of the values designated as the observed mean S_v was assessed in the net shifting exercise. The results demonstrated that although the range of values encompassed by the net shifting for each net reached a maximum of 6.6 dB, in no case did the predicted mean S_v fall within the range of observed mean S_v values demarcated by the net shifting if the difference between the original co-located observed and predicted mean S_v was greater than 0.1 dB. No bias in setback location was revealed by the net-shifting exercise. Therefore, factors other than, or in addition to, the setback co-location generated the difference between model results and the observed mean S_v.

Some general trends regarding model performance were noted. In general, in regions of strong backscattering, the model predictions calculated from the organisms caught in the nets under-predicted the observed backscatter. There are sound biological reasons such as the net avoidance discussed above that may account for this. Conversely, regions of weak backscatter tended to be over-predicted, particularly Net 1 for all three tows. In each tow, Net 1 sampled deeper than the acoustic record and consequently, these over-predictions may be an artifact if the nets captured strong scatterers deeper than the acoustic record, but this can't be verified. Sources were not

identified for the over-prediction that occurred for nets associated with weak scattering that were not Net 1.

In addition to the differences between observed and predicted mean S_v, differences were noted between frequencies. The contribution to predicted backscattering by the pneumatophores was particularly pronounced and consistently higher at 120 kHz relative to 200 kHz. This is consistent with theory (Medwin, 1977; Stanton, 1989). A gas bubble in liquid possesses a resonant mechanical oscillation frequency (Medwin, 1977). When a gas bubble is insonified at or near its natural frequency it strongly absorbs and scatters sound, resulting in a scattering cross-section that can be up to 1000 times the geometrical cross-section of the bubble (Medwin, 1977). For the pneumatophores in this study, the predicted resonance frequencies range from 10 kHz to 50 kHz, much lower than our insonification frequencies of 120 kHz and 200 kHz. However, for those same pneumatophores, the predicted TS decreases between 120 kHz and 200 kHz as the insonification frequency moves further away from the resonance frequency (Figure 2.4). At the same time, euphausiids exhibit no resonance frequency due to their fluid-like nature and, euphausiids at 120 kHz and 200 kHz are in the Rayleigh portion of their backscattering-frequency response curve. In Rayleigh scattering the target exhibits increasing target strength with increasing frequency, and hence contribute more strongly to the backscattering at 200 kHz than at 120 kHz (Figure 2.4). Hence the combination of the gas-bearing pneumatophores exhibiting higher acoustic scattering efficiency at 120 kHz and the euphausiids exhibiting higher acoustic scattering efficiency at 200 kHz accounts for the stronger

contribution at 120 kHz for the gas-bearing pneumatophores relative to their contribution at 200 kHz while the inverse is true for the euphausiids.

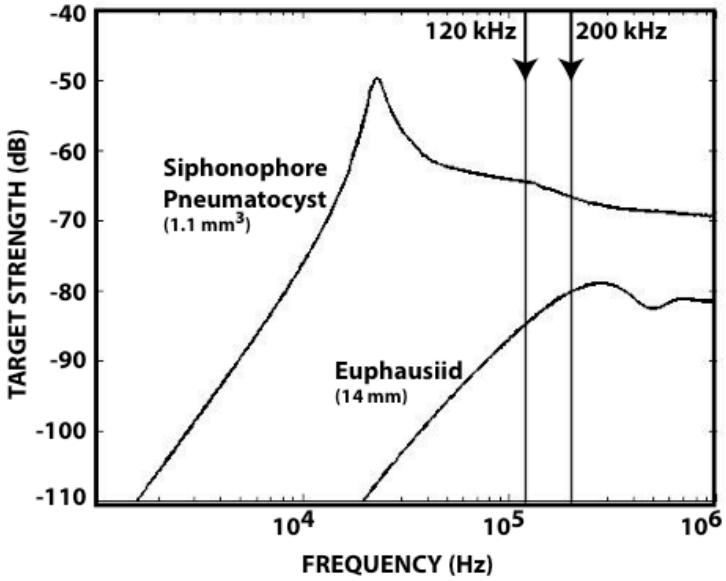

FIGURE 2.4: Predicted Target Strength (dB) as a Function of Frequency for individual siphonophore pneumatocyst and euphausiid. Prediction was made assuming a depth of 165 m, the mean depth of Net 2 in Two 5. Sizes selected for illustration are the mean size from the Tow 5 samples for Nets 1 through 4. Survey frequencies are indicated by the vertical lines.

Establishing an acoustic-derived estimate of the krill numerical density through implementation of the model-refined allocation of observed backscatter however, proved non-trivial. The acoustic-derived numerical abundance estimates were consistently greater at 120 kHz than at 200 kHz and differed by up to a factor of 4.0 between frequencies. Whereas the target strength of each animal is frequency dependent, the unequal relative contribution to the total backscatter at each frequency as illustrated above for the pneumatophores is expected. However, the numerical abundance of animals supporting the total backscatter at each frequency, if all sources

of the backscatter at appropriate target strengths are accounted for, should be the same. Given that the acoustic-derived euphausiid numerical abundance estimates were consistently greater at 120 kHz, we considered that the biased discrepancy between frequencies may indicate an undersampling of an acoustic target characterized by higher backscatter efficiency at 120 kHz relative to 200 kHz (Warren *et al.*, 2001; Mair *et al.*, 2005), such as the gas-filled pneumatophores. Although net avoidance by siphonophores has not been investigated, there is evidence that siphonophore colonies are capable of directed rapid motion at speeds commensurate with the nominal towing speed of the MOCNESS net system (Mackie, 1964; Robison *et al.*, 1998), but are unlikely to sustain the rapid initial startle response (Mackie, 1964) and in some studies exhibit little evidence of avoidance (Robison *et al.*, 1998). However, when a siphonophore layer was targeted by net sampling, very few siphonophores were captured by the net (Warren *et al.*, 2001). Therefore, the undersampling of the gas-bearing siphonophores has been noted, but it is not yet quantified. In addition, the small and inconspicuous nature of the pneumatophores make them particularly vulnerable to oversight during net washdown and transfer to sample jars, or during sample processing in which the pneumatophores may be tangled with other parts of the colony. Although there is ample support for an underrepresentation of pneumatophores, our testing of euphausiid and siphonophore undersampling estimates produced no result in which the acoustic-derived euphausiid abundance density estimates agreed at both frequencies. This may be because other acoustically important scatterers not represented in the nets, such as fish, are included in the observed backscatter but excluded from the model predictions.

Given that gas-bearing specimens more strongly backscatter sound at lower frequencies while fluid-like specimens more strongly backscatter sound at higher frequencies, we compared the backscatter at both frequencies to determine whether the presence or absence of gas-bearing specimens could be identified from the acoustic data. No conspicuous evidence was revealed. The scattering from gas-bearing specimens may have been more obvious if we had been able to examine the data on a ping-by-ping basis rather than the 15-s integrated data collected here. Likewise, if the survey included a lower frequency, such as 38-kHz which is markedly closer to the resonance peak for gas-bearing specimens, the difference in the backscattering strength between frequencies would have been amplified from less than an order of magnitude between 120 kHz and 200 kHz for both euphausiids and pneumatophores to more than an order of magnitude for the pneumatophores at 38 kHz relative to 200 kHz, and about three orders of magnitude for the euphausiids. Use of a lower frequency in conjunction with the 120 kHz and 200 kHz data, along with ping-by-ping analysis would have facilitated the effort to determine the presence and absence of gas-bearing specimens not captured by the nets (Warren *et al.*, 2001), and by extension validate the use of this technique to map the spatial heterogeneity of the siphonophores in regions not sampled by the nets.

Despite the incomplete information, implementing the forward problem to apportion the observed backscatter among the taxa proved useful and makes this technique transferrable to the specific zooplankton assemblages found at other sites. By using the forward problem to allocate the backscatter, the strong signal from the gas-bearing pneumatophores was removed from the total along with the negligible amounts

from other taxa, resulting in a portion attributable to the krill. The bias in the euphausiid abundance estimates between the two frequencies suggests that under-prediction at 200 kHz was not all attributable to the krill and therefore allocating the observed backscatter based on the apportionment derived from the net samples, rather than attributing the any under-prediction solely to krill was deemed appropriate. And this bias also suggests that in this case the 200 kHz results should be used to estimate the acoustic-derived krill abundance.

The results however, did leave us with one question: How is it that both the net-derived and the acoustic-derived krill abundance in this study are so low, on the order of 10 m^{-3} or less? The central California coast is situated in a transition zone between cold northern waters and warm southern water (Chelton *et al.*, 1982; Breaker, 2005). Consequently, the zooplankton assemblage and abundance in the Monterey Bay canyon are strongly influenced by the large-scale variations in the flow of the California current, including El Niño events (Chelton *et al.*, 1982; Roesler and Chelton, 1987; Breaker, 2005). In June 1997, the onset of El Niño conditions was marked by the arrival of an anomalous influx of warm southerly water on the central California coast (Chavez *et al.*, 2002), and in July by the sudden appearance of an adult cohort of *Nyctiphanes simplex*, a euphausiid species associated with poleward flow (Marinovic *et al.*, 2002; Brinton and Townsend, 2003). The abundance of *Euphausia pacifica* and *Thysanoessa spinifera,* both cold water species and usually the most abundant species in the Bay during a non El Niño summer, declined precipitously while zooplankton scattering values decreased dramatically (Marinovic *et al.*, 2002; Brinton and Townsend, 2003).

The El Niño event of 1997-1998 is the strongest on record, and consequently the assemblage and abundance of zooplankton were strongly affected.

Given that this study was undertaken during the anomalous conditions of an El Niño event, the extrapolation of our calculated backscattering apportionments to "normal" conditions for the canyon would be tentative at best. Missing from our understanding of how El Niño events affect the zooplankton assemblage is quantification of changes in species composition and abundance of the gas-bearing siphonophores, along with changes in relative abundance of other potentially acoustically important taxa. However, the techniques described for this study, when applied to data collect during El Niño and non-El Niño events would allow us to understand how the relative contribution to backscatter by euphausiids, by the gas-bearing pneumatophores, and by other taxa change with oceanographic conditions.

REFERENCES

Baduini, C. L. (**1997**). "Spatial and temporal patterns of zooplankton biomass in Monterey Bay, California, during the 1991-1993 El Niño, and an assessment of the sampling design," California Cooperative Oceanic Fisheries Investigations Reports **38**, 193-198.

Barham, E. G. (**1956**). "The Ecology of Sonic Scattering Layers in the Monterey Bay area, California," in *Biological Sciences* (Stanford University, Palo Alto, CA).

Benfield, M. C., Lavery, A. C., Wiebe, P. H. *et al.* (**2003**). "Distributions of physonect siphonulae in the Gulf of Maine and their potential as important sources of acoustic scattering," Canadian Journal of Fisheries and Aquatic Sciences **60**, 759-772.

Breaker, L. C. (**2005**). "What's happening in Monterey Bay on seasonal to interdecadal time scales," Continental Shelf Research **25**, 1159-1193.

Brinton, E. (**1967**). "Vertical migration and avoidance capability of euphausiids in California Current," Limnology and Oceanography **12**, 451-483.

Brinton, E., and Townsend, A. (**2003**). "Decadal variability in abundances of the dominant euphausiid species in southern sectors of the California Current," Deep-Sea Research Part II-Topical Studies in Oceanography **50**, 2449-2472.

Bucklin, A., Wiebe, P. H., Smolenack, S. B. *et al.* (**2007**). "DNA barcodes for species identification of euphausiids (Euphausiacea, Crustacea)," Journal of Plankton Research **29**, 483-493.

Chavez, F. P., Pennington, J. T., Castro, C. G. *et al.* (**2002**). "Biological and chemical consequences of the 1997-1998 El Niño in central California waters," Progress in Oceanography **54**, 205-232.

Chelton, D. B., Bernal, P. A., and McGowan, J. A. (**1982**). "Large-Scale Interannual Physical and Biological Interaction in the California Current," Journal of Marine Research **40**, 1095-1125.

Croll, D. A., Marinovic, B., Benson, S. *et al.* (**2005**). "From wind to whales: trophic links in a coastal upwelling system," Marine Ecology-Progress Series **289**, 117-130.

Davis, C. S., and Wiebe, P. H. (**1985**). "Macrozooplankton Biomass in a Warm-Core Gulf-Stream Ring - Time-Series Changes in Size Structure, Taxonomic Composition, and Vertical-Distribution," Journal of Geophysical Research-Oceans **90**, 8871-8884.

Ehrenberg, J. E., and Torkelson, T. C. (**2000**). "FM slide (chirp) signals: a technique for significantly improving the signal-to-noise performance in hydroacoustic assessment systems," Fisheries Research **47**, 193-199.

Everson, I., and Bone, D. G. (**1986**). "Effectiveness of the RMT8 System for Sampling Krill (*Euphausia superba*) Swarms," Polar Biology **6**, 83-90.

Foote, K. G. (**2000**). "Optical Methods," in *The Zooplankton Methodology Manual*, edited by R. Harris, P. H. Wiebe, J. Lenz, H. R. Skjoldal, and M. Huntley (Academic Press, London), pp. 259-295.

Greene, C. H., Wiebe, P. H., Pershing, A. J. *et al.* (**1998**). "Assessing the distribution and abundance of zooplankton: a comparison of acoustic and net-sampling methods with D-BAD MOCNESS," Deep-Sea Research Part II-Topical Studies in Oceanography **45**, 1219-1237.

Jarman, S. N., Elliott, N. G., Nicol, S. *et al.* (**2000**). "Molecular phylogenetics of circumglobal Euphausia species (Euphausiacea : Crustacea)," Canadian Journal of Fisheries and Aquatic Sciences **57**, 51-58.

Lavery, A. C., Stanton, T. K., McGehee, D. E. *et al.* (**2002**). "Three-dimensional modeling of acoustic backscattering from fluid-like zooplankton," Journal of the Acoustical Society of America **111**, 1197-1210.

Lavery, A. C., Schmitt, R. W., and Stanton, T. K. (**2003**). "High-frequency acoustic scattering from turbulent oceanic microstructure: The importance of density fluctuations," Journal of the Acoustical Society of America **114**, 2685-2697.

Lavery, A. C., Wiebe, P. H., Stanton, T. K. *et al.* (**2007**). "Determining dominant scatterers of sound in mixed zooplankton populations," Journal of the Acoustical Society of America **122**, 3304-3326.

Lawson, G. L., Wiebe, P. H., Ashjian, C. J. *et al.* (**2004**). "Acoustically-inferred zooplankton distribution in relation to hydrography west of the Antarctic Peninsula," Deep-Sea Research Part II-Topical Studies in Oceanography **51**, 2041-2072.

Lawson, G. L., Wiebe, P. H., Ashjian, C. J. *et al.* (**2006**). "Improved parameterization of Antarctic krill target strength models," Journal of the Acoustical Society of America **119**, 232-242.

Lawson, G. L., Wiebe, P. H., Stanton, T. K. *et al.* (**2008**). "Euphausiid distribution along the Western Antarctic Peninsula - Part A: Development of robust multi-frequency acoustic techniques to identify euphausiid aggregations and quantify euphausiid size, abundance, and biomass," Deep-Sea Research Part II-Topical Studies in Oceanography **55**, 412-431.

Little, W. S., and Copley, N. J. (**2003**). "WHOI Silhouette Digitizer version 1.0 User's Guide," (Woods Hole Oceanographic Institution Technical Report # 2003-05), pp. 1-63.

Mackie, G. O. (**1964**). "Analysis of locomotion in siphonophore colony," Proceedings of the Royal Society of London Series B-Biological Sciences **159**, 366-391.

Mackie, G. O. (**1985**). "Midwater Macroplankton of British-Columbia Studied by Submersible PISCES-IV," Journal of Plankton Research **7**, 753-777.

Mackie, G. O., Pugh, P. R., and Purcell, J. E. (**1987**). "Siphonophore Biology," Advances in Marine Biology **24**, 97-262.

MacLennan, D. N., Fernandes, P. G., and Dalen, J. (**2002**). "A consistent approach to definitions and symbols in fisheries acoustics," ICES Journal of Marine Science **59**, 365-369.

Mair, A. M., Fernandes, P. G., Lebourges-Dhaussy, A. *et al.* (**2005**). "An investigation into the zooplankton composition of a prominent 38-kHz scattering layer in the North Sea," Journal of Plankton Research **27**, 623-633.

Marinovic, B. B., Croll, D. A., Gong, N. *et al.* (**2002**). "Effects of the 1997-1999 El Niño and La Niña events on zooplankton abundance and euphausiid community composition within the Monterey Bay coastal upwelling system," Progress in Oceanography **54**, 265-277.

Mauchline, J., and Fisher, L. R. (eds). (**1969**). *The Biology of Euphausiids* (Academic Press Inc., New York, NY).

Mauchline, J. (**1980**). "Measurement of Body Length of Euphausia superba Dana," BIOMASS Handbook **4**.

McEwen, G. F., Johnson, M. W., and Folsom, T. R. (**1954**). "A statistical analysis of the performance of the Folsom plankton splitter, based upon test observations," Archiv fur Meteorologie, Geophysik und Bioklimatologie Serie A **7**, 502-527.

Medwin, H. (**1977**). "Counting Bubbles Acoustically - Review," Ultrasonics **15**, 7-13.

Mikami, H., Mukai, T., and Iida, K. (**2000**). "Measurements of density and sound speed contrasts for estimating krill target strength using theoretical scattering models," Nippon Suisan Gakkaishi **66**, 682-689.

Miyashita, K., Aoki, I., and Inagaki, T. (**1996**). "Swimming behaviour and target strength of isada krill (*Euphausia pacifica*)," ICES Journal of Marine Science **53**, 303-308.

Pickwell, G. V., Wilton, J. W., and Barham, E. G. (**1964**). "Carbon Monoxide Production by Bathypelagic Siphonophore," Science **144**, 860-862.

Pickwell, G. V. (**1970**). "Physiology of carbon monoxide production by deep-sea coelenterates: causes and consequences," Annals of the New York Academy of Sciences **174**, 102-115.

Pickwell, G. V., Vent, R. J., Barham, E. G. *et al.* (**1970**). "Biological Acoustic Scattering Off Southern California, Baja California and Guadalupe Island," in *Proceedings of an International Symposium on Biological Sound Scattering in the Ocean*, edited by G. B. Farquhar (Maury Center for Ocean Science, Warrenton, VA).

Robison, B. H., Reisenbichler, K. R., Sherlock, R. E. *et al.* (**1998**). "Seasonal abundance of the siphonophore, *Nanomia bijuga*, in Monterey Bay," Deep-Sea Research Part II-Topical Studies in Oceanography **45**, 1741-1751.

Roesler, C. S., and Chelton, D. B. (**1987**). "Zooplankton Variability in the California Current, 1951-1982," California Cooperative Oceanic Fisheries Investigations Reports **28**, 59-96.

Sameoto, D., Cochrane, N., and Herman, A. (**1993**). "Convergence of Acoustic, Optical, and Net-Catch Estimates of Euphausiid Abundance - Use of Artificial-Light to Reduce Net Avoidance," Canadian Journal of Fisheries and Aquatic Sciences **50**, 334-346.

Schoenherr, J. R. (**1991**). "Blue Whales Feeding on High-Concentrations of Euphausiids around Monterey Submarine-Canyon," Canadian Journal of Zoology-Revue Canadienne De Zoologie **69**, 583-594.

Skogsberg, T. (**1936**). "Hydrography of Monterey Bay, California Thermal Conditions, 1929-1933," Transactions of the American Philosophical Society **New Series 29**, 1-152.

Stanton, T. K. (**1989**). "Simple Approximate Formulas for Backscattering of Sound by Spherical and Elongated Objects," Journal of the Acoustical Society of America **86**, 1499-1510.

Stanton, T. K., Wiebe, P. H., Chu, D. Z. *et al.* (**1994**). "On Acoustic Estimates of Zooplankton Biomass," ICES Journal of Marine Science **51**, 505-512.

Stanton, T. K., Chu, D. Z., and Wiebe, P. H. (**1996**). "Acoustic scattering characteristics of several zooplankton groups," ICES Journal of Marine Science **53**, 289-295.

Stanton, T. K., Chu, D. Z., and Wiebe, P. H. (**1998a**). "Sound scattering by several zooplankton groups. II. Scattering models," Journal of the Acoustical Society of America **103**, 236-253.

Stanton, T. K., Chu, D. Z., Wiebe, P. H. *et al.* (**1998b**). "Sound scattering by several zooplankton groups. I. Experimental determination of dominant scattering mechanisms," Journal of the Acoustical Society of America **103**, 225-235.

Stanton, T. K., and Chu, D. Z. (**2000**). "Review and recommendations for the modelling of acoustic scattering by fluid-like elongated zooplankton: euphausiids and copepods," ICES Journal of Marine Science **57**, 793-807.

Totton, A. K. (**1965**). *A Synopsis of the Siphonophora* (British Museum of Natural History, London).

Trevorrow, M. V., Mackas, D. L., and Benfield, M. C. (**2005**). "Comparison of multifrequency acoustic and in situ measurements of zooplankton abundances in Knight Inlet, British Columbia," Journal of the Acoustical Society of America **117**, 3574-3588.

Warren, J. D., Stanton, T. K., Benfield, M. C. *et al.* (**2001**). "*In situ* measurements of acoustic target strengths of gas-bearing siphonophores," ICES Journal of Marine Science **58**, 740-749.

Wiebe, P. H., Boyd, S., and Cox, J. L. (**1975**). "Relationships between Zooplankton Displacement Volume, Wet Weight, Dry Weight, and Carbon," Fishery Bulletin **73**, 777-786.

Wiebe, P. H., Boyd, S. H., Davis, B. M. *et al.* (**1982**). "Avoidance of towed nets by the euphausiid *Nematoscelis megalops*," Fishery Bulletin **80**, 75-91.

Wiebe, P. H., Morton, A. W., Bradley, A. M. *et al.* (**1985**). "New Developments in the MOCNESS, an Apparatus for Sampling Zooplankton and Micronekton," Marine Biology **87**, 313-323.

Wiebe, P. H. (**1988**). "Functional Regression Equations for Zooplankton Displacement Volume, Wet Weight, Dry-Weight, and Carbon - a Correction," Fishery Bulletin **86**, 833-835.

Wiebe, P. H., Mountain, D. G., Stanton, T. K. *et al.* (**1996**). "Acoustical study of the spatial distribution of plankton on Georges Bank and the relationship between volume backscattering strength and the taxonomic composition of the plankton," Deep-Sea Research Part II-Topical Studies in Oceanography **43**, 1971-2000.

Wiebe, P. H., Stanton, T. K., Benfield, M. C. *et al.* (**1997**). "High-frequency acoustic volume backscattering in the Georges Bank coastal region and its interpretation using scattering models," IEEE Journal of Oceanic Engineering **22**, 445-464.

Wiebe, P. H., and Benfield, M. C. (**2003**). "From the Hensen net toward four-dimensional biological oceanography," Progress in Oceanography **56**, 7-136.

Wiebe, P. H., Ashjian, C. J., Gallager, S. M. *et al.* (**2004**). "Using a high-powered strobe light to increase the catch of Antarctic krill," Marine Biology **144**, 493-502.

Wiebe, P. H., Lawson, G. L., Lavery, A. C. *et al.* (**2013**). "Improved agreement of net and acoustical methods for surveying euphausiids by mitigating avoidance using a net-based LED strobe light system," ICES Journal of Marine Science **70**, 650-664.

Yen, P. P. W., Sydeman, W. J., and Hyrenbach, K. D. (**2004**). "Marine bird and cetacean associations with bathymetric habitats and shallow-water topographies: implications for trophic transfer and conservation," Journal of Marine Systems **50**, 79-99.

CHAPTER 3

Diving behavior and efficiency of a blue whale (Balaenoptera musculus) foraging in its three-dimensional prey field

ABSTRACT

Blue whales (*Balaenoptera musculus*) are the largest animals to have lived on the planet. Paradoxically, their feeding strategy is to feed on euphausiids, a very small shrimp-like crustacean that occur in patchy and ephemeral aggregations at depths of 150 to 200 m, while employing an energetically costly lunge-feeding maneuver. To improve our understanding as to how the whales locate and exploit patches of sufficiently high krill density, and the foraging efficiency that the whales may be achieving, we tracked the behavior of an individual whale as it searched and exploited the krill sound-scattering layer adjacent to the wall of the Monterey Bay Submarine Canyon. The specific objectives were to 1) quantitatively characterize the predator's three-dimensional prey field, 2) track the predator's foraging behavior within that prey field, 3) estimate the predator's foraging efficiency, and 4) develop a series of hypotheses about the general patch-foraging strategies employed by blue whales. The results of our analysis suggest that the search behavior of the whale is consistent with behavior that theory predicts would optimize their encounter rate with krill patches of sufficiently

high prey density. The results also provide compelling evidence that within the foraging habitat, the whale focused its foraging effort in a discrete high-density patch where the achievable foraging efficiency was an order of magnitude greater than in other regions tested and rejected by the whale.

INTRODUCTION

Blue whales (*Balaenoptera musculus*), a baleen whale, are the largest animals to have lived on the planet. They reach sizes that exceed 30 m and can well exceed 100 ton (Rice, 1978; Yochem and Leatherwood, 1985). Their great size, mammalian metabolism and investment in reproduction, and basin-scale migrations, result in extremely high metabolic requirements. Paradoxically, they feed on patchy, ephemeral aggregations of euphausiids (Gaskin, 1982; Croll *et al.*, 2005), also known as krill, a very small shrimp-like order of crustaceans that are less than 5 cm in length and distributed throughout the world's oceans (Mauchline and Fisher, 1969). In order to support their metabolic needs, blue whales must consume up to 2 ton or 20 million krill per day (Rice, 1978).

Although the whales require significant quantities of prey, the mechanisms by which they detect and ingest their prey are energetically costly. It is thought that the foraging whales sense the presence and abundance of their prey through direct contact with the vibrissae (Ling, 1977; Slijper, 1979; Kenney *et al.*, 2001). As their prey are often found at depths of 150 to 200 m (Mauchline and Fisher, 1969; Croll *et al.*, 1998), direct contact requires a whale to commit to the substantial energetic investment of a dive to 200 m to sample the foraging environment. In addition, these baleen whales feed by engulfing their prey using an energetically demanding lunge-feeding behavior; a maneuver that requires the whale to cease its descent, turn upwards, and, in preparation for engulfment, accelerate to an attacking speed sufficient to overcome the significant drag forces brought on by opening its great mouth and the extension of its throat pleats

(Croll *et al.*, 2001; Calambokidis *et al.*, 2007; Goldbogen *et al.*, 2007). In addition to the costly nature of their foraging and feeding, the number of engulfments in each successful feeding dive is limited by the round trip travel time and the requirement to return to the surface to breathe. The short duration of blue whale dives relative to their great size, ~ 10 minutes between ventilations, is indicative of the energetic costs imposed by executing lunge-feeding maneuvers (Croll *et al.*, 2001; Acevedo-Gutierrez *et al.*, 2002; Goldbogen *et al.*, 2008). To support their metabolic needs, successful foraging dives must yield energetic returns that substantially exceed the costs of exploratory dives and the costs of executing multiple engulfment lunges while at depth. This requires that blue whales locate sufficiently large patches of highly concentrated krill.

Krill are distributed worldwide but the density at which they aggregate, due to physical, biological and behavioral factors, varies widely across the scales of time and space (Mauchline and Fisher, 1969). At the regional scale, krill are typically found aggregated in nutrient-rich zones, and for some species, associated with topographical breaks (Brinton, 1962; Croll *et al.*, 1998; Fiedler *et al.*, 1998; Santora *et al.*, 2011). Feeding grounds for the blue whales are defined at this scale. It is thought that the location of feeding grounds are known to the whales as there is a strong correlation between sightings of feeding blue whales and their krill prey during their annual migrations (Simard and Lavoie, 1999; Burtenshaw *et al.*, 2004; Barlow and Forney, 2007; Calambokidis *et al.*, 2009; Block *et al.*, 2011).

On the feeding grounds, the krill are not uniformly distributed. Due to their aggregating behavior most of their total biomass is aggregated within a small fraction of

the available ocean habitat (Mauchline and Fisher, 1969; Simard and Mackas, 1989; Mackas *et al.*, 1997; Simard and Lavoie, 1999). This results in localized aggregations, at the scale of meters to kilometers, for which the biomass concentration is one or more orders of magnitude greater than in the area surrounding the aggregations (Ichii *et al.*, 1998; Croll *et al.*, 2005). Within aggregations, concentration varies again on the order of magnitudes resulting in highly localized, highly concentrated patches of krill (Zamon *et al.*, 1996). The detection of the background density within the aggregation is thought to signal to the predator a high probability of finding rich patches of sufficient density, but as there is no structure inherent in the aggregations to guide the predator to finding the rich patches, feeding success is dependent on efficient tactics to find the rich patches (Simard and Lavoie, 1999).

The overall success of blue whale foraging strategy is demonstrated by the great size that they able to achieve as well as their ability to survive and reproduce in an ocean environment characterized by high inter-annual and oceanographic variability in prey abundance (e.g. shifts in geographic distribution of prey species due to El-Niño; see (Benson *et al.*, 2002; Burtenshaw *et al.*, 2004; Tynan, 2004)). However, the question remains as to how the whales locate and exploit patches of sufficiently high krill density, and the achievable foraging efficiencies experienced by individual whales within their feeding grounds. To answer these questions, it is critical to track the behaviors of individual whales as they interact with their three-dimensional prey field. Here, we report the diving behavior of an individual blue whale as it searches and exploits the three-dimensional krill sound-scattering layers adjacent to the wall of the Monterey Bay Submarine Canyon. The specific objectives were to 1) quantitatively

characterize the predator's three-dimensional prey field, 2) track the predator's foraging behavior within that prey field, 3) estimate the predator's foraging efficiency, and 4) develop a series of hypotheses about the general patch-foraging strategies employed by blue whales.

METHODS

Study area

Monterey Bay is an open embayment on the Central California continental shelf; its mouth measures 37 km in width between Point Santa Cruz and Point Piños. The shelf underlying the bay is bisected by the Monterey Bay Submarine Canyon (MBSC) reaching depths of 2 km and providing unrestricted access to the deep ocean (Martin and Emery, 1967). Krill within the canyon are reliably found in dense daytime aggregations at depths of 150 to 200 m, adjacent to the canyon walls seasonally from June to November (Croll *et al.*, 2005). Blue whales of the eastern North Pacific stock regularly feed within Monterey Bay and its associated submarine canyon (Schoenherr, 1991; Croll *et al.*, 1998; Barlow and Forney, 2007). The distribution of the foraging whales within the Bay is associated with the areas of predictably high krill densities (Croll *et al.*, 1998). Our study took place in an 11 km by 6 km region of the Monterey Bay Submarine Canyon (122.0 W to 121.9 W and 36.7 N to 36.8 N; Figure 3.1) adjacent to the canyon wall and commonly frequented by feeding blue whales.

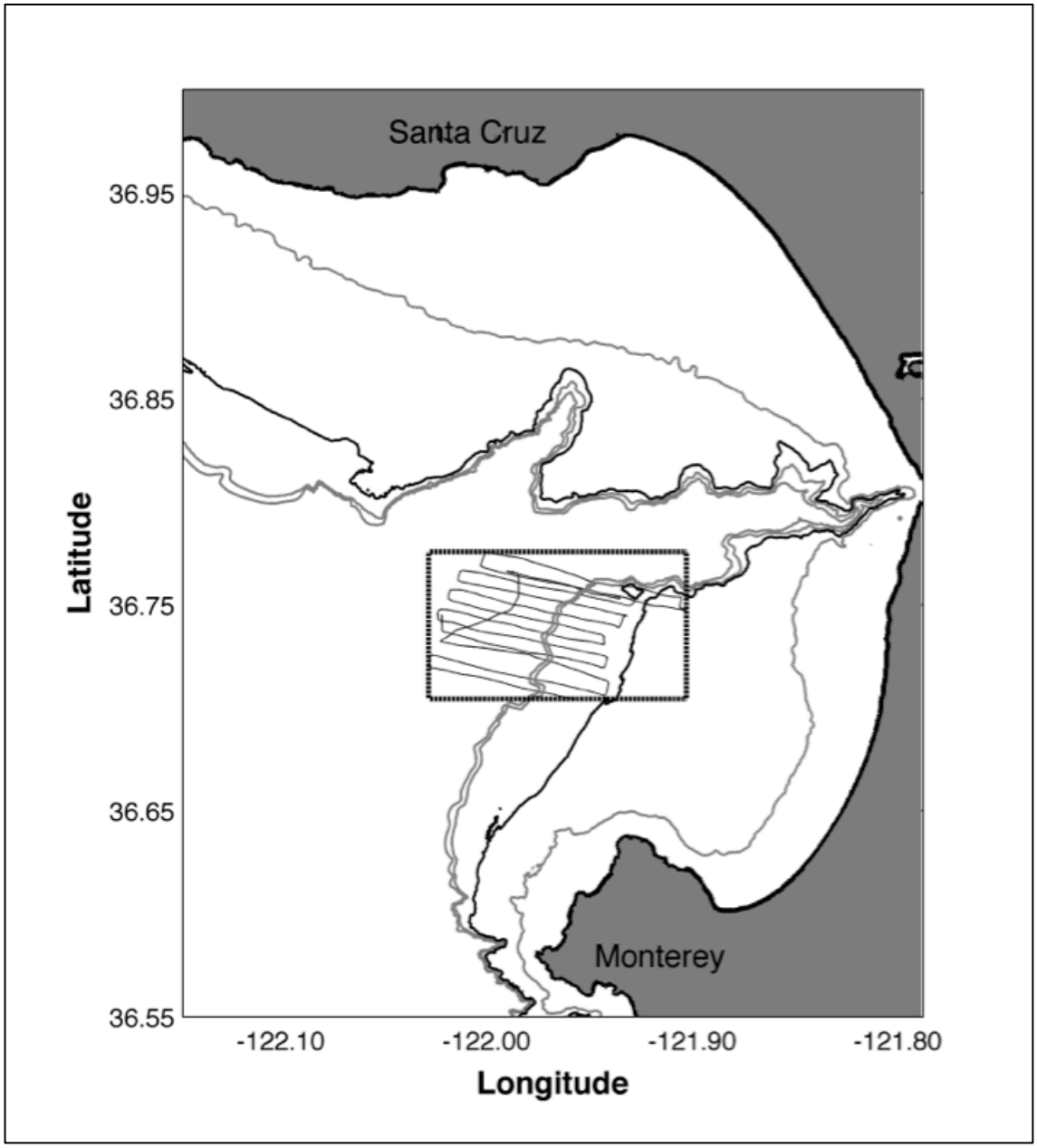

FIGURE 3.1: Map View of Foraging Habitat Survey in Monterey Bay, California showing shiptrack from the acoustic survey. Contours: 0 to 200 m in intervals of 50 m. Those of 0 and 100 m emphasized in black.

Data Collection and Processing – Acoustic Backscatter

Acoustic volume backscattering strength was measured from the surface to a depth of 185 m using a hull-mounted Simrad EY 500 (Simrad, Lynnwood, Washington) downward-looking echosounder. Data were collected on 22 August 1996, from 0800 h to 1630 h using two single-beam transducers transmitting at frequencies of 38 kHz and 200 kHz. The regularly spaced survey grid formed generally northwest-southeast elongated tracks (~6 km) oriented perpendicular to the canyon wall, and short, interconnecting northeast-southwest tracks (<1 km) (Figure 3.1). Due to poor data quality at 38 kHz, only the 200-kHz data were used for this study.

The acoustic data were integrated into 30-second horizontal and 5-meter vertical bins. A noise threshold was defined as the minimum mean volume backscattering coefficient (s_v, units of m^2/m^3) recorded at 150 m. To remove noise and the associated time-varied amplification, a $20\log_{10}(\text{depth})$ equation was developed to match the minimum at 150 m, and the resulting values, appropriate to each depth bin, were subtracted from the dataset.

To eliminate suspect returns, the top two depth bins (10 m) and one 5-meter depth bin above the bottom were removed, as were bins immediately adjacent (30 s) to the steep canyon walls if their values were greater than or equal to the bottom returns. Upon visual inspection, a few additional high-value data points that appeared to be associated with the bathymetry were removed. Depth to the bottom was corroborated using the National Geophysical Data Center (NGDC) bathymetric dataset.

Values for the unsampled regions between the tracklines were estimated using two-dimensional ordinary kriging, a geospatial interpolation technique (Isaaks and

Srivastava, 1989). A model fit to the empirical semi-variogram for each depth bin was used to interpolate volume backscattering coefficient (s_v) values onto a regularly spaced grid (EasyKrig: Chu, 1998) defined by the survey boundaries and a grid spacing of 400 m. The interpolated layers were stacked to create a 3-dimensional representation of the volume backscattering.

To delineate the area of interest within the interpolated volume, the kriged values were converted to mean volume backscattering strength (S_v, units dB re 1 m^{-1}, herein referred to as dB) by the following relationship (MacLennan *et al.*, 2002):

$$S_v = 10 * log_{10}(s_v) \qquad \text{EQUATION 3.1}$$

A cumulative histogram of estimated mean volume backscattering strength (S_v) for the entire volume was inspected and an isosurface threshold, -50 dB, was selected to highlight the most intense regions of the estimated backscatter. Using backscatter intensity as proxy for krill density, this region, 6.8% of the kriged values, defines the densest regions of the aggregations of krill.

Although we can not verify that the backscatter is attributable entirely to krill due to lack of direct sampling, previous studies have shown that the strong sound-scattering layer regularly found at depths of 100 to 200 m adjacent to the Monterey Bay Canyon walls is dominated by krill biomass (Schoenherr, 1991; Croll *et al.*, 2005). Of importance to this study is a location of markedly high measured backscatter. The high backscatter was measured throughout the horizontal and vertical dimension of the krill sound-scattering layer (SSL) traversed by the acoustic survey during Transect 1. The continuity of the high backscatter suggests that the survey ensonified a particularly

dense patch of euphausiids rather than encountering the rare but strongly scattering gas-bearing siphonophores that can contribute substantially to the measured backscatter in Monterey Bay (see backscatter modeling chapter of this dissertation). Therefore, in this study we use the measured acoustic backscatter as a proxy for krill biomass, and use S_v and krill biomass interchangeably. All calculations using acoustic data were made using the linear form, s_v, and then converted, using the relationship above, to the decibel form, S_v, for reporting.

Data Collection and Processing - Time-Depth Recorder

At 1200 h, a time-depth recorder (TDR) tag was attached 2-3 m behind the blowhole of a blue whale feeding within the boundaries of the hydroacoustic survey. The tag included three components: (1) a Wildlife Computers (Redmond, Washington) Mk 5 time/depth/temperature recording device (TDR); (2) a VHF radio transmitter (Advanced Telemetry Systems, Isanti, Minnesota) to track the tagged whale; and (3) a radio activated release mechanism (Jamie Stamps, Livermore, California). A more complete description of the TDR tag and the methodology employed to attach it is provided by Croll *et al*. (1998; 2001). The tagged whale is identified as "Bootsie" in the literature (Croll *et al.*, 2001).

Upon tagging, the whale was followed by a 15-m vessel at a distance of 100-200 m. For every surface interval, the behavior of the tagged whale was observed and recorded in the respiration data log. When the tag was released from the whale at approximately 1630 h, it was localized with a directional VHF system and recovered. Time, depth, and temperature were logged by the tag at 1-s intervals.

To generate a 3-dimensional representation of the whale's location over time, the latitudinal and longitudinal position of the whale at the surface was matched to the TDR data record based on the time of surfacing recorded in the respiration data log. The whale's position at each time stamp between the respiration data log entries was estimated using a linear interpolation for which the distance traveled in the horizontal plane was proportional to the time that had lapsed since the previous surfacing. The result is a 3-dimensional pseudo-track for the whale in which the depth of the whale at each time-step is the depth recorded by the tag, and the horizontal position at each depth location is a linear interpolation between the known positions at each surfacing.

To reduce the size of the TDR dataset, a subset consisting of every third position was extracted for use in subsequent analyses. The resulting dive record was examined for feeding-lunge behavior characterized by vertical excursions greater than 8 meters (Croll *et al.*, 2001) and the presence, within the characteristic depths of the lunge-feeding behavior, of a pause during the final ascent to the surface (Calambokidis *et al.*, 2007; Doniol-Valcroze *et al.*, 2011).

Data Analysis – Prey Field with Predator Behavior

The volumetric representation of the estimated mean acoustic volume backscattering strength (S_v), our proxy for the prey field structure, and the interpolated positions of the feeding blue whale were combined and visualized in 3-dimensional space. Each depth bin between 140 and 185 m, the depths in which the whale executed lunge behavior, was examined for the presence of high-density krill biomass, indicated by patches of intense backscatter (> -50 dB), and the co-location of whale positions.

The number and placement of the whale positions within the prey field for each 5-meter depth bin was assumed indicative of the foraging effort. To summarize the foraging effort, the mean volume backscattering coefficient (s_v) was integrated through the depths of 140 to 185 m, as was the number of whale positional data points. For later use in calculating foraging efficiency, estimated S_v was extracted from the volumetric representation of the prey field at each interpolated whale position.

Data Analysis – Foraging Efficiency

To calculate the foraging efficiency of the whale, both the energetic costs of the dive and the energy assimilated from the consumed prey need to be estimated. For this study, we assume a 25-m whale diving to 200 m as modeled by Goldbogen *et al*., (2011b; see their Table 3). The energy assimilated was calculated following Goldbogen *et al*., (2011a) using the S_v values calculated here, converted to krill biomass in units of kg m^{-3}. No net tows were available with this survey; therefore the conversion of S_v to krill biomass was constructed from the literature using the following procedure.

The length distribution of an assemblage of krill (after Croll *et al.*, 2005; see their Figure 6; "whale diet") was used to parameterize a euphausiid backscattering model to establish the mean volume backscattering strength (S_v) expected from the assemblage at 200 kHz. See Chapter 2 of this dissertation for details. The biomass of the assemblage was predicted using a length-to-weight conversion derived from Euphausiacea species (Mauchline, 1980)

$$log_{10}(weight) = 2.58 * log_{10}(length) - 4.52 \qquad \text{EQUATION 3.2}$$

for which the units of weight and length are grams and millimeters, respectively. The conversion was applied to each length in the assemblage, resulting in a prediction of the formalin-preserved wet weight. The formalin-preserved wet weights were converted to fresh wet weights by assuming a 15.4% weight loss associated with formalin preservation (Kulka and Corey, 1982). The resulting conversion of S_v to krill biomass in units of g m^{-3} is as follows:

$$log_{10}(biomass) = 0.1 * S_v + 6.5348 \qquad \text{EQUATION 3.3}$$

To determine appropriate S_v values to convert to krill biomass we considered both the interpolated and the measured prey-field data. The interpolated prey-field data allows us to examine foraging efficiency on a per-dive basis. Each time-step of the whale track was coded with the S_v value extracted from the interpolated prey-field data, and the acceleration or deceleration rate computed from the dive record. The ascent-portion of each lunge, including the portion of the final ascent within the lunge depths, was examined for evidence of the feeding engulfment sequence consistent with ram feeding events (Goldbogen *et al.*, 2006; Calambokidis *et al.*, 2007). If the sequence was present in the coded dive track, and the position of maximum deceleration co-occurred with encounter of backscatter greater than our threshold of -50 dB, the position of maximum deceleration was considered a reliable indicator of an engulfment event.

Without the benefit of additional data (e.g., from audio, visual, and multiple-axis accelerometer instruments), we know the whale's behavior only in the vertical plane, from which it is difficult to confidently identify the locations of feeding bouts (Goldbogen *et al.*, 2006; Calambokidis *et al.*, 2007; Hazen *et al.*, 2009). Therefore,

multiple schemes were employed to identify the S_v at which the whale may have been feeding, including a best-case scenario of maximum S_v encountered during the ascent portion of each lunge. If a pause in the vertical ascent was evident in the lunge-feeding depths during the final ascent to the surface, it was counted as a feeding event (Calambokidis *et al.*, 2007; Doniol-Valcroze *et al.*, 2011) and included in the foraging efficiency calculation for that dive.

Recognizing that the foraging efficiency calculated using the interpolated movement of the whale through the interpolated prey field may not be fully representative of the range of foraging efficiencies experienced by the whale, we made additional calculations using S_v values measured nearest the locations at which the whale was diving. For these additional calculations of foraging efficiency, engulfment events per dive were assumed to be two, the average number of feeding bouts found in this data set.

Using each of the S_v scenarios above, and the S_v-to-biomass conversion (Equation 3.3), a krill density (kg m^{-3}) was specified for each engulfment event. Assuming an engulfment volume of 80 m^3 (Goldbogen *et al.*, 2011a), the biomass of krill ingested was calculated and then converted to energy assimilated using a conversion factor of 4,600 kJ kg^{-1} krill (Clarke, 1980) and an assimilation efficiency of 84% (Goldbogen *et al.*, 2011a). The energy for each feeding bout was then summed to determine the total energy obtained from each dive. A metabolic energy cost of 6,300 kJ (Goldbogen *et al.*, 2011b) was multiplied by the number of lunges per dive and added to the active metabolic rate (AMR) of 41,403 kJ (Goldbogen *et al.*, 2011b) to account for the costs of the dive and surface time. The foraging efficiency for each dive was

calculated as the ratio of total energy obtained from krill ingested during the dive divided by the total metabolic energy costs for the foraging dive including recovery time (Williams and Yeates, 2004; Goldbogen *et al.*, 2011a). The active metabolic rate of 41,403 kJ reported by Goldbogen *et al*., (2011b) includes the costs associated with the filtering phase for the 3.5 feeding lunges per dive assumed in their study. Therefore, the metabolic costs used here are somewhat overstated and result in conservative estimates of foraging efficiency.

To assess the stability of the results of our analysis, additional calculations of the foraging efficiency estimates were made. These additional estimates tested (1) the sensitivity to the prey size assumption by using single-size krill-length assemblages of 16 mm, 18 mm, 26 mm and 28 mm to bracket the mixed-length assemblage, mean 22.2 mm, used here, (2) the sensitivity to the number of engulfment lunges per dive by assuming one, three, and four, in addition to the two used here, completing the range of engulfments per dive found in this dataset, and (3) the sensitivity to the predator size by using the parameters for a 22 m and 27 m whale as reported by Goldbogen *et al*., (2011b).

RESULTS

Foraging Habitat

High intensity backscatter was recorded within 1 km of the canyon wall along a 5 km stretch. The long axis of the sound-scattering layer (SSL) was generally parallel to the canyon wall. The width of the SSL was approximately 600 m and found at depths of

140 m or deeper. The three-dimensional rendering of the interpolated acoustic backscatter revealed that the SSL decreased in areal extent through the depths of 160 m to the maximum depth recorded by the transducer at 185 m. The backscattering within the layer was one to two orders of magnitude greater than background scattering levels outside the layer.

A region of markedly high backscatter was measured when the acoustic survey traversed the SSL during Transect 1. This region was notable because, unlike other regions traversed by the transects, the high backscatter (mean: -36.3 dB and median: 36.7 dB or 800 g m^{-3} and 730 g m^{-3} of krill, respectively) was consistent throughout the horizontal (~ 600 m) and vertical (depths including 140 m thru 185 m) dimensions of the SSL (Figure 3.2). We will refer to the SSL found adjacent to the canyon wall as the "foraging habitat", and the region of markedly high backscatter within that habitat as the "patch". Background scattering levels within the habitat, exclusive of the patch, were -44.8 dB and -53.0 dB corresponding to krill biomass of 110 g m^{-3} and 20 g m^{-3}, mean and median, respectively. Acoustic measurements along transects 1 through 8 of the survey were completed before the whale was tagged. A second region of strong backscattering, found 3 km away from the canyon wall, outside the boundary of the whale movement, and at depths of 140 m to 160 m was not investigated in this study.

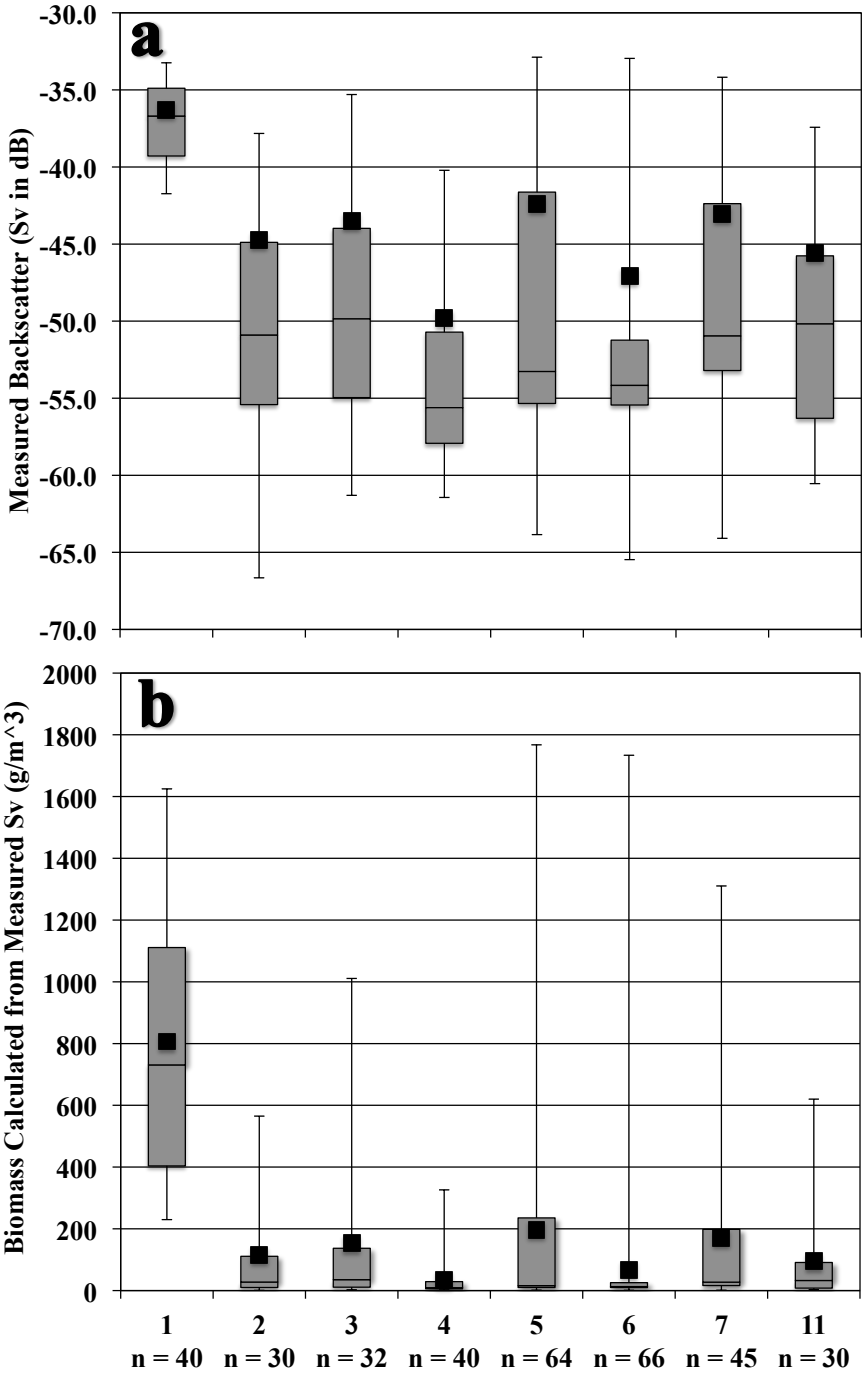

FIGURE 3.2: Boxplots of Backscatter and Euphausiid Biomass "Foraging Habitat"
For the seven transects oriented normal to the canyon wall, boxplots of a) measured backscatter (Sv in dB), and b) euphausiid biomass (g m-3) calculated from measured backscatter. Criteria for inclusion: depth range 140 m to 185 m within the sound-scattering layer along each transect. Only transect within the boundary of the area foraged by the whale are included. Shaded box designates the rang of the interquartile with line marking the median. Whiskers designate range to minimum and maximum. Solid squares designate the mean. Data are for all pings for which any value in depth bins 26 through 35 was greater than -45 dB.

Whale Dive Record – Movement and Interactions with Prey Field

All recorded whale movement took place within the surveyed foraging habitat (Figure 3.3), with the whale diving below the SSL and then lunging up through it. Twenty-four dives were recorded in which the whale dove to maximum depths of 145 to 198 m (172.8 and 14.72, mean and standard deviation, respectively). At the bottom of the dives, the whale lunged up to 4 times with a mean of 2.1 lunges per dive (S.D. 0.9) (Figure 3.4). Additional data on the dive behavior of the whale during this survey can be found in Croll *et al.* (2001). Because transects 1 through 8 of the acoustic survey were completed before the whale was tagged, all reported whale movements within the foraging habitat were nearly simultaneous with the acoustic measurements and those measurements used in referencing the whale movement relative to the foraging habitat are not confounded by post-feeding prey-field depletion by this whale.

Examination of the whale positions in the lunge-feeding depths showed good agreement between the interpolated 3-dimensional positions of the whale and the kriged prey-field structure (Figure 3.5). In the depths where the areal extent of the high-density patch narrows, the focal zone of the whale positions in those depth bins reflects that narrowing, indicating the targeting of the high-density region by the whale. Fifty six percent of the total time the whale spent in the lunge behavior depths of 140 to 185 m was spent in this region of the most intense mean volume backscattering strength (Figure 3.6). A map-view with a connecting line between the start positions of each of the dives shows that the net movement of the whale was generally parallel to the long axis of the elongated sound-scattering layer.

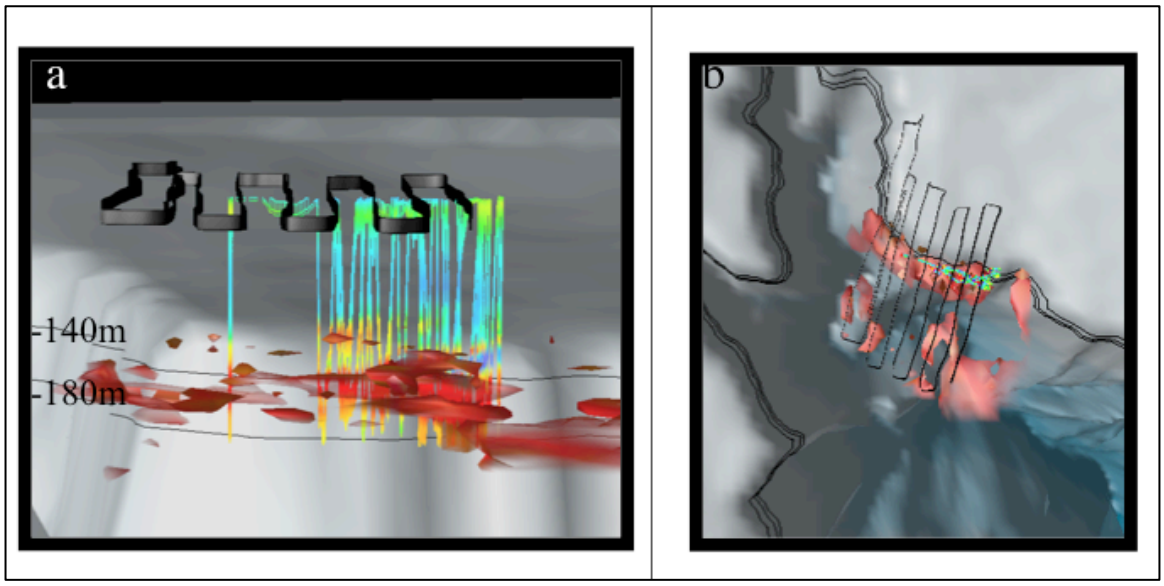

FIGURE 3.3: Whale Dive Track, Canyon, and Krill Prey Field
Pseudo-track of whale dive behavior and foraging habitat, a) side view and b) top view. Whale track: color designates backscatter intensity (proxy for krill density) through which the whale is diving. Foraging habitat: red patches designate regions where interpolated Sv dataset exceeds -50 dB. Acoustic survey trackline: black. Bathymetry: grey region for which contour lines designate depths of 140 m to 180 m.

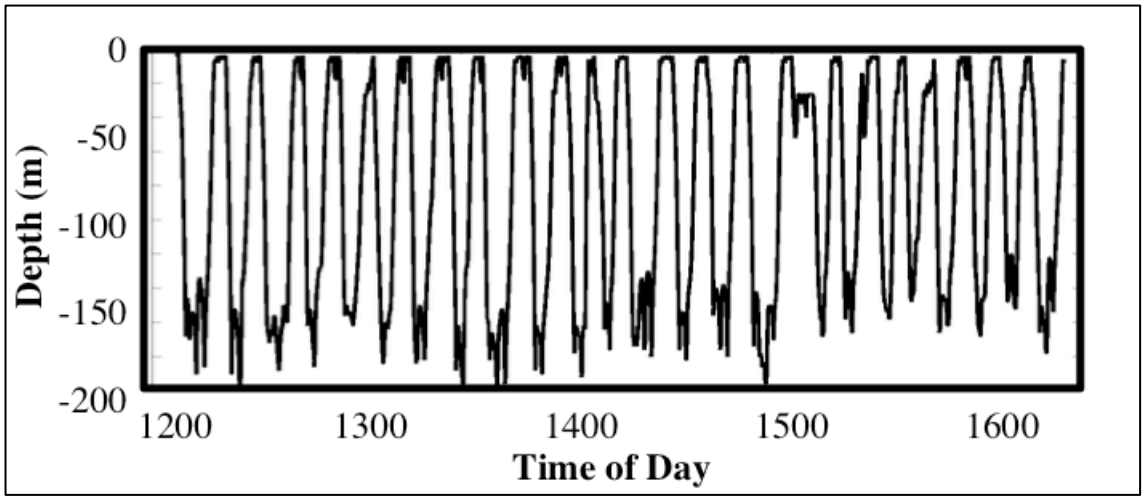

FIGURE 3.4: Time Depth Record of Whale Dive Behavior
as recorded by the time-depth recorder attached to the whale.

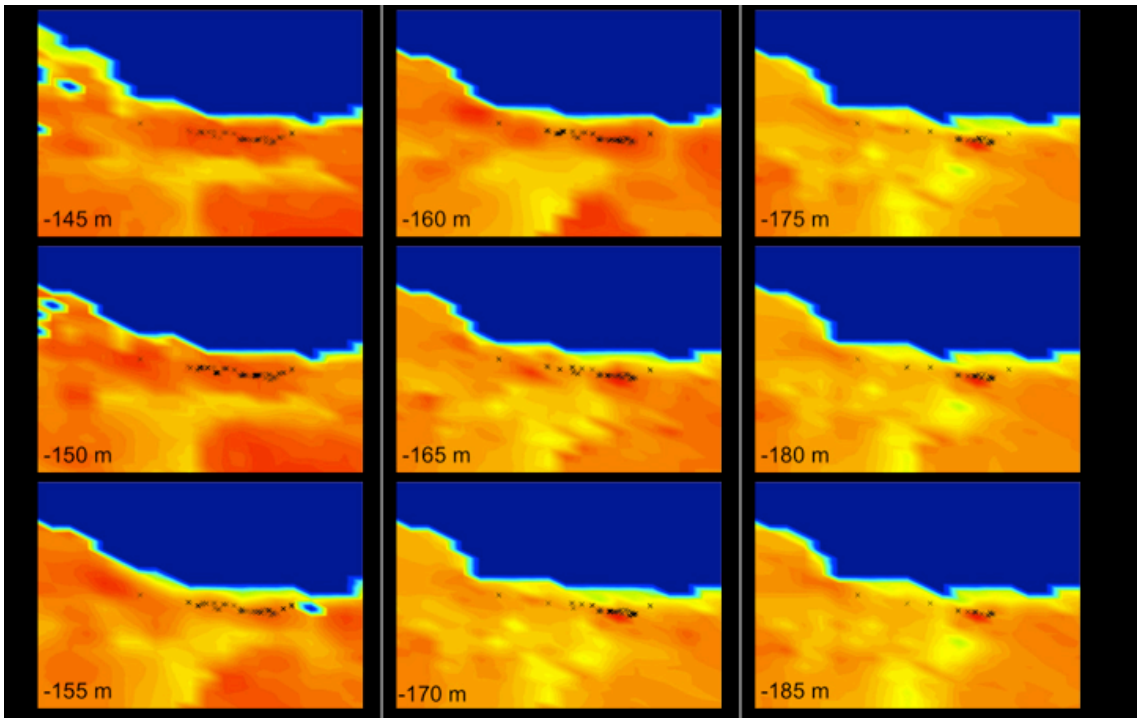

FIGURE 3.5: Co-location of Interpolated Whale Positions and Krill Hotspot
Nine panels showing map view of canyon shelf (blue) and interpolated backscatter (S_v; yellows and oranges). Numbers in each panel designates the depth bin. Interpolated location of whale in each depth bin is included (black x). Whale location shows good agreement with patches of high-density krill (intense backscatter), and focuses its diving in the discrete, high-density patch (deep orange).

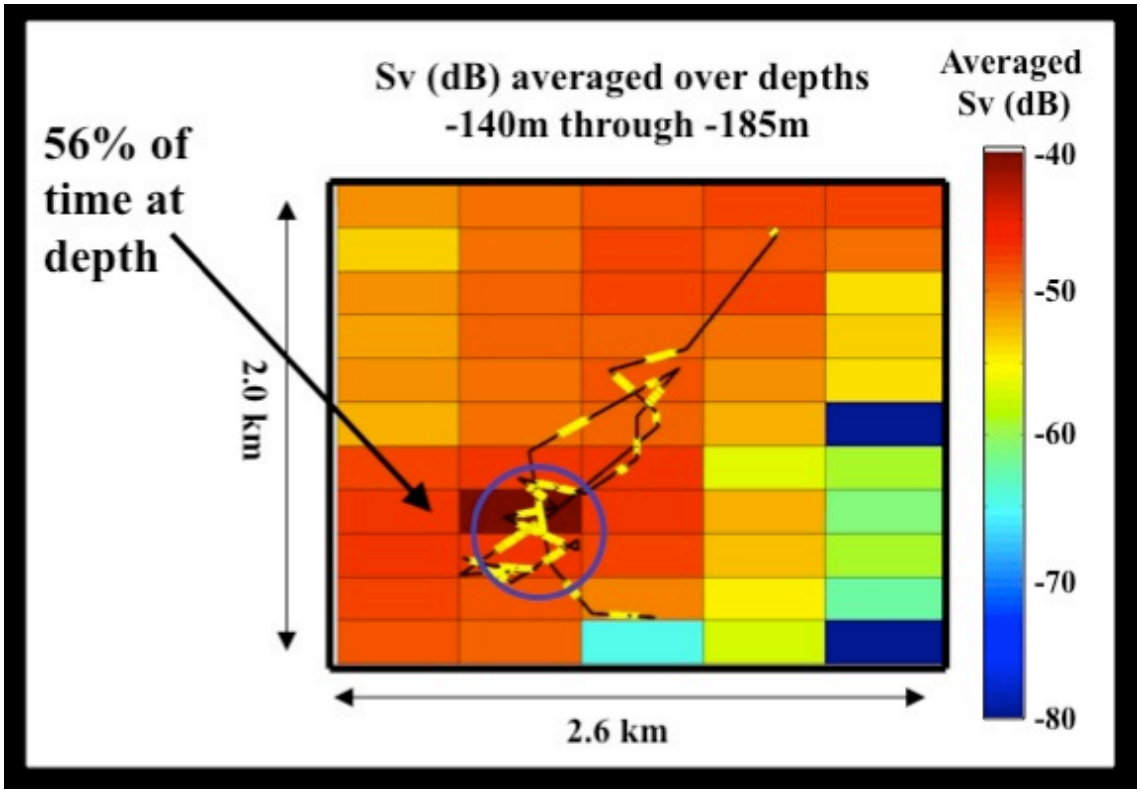

FIGURE 3.6: Map View of the Gridded Prey Field and Whale Positions
Gridded image was constructed with interpolated backscatter averaged through the depths of the lunge-feeding behavior (140 m through 185 m). Black line denotes surface expression of the movements of the whale. Each yellow X marks the pseudo-track position for each log entry from the tag for which the whale was in the depths of 140 m through 185 m. The number and placement of the whale positions (yellow X's) is assumed indicative of the foraging effort. The long axis of the foraging habitat, and the whale movement, was generally parallel to the canyon wall. Placement of the canyon wall is just off the lower right of the image (blue region designates canyon wall or shelf).

A description of that movement (Figure 3.7) is as follows. The whale executed two sequences consisting of three dives followed by a ~ 1 km traverse at the surface. The horizontal ground covered while submerged was ~ 400 m and less than 150 m for the first two dives and the third dive of each sequence, respectively. Very low turning angles between the dives kept the whale on a trajectory generally parallel to the long axis of the SSL. At Dive 7 near our Transect 1, after the second 1 km traverse at the surface, the whale first encountered elevated backscatter. Rather than surfacing 400 m away as seen for the dives in the two three-dive sequences, the whale surfaced 600 m away and began a sequence of four dives (Dive 8 thru 11) for which the movement shifted from the long-axis trajectory to perpendicular, for which the distance between surfacings was ~ 200 m, and for which the azimuth change between dives were nearly 180° keeping the whale over a 200 m sector of the krill SSL for the four dives. The cumulative horizontal distance traveled by the whale and its cumulative net horizontal displacement from the origin diverged at Dive 7, consistent with the commencement of dives with tighter turning angles (Figure 3.8). After completing Dive 11, the whale began a sequence of five dives, 12 through 16, for which the turning radius was still high, but not 180°, resulting in a generally zigzag pattern involving a greater perpendicular component than the original along-habitat movement, but still resulted in net movement generally parallel to the long-axis of the habitat. The net distance offset for these dives ranged from ~ 200 m to ~ 400 m. The end of this sequence brought the whale back to the region of Dive 7, where it first encountered the high concentration of krill. After reoccupying the area near Dive 7, the whale began a sequence of dives with characteristics similar to the original; the distance covered while submerged was

~ 400 m to ~ 500 m and the movement was again generally parallel to the long-axis of the foraging habitat. These dives, 17 through 22, were executed in the ~ 1 km distance between Dive 7 and Dive 6 for which the distance between these two dives was originally transected while the whale was at or near the surface. Dive 17 through 19 were “inside”, between the surface transect and the canyon wall, bringing the whale to the area near Dive 6. The whale then reversed its net direction and Dives 20 through 22, “outside” the surface transect, brought the whale again to the area near Dive 7 occupying that location for the third time. In Dive 22 the whale moved 800 m through the region of the elevated backscatter while submerged. Once past that area, the whale executed Dive 23 covering 400 m and at Dive 24 the tag was released and recovered.

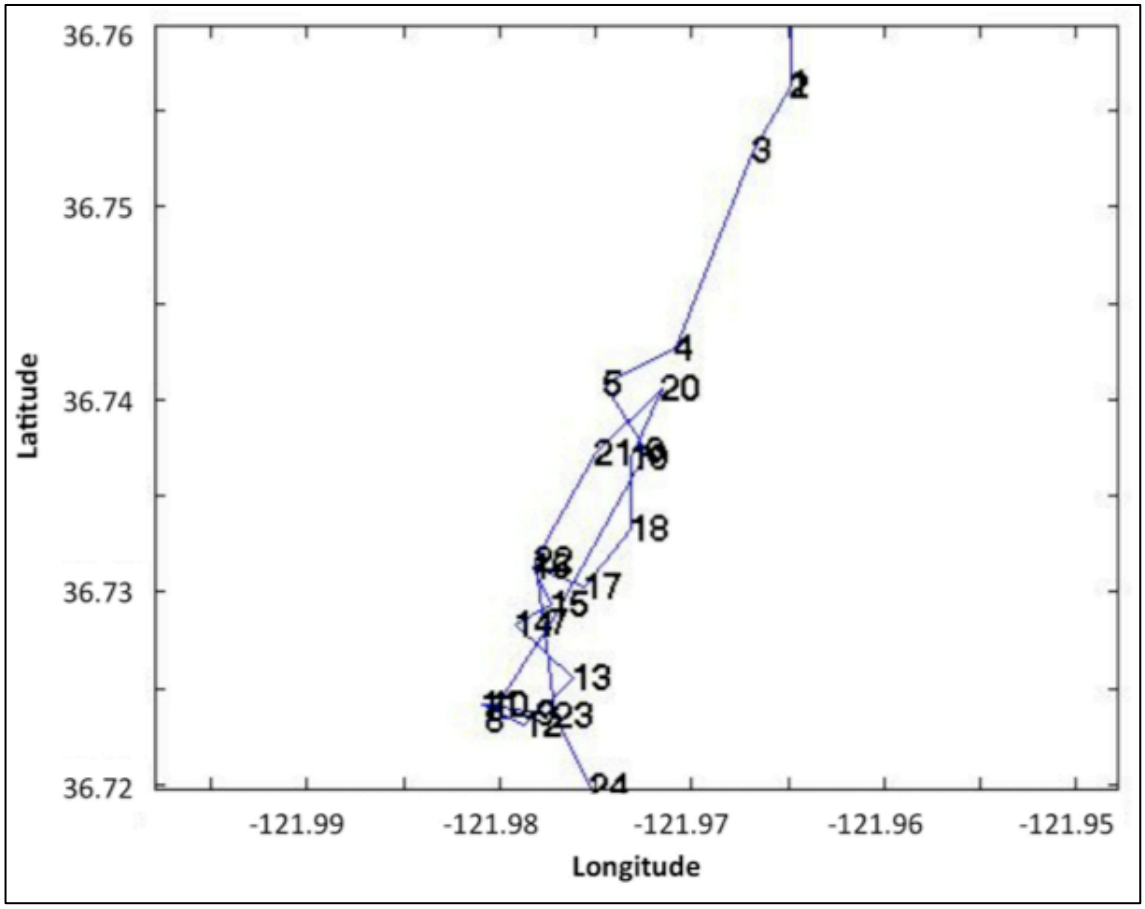

Figure 3.7: Map View of Whale Dive Start Locations
Blue line denotes surface expression of the movement of the whale. Numbers denote location of start position for each of the 24 deep dives.

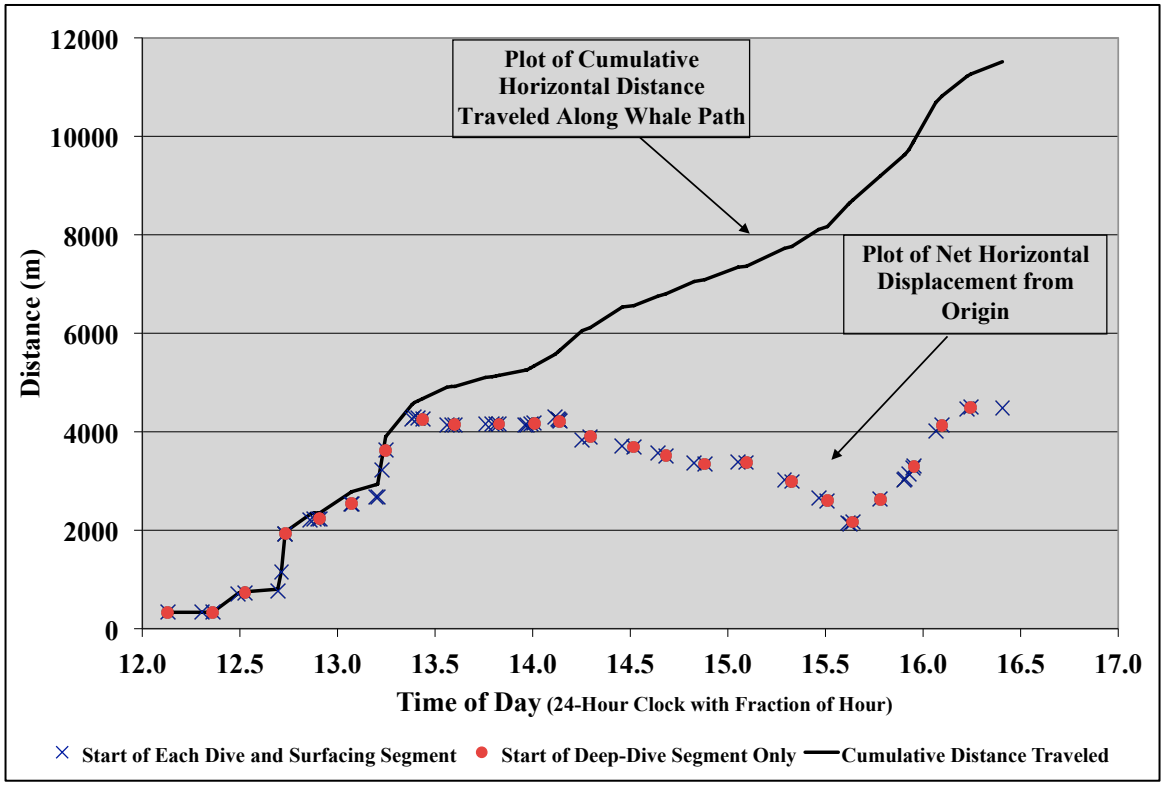

Figure 3.8: Cumulative and Net Horizontal Displacement from Origin
From the location of the first dive, cumulative horizontal displacement of the whale (line), and net horizontal displacement distance (glyphs). Consistent with the start of tight turns between dives, the two lines diverge after Dive 7 where the whale first encountered elevated krill density. Blue x marks the start of each dive and location of surfacing. Red circle marks the location of the start of deep dives only.

Whale Foraging – Engulfments and Foraging Efficiency

Detailed examination of the whale dive through the interpolated prey field data provides little insight as to where engulfment events occurred along the dive track. Ascents three and four of Dive 1 exhibit behavior consistent with the literature (Goldbogen *et al.*, 2006; Calambokidis *et al.*, 2007): on the ascent phase of the lunge, acceleration consistent with readying an increase in attacking speed was followed by maximum deceleration co-located with the high backscatter indicative of the increased drag forces due to mouth opening at the onset of a high biomass of prey. However, the evidence was not nearly so consistent with expectations based on the literature for the remaining two lunges of Dive 1, and for the remaining 23 dives.

Given the inability to identify definitive engulfment locations, six scenarios were used to extract representative Sv from the interpolated prey-field data along the ascent phase of each lunge. None of the scenarios resulted in estimates of the foraging efficiency, on a dive-by-dive basis, consistently greater than one. The calculations using the measured backscatter from Transect 1 resulted in estimated foraging efficiencies from 2.6 to 18.6 with a median of 8.4. The median foraging efficiency calculated within the SSL for each of the other transects was 0.5 leaving Transect 1, the region in which the whale focused its foraging dives, the only transect for which the foraging efficiencies exceeded one throughout the horizontal (~ 600 m) and vertical (depths including 140 thru 185 m) dimensions of the SSL (Figure 3.9). The foraging efficiencies reported here were based on the variability of the backscatter measured throughout the foraging habitat and a stable set of assumptions (e.g. two engulfments per dive, krill length distribution) allowing us to use the resulting foraging efficiency to

examine the foraging behavior of the whale in the context of the prey field variability. The tests of the stability of the estimated maximum foraging efficiency suggest that the above value for the region where the whale focused its foraging may range from a low of 10 (25 m whale, one engulfment, 18 mm krill), to a high of 45 (22 m whale, four engulfments, 28 mm krill).

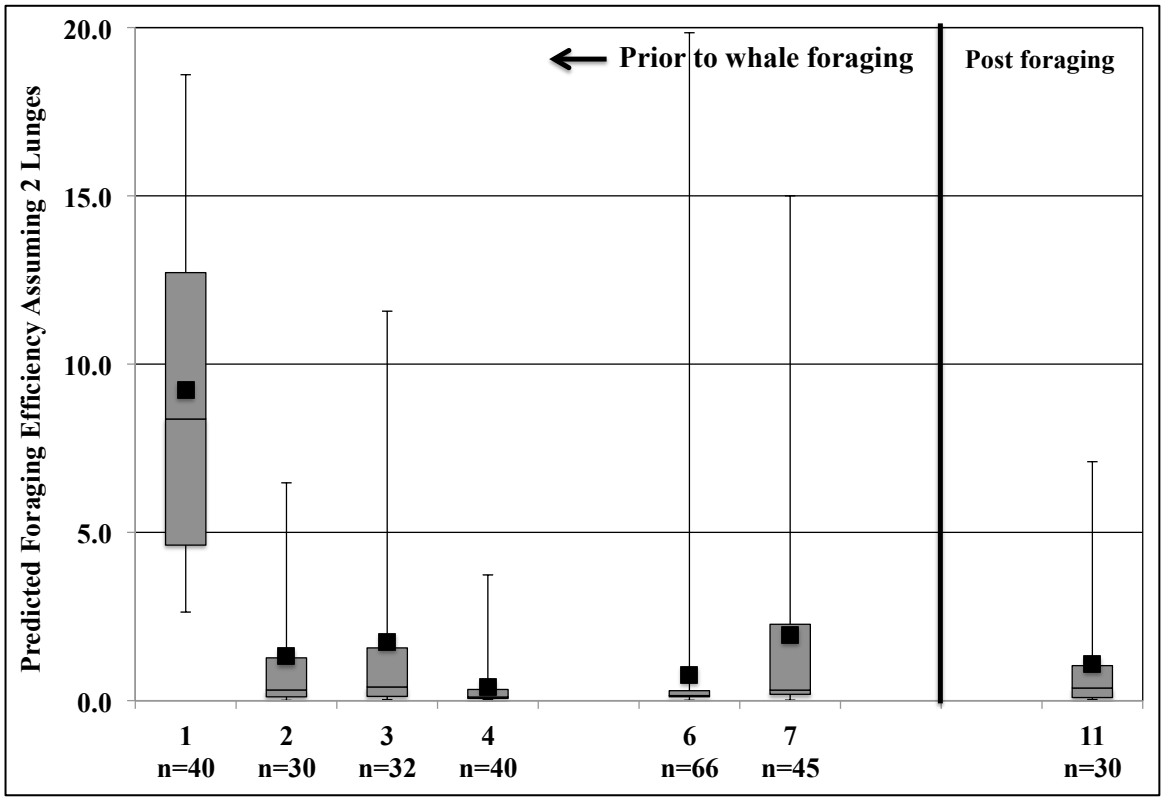

Figure 3.9: Ranges of Potentially Achievable Foraging Efficiency
estimated in depth range 140 m to 185 m within the sound-scattering layer along each transect. Only transects near which the foraging whale dove are shown. Transect 11 reoccupied the region near the strong backscattering of Transect 1 after the whale foraged. Shaded box designates range of the interquartile with line marking the median. Whiskers designate range to minimum and maximum. Solid squares designate the mean.

DISCUSSION

The work of Schoenherr (1991) and Croll and colleagues (1998; 2005) showed that feeding blue whales in Monterey Bay concentrate their foraging efforts in the dense krill aggregations that are found in elongated sound-scattering layers (SSL) adjacent to the canyon walls. Building on their work, we present compelling evidence that within these elongated foraging habitats of high krill biomass, a blue whale will focus its feeding effort in patches where the achievable foraging efficiency is markedly higher than in other portions tested and rejected by the whale. In this case, the region of focus was a hotspot in which the markedly higher backscatter was found throughout the horizontal and vertical dimensions of the SSL, and in which the estimated achievable foraging efficiencies were an order of magnitude greater than the background levels within the habitat. In addition, the behavior of the whale within the context of its prey-field structure suggests that the foraging strategy employed by the whale is consistent with theory. Two different but complementary data streams were used. Measured backscatter was used to quantify the foraging efficiency potentially experienced by the whale. Interpolated data, providing a three-dimensional representation of the behavior of the whale in the context of the prey-field structure, proved valuable in providing insight when comparing behavior to theory.

The location of the strongest backscatter measured in each depth bin of the lunge-feeding depths is within the hotspot found in the SSL. This location, on Transect 1, is notable not only due to the strength of the backscatter but also that the markedly high backscatter is consistent throughout the horizontal and vertical

dimensions of the SSL traversed by the transect. All other transects recorded a maximum backscattering level within the range of the scattering found in Transect 1, but those maximum levels are outliers and not representative of the backscattering found on each of those transects; and therefore, not representative of the krill biomass found at those locations (Figure 3.2). The consistently high backscatter measured during Transect 1 suggests high krill biomass throughout the horizontal and vertical dimensions of the SSL and therefore consistently high krill biomass in the depths in which the whale was feeding. The krill biomass estimated from the measured backscatter suggests that the median of the biomass found in the hotspot is 730 g m^{-3} whereas the median for all other transects is less than 40 g m^{-3}. Converting the biomass to foraging efficiency revealed a median of 8.4 for the foraging potentially attainable within the SSL on Transect 1, in contrast with the median on all other transects at less than 0.5. As none of the other transects had a biomass density sufficient to consistently exceed a foraging efficiency of one, interpretation of the whale's behavior may indicate that the whale targeted the region of highest biomass, or indicate the whale targeted biomass consistently high enough to exceed a foraging efficiency of one, the threshold at which the whale is assimilating sufficient biomass to offset the metabolic costs of the foraging dive. It is significant, however, that after testing and rejecting other measured regions of the prey field, the focus of the whale foraging was coincident with the highest measured backscatter, our proxy for krill biomass.

To examine these data for insight into the foraging tactics potentially employed by the whale, we sought to quantitatively characterize the predator's three-dimensional prey field and to track the predator's foraging behavior within that prey field. Two

assumptions were inherent in the construct of the three-dimensional analysis. First, the structure of the prey-field, and therefore the relative density of krill throughout foraging habitat, did not materially shift between the time that it was ensonified and the time when the whale foraged in those measured areas. Second, the SSL exhibited isotropic properties indicating that the spatial structure of the krill aggregations measured in the along-transect direction is representative of the spatial structure in the between-transect direction. A third factor impacted the quantification of the prey-field structure: due to analytical limitations, the geospatial interpolation smoothed the extremes of the prey-field values. It did, however, retain sufficient dynamic range to highlight hotspots within the foraging habitat, suggesting that the interpolation characterizes the distribution of the krill SSL but underestimates the concentrations within high-biomass patches. The dynamic range, in conjunction with the co-location of the pseudo-track of the whale and the prey-field hotspot, all the way down to 185 m where the hotspot narrows considerably, provided persuasive evidence that the interpolations were sufficient for use in gaining insight into the movements of the whale in the context of the prey-field structure.

The interpolated three-dimensional prey-field data revealed a structure characterized as a hierarchical patch system in which there are high-density patches at small scales nested within a low density foraging habitat at a larger scale (e.g. Fauchald, 1999). The behavior exhibited by this whale is consistent with optimizing search behavior in a hierarchical patch system when no information is available about the position of high-density patches: search in generally straight line with long distances between sampling (Bell, 1991; Fauchald, 1999). In this case, the whale performed

sampling dives with a net horizontal movement of ~ 400 m interspersed with ~ 1 km treks at the surface, all generally parallel to the long axis of the habitat until it first encountered elevated prey density. We interpret the behavior of these initial dives to indicate sampling dives for which the prey density encountered was insufficient. Consistent with the benefit of altering behavior in response to the perceived local prey density in the patchy environment (Thompson and Fedak, 2001), at the first encounter with elevated krill biomass, the whale executed a particularly long dive, ~ 600 m between surfacings. This long dive may indicate that the whale changed its behavior to "local search" (Bell, 1991) and used its time while submerged to trace the prey concentration gradient to the location of highest density, thereby targeting the location at which to begin patch exploitation: upon surfacing from this dive the whale commenced a sequence of dives for which the distance of, and the turning radius between, kept the whale over a 200 m sector of the krill SSL, rather than continuing on a trajectory parallel to the long axis of the habitat.

After completing the last of the in-patch sequence of four dives, a generally zigzag trajectory between dives brought the whale back to the region of Dive 7. This behavior may be indicative of the whale the exploiting region of elevated backscatter between the high-density patch of Dives 8 through 11, and Dive 7 where it first encountered the elevated prey concentration. After reoccupying the area near Dive 7, the turning radius decayed further and the whale began a sequence of fairly straight, ~ 400 m dives between the locations of Dive 7 and Dive 6. The ~ 1 km distance between these two dives was originally transected while the whale was near the surface. This behavior of sampling within the ~ 1 km region originally passed over is consistent with

testing for overrun errors (Krebs *et al.*, 1983). The whale then moved through the original high-concentration patch executing Dive 22, moving ~ 800 m while submerged. Having passed out of the region of its foraging, the whale then continued its original, fairly straight, trajectory generally paralleling the long axis habitat executing ~ 400 m dives, suggesting that the whale had completed its foraging in the area. Dives 23 and 24 were executed and the tag was released and recovered.

Following the whale's departure from the patch, but before Dive 22 its last pass through the patch region, the acoustic survey made a second pass within 30 m of the location of highest measured backscatter. With Transect 11, we now had measurements post-foraging to compare with measurements collected pre-foraging on Transect 1. The backscatter measured post-foraging was comparable to the habitat background scattering intensity. We considered whether the whale may have depleted the patch to background densities, however, estimates of the prey consumed by the whale during its foraging in the patch could not account for the biomass difference. An alternative explanation for the difference is that the dense initial aggregation inferred from the acoustic survey either moved or dispersed in response to the recurrent foraging, leaving the density at the site of the original aggregation at background levels. Although patch depletion through consumption couldn't account for the difference between the pre- and post-foraging measurements, the measurements do support the earlier observations that the krill aggregations at the background densities measured in this habitat are not sufficient for a whale to focus its foraging. In this way the whale maximizes the net energy intake by focusing its foraging on a dense aggregation of prey until the location

is depleted to background levels through consumption, advection, or dispersion. See Bell (1991) for a review of predator moving-on threshold decisions.

No dive characteristic (horizontal displacement during the dive, turning radii between dives, dive duration, or number of lunges performed during the dive) by itself was sufficient to signal the patch quality experienced by the whale. Concurrent changes in the horizontal displacement during a dive and the turning radii between dives appears to be the best dive-record signal of the patch quality experienced by the whale, although the interpretation of these is confounded by the decay in the turning radii while maintaining ~ 200 m horizontal displacement during each dive after the whale left the location of the four in-patch dives. The resulting zigzag trajectory that brought the whale back to the location of Dive 7, where it first experienced the elevated prey density, may be indicative of an intermediate prey density but without higher resolution data set, we cannot discern whether the decay in turning radii was a response to environmental cues or a search tactic employed upon departure from a high-quality patch.

The number of lunges performed by a whale during its foraging dive has been suggested as indicative of the prey-patch quality (Goldbogen *et al.*, 2008). Given the presence of the patch of markedly high biomass, we expected to observe a significant increase in the number of lunges per dive co-located with the patch. We did not find that here. Potential explanations include: 1) the number of engulfments for each dive was estimated from the behavior recorded by a TDR tag which has been shown insufficient for confidently quantifying engulfments (Goldbogen *et al.*, 2006; Calambokidis *et al.*, 2007), 2) the prey-patch quality was measured at temporal and

spatial resolutions that preclude an exact quantification of the prey density the whale experienced during each individual dive, and 3) the foraging energetics required for lunge feeding at depth. The model developed by Goldbogen et al., (2011a) suggests that the metabolic costs to execute a lunge are 10-20% of the energy loss generated by the dive to reach the prey at 200 m. Therefore the threshold at which an optimal forager might execute a lunge may include what otherwise might be deemed an insufficient patch. As long as the net energy gained from the lunge itself is greater than the cost of the lunge, performing a lunge will contribute an offset to the cost of the dive to reach the patch, thereby providing a benefit even if it does not provide enough to completely offset the total cost of the dive. Executing engulfment lunges in suboptimal patches is consistent with modeled optimal dive behavior when the model is parameterized with prey-patch quality and depth to prey: net benefit gained by terminating dives in suboptimal patches was reduced with deeper dives (Thompson and Fedak, 2001). A positive consequence to executing multiple engulfment lunges, is that with each added engulfment during a dive, the prey density required for achieving a foraging efficiency for the entire dive is lowered. Optimizing the number of lunges for a given dive requires assessing the competing demands: 1) the commitment to the cost of a dive in order to gain information about prey density, 2) as an air breather, the time available for searching and feeding while submerged is limited, and 3) high quality patches of prey are a subset of the foraging habitat.

CONCLUSION

In this paper, we analyzed the behavior of an individual tagged blue whale as it was tracked while foraging in the Monterey Bay Submarine Canyon. The three-dimensional prey field experienced by this diving predator was reconstructed and visualized from acoustic survey data collected in the vicinity of the foraging whale. The results of our analysis provide compelling evidence that the whale focused its foraging effort in a discrete high-density patch within the foraging habitat. Krill abundance estimates inferred from the acoustic data allowed us to quantify the potential foraging success experienced by the whale. The results indicate that the prey abundances and subsequent foraging efficiencies experienced by the whale while it was feeding in the patch were at least an order of magnitude higher than in other locations tested and rejected by the whale. Although one must be cautious in interpreting results from the observations of a single whale, this study provides unique insights into the tactics that may be employed by blue whales and other diving predators as they explore and exploit a three-dimensional prey environment that is patchy in both time and space.

REFERENCES

Acevedo-Gutierrez, A., Croll, D. A., and Tershy, B. R. (**2002**). "High feeding costs limit dive time in the largest whales," Journal of Experimental Biology **205**, 1747-1753.

Barlow, J., and Forney, K. A. (**2007**). "Abundance and population density of cetaceans in the California Current ecosystem," Fishery Bulletin **105**, 509-526.

Bell, W. J. (**1991**). *Searching Behaviour: the behavioural ecology of finding resources* (Chapman and Hall, London).

Benson, S. R., Croll, D. A., Marinovic, B. B. *et al.* (**2002**). "Changes in the cetacean assemblage of a coastal upwelling ecosystem during El Niño 1997-98 and La Niña 1999," Progress in Oceanography **54**, 279-291.

Block, B. A., Jonsen, I. D., Jorgensen, S. J. *et al.* (**2011**). "Tracking apex marine predator movements in a dynamic ocean," Nature **475**, 86-90.

Brinton, E. (**1962**). "The Distribution of Pacific Euphausiids," Bulletin of the Scripps Institution of Oceanography of the University of California, La Jolla, California **8**, 51-270.

Burtenshaw, J. C., Oleson, E. M., Hildebrand, J. A. *et al.* (**2004**). "Acoustic and satellite remote sensing of blue whale seasonality and habitat in the Northeast Pacific," Deep-Sea Research Part II-Topical Studies in Oceanography **51**, 967-986.

Calambokidis, J., Schorr, G. S., Steiger, G. H. *et al.* (**2007**). "Insights into the underwater diving, feeding, and calling behavior of blue whales from a suction-cup-attached video-imaging tag (CRITTERCAM)," Marine Technology Society Journal **41**, 19-29.

Calambokidis, J., Barlow, J., Ford, J. K. B. *et al.* (**2009**). "Insights into the population structure of blue whales in the Eastern North Pacific from recent sightings and photographic identification," Marine Mammal Science **25**, 816-832.

Chu, D. (**1998**). "The GLOBEC Kriging Software Package - EasyKrig 2.1," (Woods Hole Oceanographic Institution).

Clarke, A. (**1980**). "The biochemical composition of krill, *Euphausia superba* Dana, from South Georgia," Journal of Experimental Marine Biology and Ecology **43**, 221-236.

Croll, D. A., Tershy, B. R., Hewitt, R. P. *et al.* (**1998**). "An integrated approach to the foraging ecology of marine birds and mammals," Deep-Sea Research Part II-Topical Studies in Oceanography **45**, 1353-1371.

Croll, D. A., Acevedo-Gutierrez, A., Tershy, B. R. *et al.* (**2001**). "The diving behavior of blue and fin whales: is dive duration shorter than expected based on oxygen stores?," Comparative Biochemistry and Physiology a-Molecular & Integrative Physiology **129**, 797-809.

Croll, D. A., Marinovic, B., Benson, S. *et al.* (**2005**). "From wind to whales: trophic links in a coastal upwelling system," Marine Ecology-Progress Series **289**, 117-130.

Doniol-Valcroze, T., Lesage, V., Giard, J. *et al.* (**2011**). "Optimal foraging theory predicts diving and feeding strategies of the largest marine predator," Behavioral Ecology **22**, 880-888.

Fauchald, P. (**1999**). "Foraging in a hierarchical patch system," American Naturalist **153**, 603-613.

Fiedler, P. C., Reilly, S. B., Hewitt, R. P. *et al.* (**1998**). "Blue whale habitat and prey in the California Channel Islands," Deep-Sea Research Part II-Topical Studies in Oceanography **45**, 1781-1801.

Gaskin, D. E. (**1982**). *Ecology of Whales and Dolphins* (Heinemann, London).

Goldbogen, J. A., Calambokidis, J., Shadwick, R. E. *et al.* (**2006**). "Kinematics of foraging dives and lunge-feeding in fin whales," Journal of Experimental Biology **209**, 1231-1244.

Goldbogen, J. A., Pyenson, N. D., and Shadwick, R. E. (**2007**). "Big gulps require high drag for fin whale lunge feeding," Marine Ecology-Progress Series **349**, 289-301.

Goldbogen, J. A., Calambokidis, J., Croll, D. A. *et al.* (**2008**). "Foraging behavior of humpback whales: kinematic and respiratory patterns suggest a high cost for a lunge," Journal of Experimental Biology **211**, 3712-3719.

Goldbogen, J. A., Calambokidis, J., Oleson, E. *et al.* (**2011a**). "Mechanics, hydrodynamics and energetics of blue whale lunge feeding: efficiency dependence on krill density," Journal of Experimental Biology **214**, 131-146.

Goldbogen, J. A., Calambokidis, J., Oleson, E. *et al.* (**2011b**). "Mechanics, hydrodynamics and energetics of blue whale lunge feeding: efficiency dependence on krill density (vol 214, pg 131, 2011)," Journal of Experimental Biology **214**, 698-699.

Hazen, E. L., Friedlaender, A. S., Thompson, M. A. *et al.* (**2009**). "Fine-scale prey aggregations and foraging ecology of humpback whales (*Megaptera novaeangliae)*," Marine Ecology-Progress Series **395**, 75-89.

Ichii, T., Katayama, K., Obitsu, N. *et al.* (**1998**). "Occurrence of Antarctic krill (*Euphausia superba*) concentrations in the vicinity of the South Shetland Islands: relationship to environmental parameters," Deep-Sea Research Part I-Oceanographic Research Papers **45**, 1235-1262.

Isaaks, E. H., and Srivastava, R. M. (**1989**). *Applied Geostatistics* (Oxford University Press, New York, New York).

Kenney, R. D., Mayo, C. A., and Winn, H. E. (**2001**). "Migration and foraging strategies at varying spatial scales in western North Atlantic right whales: a review of hypotheses," Journal of Cetacean Research and Management **2**, 251-260.

Krebs, J. R., Stephens, D. W., Sutherland, W. J. *et al.* (**1983**). "Perspectives in optimal foraging," in *Perspectives in Ornithology*, edited by A. H. Brush, and G. A. Clark Jr. (Cambridge University Press, Cambridge), pp. 165-222.

Kulka, D. W., and Corey, S. (**1982**). "Length and Weight Relationships of Euphausiids and Caloric Values of *Meganyctiphanes norvegica* (M. Sars) in the Bay of Fundy," Journal of Crustacean Biology **2**, 239-247.

Ling, J. K. (**1977**). "Vibrissae of marine mammals," in *Functional Anatomy of Marine Mammals*, edited by R. J. Harrison (Academic Press, London), pp. 387-415.

Mackas, D. L., Kieser, R., Saunders, M. *et al.* (**1997**). "Aggregation of euphausiids and Pacific hake (*Merluccius productus*) along the outer continental shelf off Vancouver Island," Canadian Journal of Fisheries and Aquatic Sciences **54**, 2080-2096.

MacLennan, D. N., Fernandes, P. G., and Dalen, J. (**2002**). "A consistent approach to definitions and symbols in fisheries acoustics," ICES Journal of Marine Science **59**, 365-369.

Martin, B. D., and Emery, K. O. (**1967**). "Geology of Monterey Canyon, California," American Association of Petroleum Geologists Bulletin **51**, 2281-2304.

Mauchline, J., and Fisher, L. R. (eds). (**1969**). *The Biology of Euphausiids* (Academic Press Inc., New York, NY).

Mauchline, J. (**1980**). "The biology of mysids and euphausiids," Advances in Marine Biology **18**, 373-681.

Rice, D. W. (**1978**). "Blue Whale," in *Marine Mammals of Eastern North Pacific and Arctic Waters*, edited by D. Haley (Pacific Search Press, Seattle, Washington), pp. 40-45.

Santora, J. A., Sydeman, W. J., Schroeder, I. D. *et al.* (**2011**). "Mesoscale structure and oceanographic determinants of krill hotspots in the California Current: Implications for trophic transfer and conservation," Progress in Oceanography **91**, 397-409.

Schoenherr, J. R. (**1991**). "Blue Whales Feeding on High-Concentrations of Euphausiids around Monterey Submarine-Canyon," Canadian Journal of Zoology-Revue Canadienne De Zoologie **69**, 583-594.

Simard, Y., and Mackas, D. L. (**1989**). "Mesoscale Aggregations of Euphausiid Sound Scattering Layers on the Continental-Shelf of Vancouver Island," Canadian Journal of Fisheries and Aquatic Sciences **46**, 1238-1249.

Simard, Y., and Lavoie, D. (**1999**). "The rich krill aggregation of the Saguenay - St. Lawrence Marine Park: hydroacoustic and geostatistical biomass estimates, structure, variability and signficance for whales," Canadian Journal of Fisheries and Aquatic Sciences **56**, 1182-1197.

Slijper, E. J. (**1979**). *Whales* (Cornell University Press, Ithaca, New York).

Thompson, D., and Fedak, M. A. (**2001**). "How long should a dive last? A simple model of foraging decisions by breath-hold divers in a patchy environment," Animal Behaviour **61**, 287-296.

Tynan, C. T. (**2004**). "Cetacean populations on the SE Bering Sea shelf during the late 1990s: implications for decadal changes in ecosystem structure and carbon flow," Marine Ecology-Progress Series **272**, 281-300.

Williams, T. M., and Yeates, L. (**2004**). "The energetics of foraging in large mammals: a comparison of marine and terrestrial predators," International Congress Series **1275**, 351-358.

Yochem, P. K., and Leatherwood, S. (**1985**). "Blue whale (*Baleaenoptera musculus*) (Linnaeus, 1758)," in *Handbook of marine mammals*, edited by S. H. Ridgway, and R. J. Harrison (Academic Press, London), pp. 193-240.

Zamon, J. E., Greene, C. H., Eli, M. T. *et al.* (**1996**). "Acoustic characterization of the three-dimensional prey field of foraging chinstrap penguins," Marine Ecology-Progress Series **131**, 1-10.